NUMERICAL AND EXPERIMENTAL STUDY OF GROUTED ROCK BOLTS AND THEIR DEFECTS USING ULTRASONIC GUIDED WAVES

by

Yan Cui

Submitted in partial fulfilment of the requirements
for the degree of Doctor of Philosophy

at

Dalhousie University
Halifax, Nova Scotia
May 2013

DALHOUSIE UNIVERSITY

DEPARTMENT OF CIVIL AND RESOURCE ENGINEERING

The undersigned hereby certify that they have read and recommend to the Faculty of Graduate Studies for acceptance a thesis entitled "NUMERICAL AND EXPERIMENTAL STUDY OF GROUTED ROCK BOLTS AND THEIR DEFECTS USING ULTRASONIC GUIDED WAVES" by Yan Cui in partial fulfilment of the requirements for the degree of Doctor of Philosophy.

Dated: May 3, 2013

External Examiner: _____

Research Supervisor: _____

Examining Committee: _____

_____

Departmental Representative: _____

DALHOUSIE UNIVERSITY

DATE: May 3, 2013

AUTHOR: Yan Cui

TITLE: Numerical and Experimental Study of Grouted Rock Bolts and Their Defects using Ultrasonic Guided Waves

DEPARTMENT OR SCHOOL: Department of Civil and Resource Engineering

DEGREE: PhD CONVOCATION: October YEAR: 2013

_____

Signature of Author

TABLE OF CONTENTS

LIST OF TABLES

LIST OF FIGURES

ABSTRACT

A rock bolt installed in field has only one short exposed end on the rock surface. This condition has posed challenges in field instrumentation and made it difficult to use the ultrasonic guided wave method for rock bolt monitoring. In rock bolt laboratory tests using ultrasonic guided waves, the input and receiving transducers are typically installed at the two exposed ends of a bolt. This is suitable to laboratory conditions but not practical in the field because one of the ends of a rock bolt is embedded in the rock mass. A method needs to be found to install the receiving transducer at a suitable location in the field for receiving valid wave data.

In this thesis, a practical approach is proposed for conducting field tests with the installation of the receiving transducer on the grout surface near the exposed end of the bolt. The effects of the installation location of the receiving transducer are studied with numerical modeling. Experiments are conducted to verify the numerical modeling results. The results indicate that the data obtained from the receiving transducer installed on the grout surface at a proper location are representative and can be analyzed through the established correlations to determine the required parameters.

Previous researches have mostly focused on the feasibility of the ultrasonic guided wave method for rock bolt tests and on the behavior of ultrasonic guided waves of fully grouted rock bolts in laboratory conditions. No further study has been performed to identify the grout defects in grouted rock bolts. Adequate understanding of the behaviour of ultrasonic guided waves in rock bolts with defects is therefore prerequisite for this method to be applied in practice. This thesis investigates the effects of some typical defects (e.g., an insufficient rebar length, a missing grout at the ground end, and a void in grout) in grouted rock bolts using the developed field measurement method and numerical modeling. The results are verified by laboratory tests using the equipment set-up established in this research. The results indicate that it is practically possible to identify those grout defects using ultrasonic guided waves.

LIST OF ABBREVIATIONS AND SYMBOLS USED

A_a	Amplitude at location *a*
A_b	Amplitude at location *b*
A_e	Amplitude of echo
A_f	Amplitude of input group
A_{eC}	Average amplitude of the echo at Point C on the grout surface
A_{eB}	Average amplitude of the echo at Point B
A_{fC}	Average amplitude of the input group at Point C on the grout surface
A_{fB}	Average amplitude of the input group at Point B
G	Correction factor to account for the wave energy propagating into the un-grouted portion
H	Correction factor to account for the wave energy propagating into the grout
K_b	Boundary correction factor
K_f	Fixed energy loss factor
K_I	Boundary correction factor for rock bolts with an insufficient rebar length at the ground end.
K_{IR}	Correction factor for boundary conditions and the energy loss at the first reflection point for rock bolts with an insufficient rebar length.
K_l	Location correction factor
K_m	Boundary correction factor for rock bolts with a missing grout length at the ground end
K_{MG}	Correction factor for boundary conditions and the energy loss at the first reflection point for rock bolts with a portion of missing grout
K_v	Boundary correction factor for rock bolts with a grout void
k	Stiffness
L	Grout length
L_i	Travel distance affected by the *i*th factor
L_{FG500}	Grouted rebar length of Sample FG500

L_{FG750}	Grouted rebar length of Sample FG750
L_{FG1000}	Grouted rebar length of Sample FG1000
L_{IR500}	Grouted rebar length of Sample IR500
L_{IR750}	Grouted rebar length of Sample IR750
L_{MG750}	Grouted rebar length of Sample MG750
L_{MG1000}	Grouted rebar length of Sample MG1000
R	Amplitude ratio
R_{FG500}	Amplitude ratios of the echo and input group of Sample FG500
R_{FG750}	Amplitude ratio of the echo and input group of Sample FG750
R_{FG1000}	Amplitude ratio of the echo and input group of Sample FG1000
R_{IR500}	Amplitude ratios of the echo and input group of Sample IR500
R_{IR750}	Amplitude ratios of the echo and input group of Sample IR750
R_{MG750}	Amplitude ratio of the echo and input group of Sample MG750
R_{MG1000}	Amplitude ratio of the echo and input group of Sample MG1000
R_c	Amplitude ratio at point C
R_B	Amplitude ratio at point B
R_e	Echo amplitude ratio
R_f	Input group amplitude ratio
R_i	Amplitude ratio after attenuation of the *i*th component
R_m	Measured amplitude ratio
α	Attenuation coefficient
α_i	Attenuation coefficient of the *i*th component,
α_t	Total attenuation coefficient
$v_i(t)$	Recorded wave amplitude
Δt	Lateral travel time

ACKNOWLEDGEMENTS

The research outlined in this thesis is part of an ongoing research program of ultrasonic guided waves for rock bolt monitoring and the grout quality tests led by Dr. D. H. Zou in Dalhousie University. Some of the test equipment used in this study was developed in this research program. This research is partially supported by NSERC, which made this study possible.

The reported study was directed by Dr. D. H. Zou, as my supervisor, and Dr. F. Taheri and Dr. M. Rockwell, as the guiding committee members. They gave valuable suggestions and supports during experiments and numerical analysis of this study. Financial supports were mostly provided by the research assistantship from Dr. Zou`s research funding and partially by the Graduate Assistantship of the Faculty of Graduate Studies in Dalhousie University.

CHAPTER 1 INTRODUCTION

Rockbolting is one of the most important developments in the history of rock mechanics. It revolutionized both reinforcement practice and theory. Today, it is a standard rock mass reinforcement means for a wide range of ground control problems encountered in mining, civil and geotechnical engineering.

Rock bolts, in many applications, are installed into the ground and grouted with cement or resin. The efficiency of rock bolting is largely determined by the installation quality, which is affected by many factors. An important aspect of rockbolting is therefore testing and evaluating the installation quality.

Traditional methods, such as pull-out tests, are usually destructive, expensive and time consuming. A non-destrictive method which possesses the potential for significantly improving the efficiency of this evaluation process is required.

In recent years, there have been a number of research initiatives in non-destructive rock bolt tests, most noticeable the method using guided ultrasonic waves (Achenbach 1973, Thurner 1988, Beard and Lowe 2003, Madenga 2004, Cui and Zou 2006, Zou et al 2007, Han et al 2009, Zou et al 2010, Zou and Cui 2011, Cui and Zou 2012 and Zou and Cui 2012).

When guided ultrasonic waves traveling along a rock bolt, the wave travel time is determined from the bolt length and the wave group velocity. With the knowledge that the travel time is different in the grout length from that in the non-grout length, the measured travel time may be useful to estimate the grout length. It is also known that an ultrasonic guided wave loses energy as it propagates in a grouted rock bolt, resulting in the amplitude reduction, an effect of wave attenuation. The attenuation magnitude may also be used to estimate the grout length and the grout quality of rock bolts.

In a grouted bolt, the wave behaviour depends not only on the grout length and the

properties of grouting materials, but also on the wave frequency (Rose 1999). In addition, defects in grout may also play important roles. Adequate understanding of the effects of the grout length, grout material property, wave frequency and grout defects on the group velocity and wave attenuation is essential for using ultrasonic guided waves in non-destructive rock bolt tests.

Previous researches (Beard et al 2003, Madenga 2004, Cui 2005, Zou et al 2007 and Han 2009) have achieved some important results in using ultrasonic guided waves in rock bolt grout quality tests. The major difficulty for practically using this method is that so far reported studies on this method are restricted to the arrangement that the input transducer and receiving transducer are at the two ends of the rock bolt as illustrated in Figure 1-1.

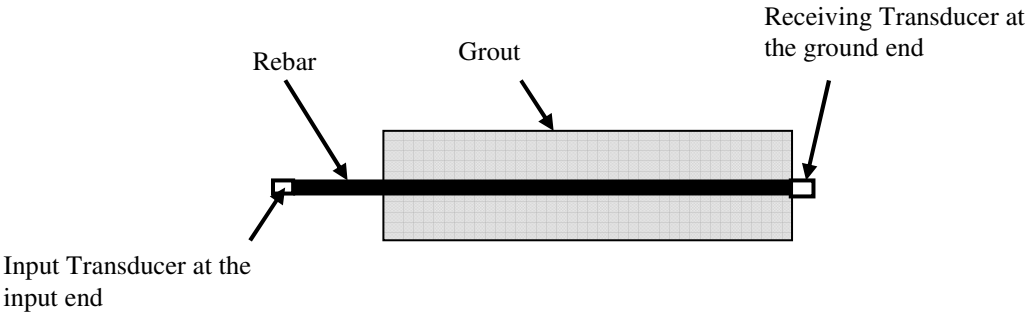

Figure 1-1 Transducer locations in transmission-through set-up

This set-up is suitable to study wave behaviors in laboratory settings, but is not practical in the field, because one end of the bolt has to be embedded into the ground in such case. To be a practical method using ultrasonic guided waves, both the input and receiving transducers must be at the exposed end. The first step to apply the ultrasonic guided wave method to field practice is to find a suitable installation location for the installation of the receiving transducer in the field environment.

For clarification, the rock bolt end where the input transducer is installed is called the input end, and the end in the ground is called the ground end in this thesis.

Previous researches have mostly focused on the feasibility of the ultrasonic guided wave method for rock bolt tests. Results regarding the ultrasonic guided wave behaviours along the rebar of a fully grouted rock bolt (Figure 1-1) were available (Cui and Zou 2006 and Zou et al 2007). However, one of the objectives of the tests is to identify the grout defects in the grouted rock bolts. Understanding of the ultrasonic guided wave behaviours in rock bolts with defects is essential before this method can be used in practice.

1.1 RESEARCH OBJECTIVES

The ultimate goal of the research on using the ultrasonic guided waves for rock bolt tests is for the field evaluation of the capacity of the grouted rock bolts. Since the rock bolt capacity partly depends on the grout length and grout quality, this study focuses on identifying the grout defects of the rock bolts and assessing the effectively grout length.

The transmission-through equipment set-up (Figure 1-1) used in previous researches is not practical for field use. Configuring a suitable equipment set-up is the first priority in conducting rock bolt tests using the ultrasonic guided wave method.

The objectives of this research are:

1) to study the feasibility of a proposed field measurement method. A transmission-echo-off-path set-up as shown in Figure 1-2 is proposed. The input transducer is installed at the input end of the rebar (Point A in Figure 1-2) and the receiving transducer is installed on the grout surface near the input end (Point C in Figure 1-2).

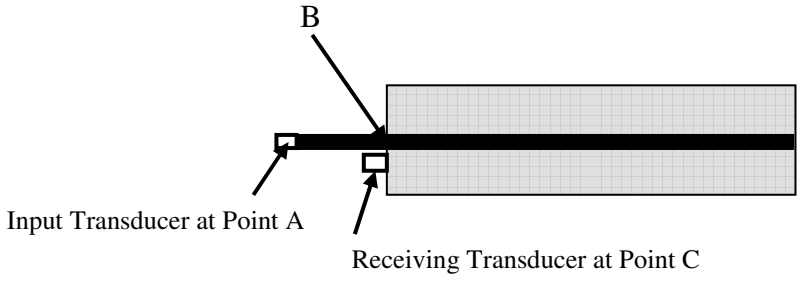

Figure 1-2 Transducer locations in transmission-echo-off-path set-up

2) to find a suitable location for the receiving transducer installation. With the transmission-echo-off-path set-up shown in Figure 1-2, it is expected that the distance between Point B (the center of the rebar) and Point C affects the measurement results. In Addition, wave attenuation and wave travel time measured at the location of Point C are required to be correlated to a location along the axis of the rebar (Point B).

3) to study the effects of some typical grout defects (insufficient rebar length, a missing grout at the ground end and a void in grout) on the wave attenuation and group velocity when using the proposed field measurement method shown in Figure 1-2.

This study aims at providing a practical application to field evaluate grout length of rock bolts, and is limited to laboratory experiments and numerical analysis. The results are specific to the experimental situation and material properties. However, the conclusions and the suggested testing methods are considered to be suitable to test rock bolts in other experimental circumstances or in the field.

1.2 THESIS OUTLINE

Chapter 1 presents an introduction and outline of this thesis.

In Chapter 2, published literatures on rock bolts are reviewed; traditional and non-destructive test methods for evaluating rock bolt quality are summarized; and the limitations of those testing methods are illustrated.

Chapter 3 provides the basic concepts and relevant theories of ultrasonic guided waves. This is the fundamental knowledge of this reported study.

Chapter 4 describes general methodologies, experimental devices and data analysis methods of this research.

The numerical studies on the effects of receiving transducer locations on the attenuation and wave travel time in fully grouted rock bolt samples are presented in Chapter 5. Results obtained from the numerical study are verified by laboratory tests.

Details of numerical studies of ultrasonic guided waves in rock bolts with a portion of missing grout at the ground end are described in Chapter 6. The verification of the numerical study results using laboratory experiments is also presented in this chapter.

The laboratory and numerical studies on rock bolts with an insufficient rebar length at the ground end are described in Chapter 7.

In Chapter 8, the effects of a void in grout of rock bolts are studied by numerical modeling. Simplifications are applied to the void and the details are provided in Chapter 8. The experimental verification for the numerical results is also included in this chapter.

Chapter 9 summarizes conclusions of the research, and recommends on future researches required for the proposed guided ultrasonic wave method.

The scientific literature cited in this thesis is listed in the Bibliography.

At the end of this thesis, typical computer input files used in this study are illustrated in Appendices.

CHAPTER 2 LITERATURE REVIEW

In 1927, a United States metal mine began to use a new support technology, very primitive steel slot-and-wedge rock bolts (Bolstad and Hill 1983). In 1984, the United States Bureau of Mines estimated that about 120 million roof bolts were used in United States and over 90% of underground coal production taken place under bolted roofs (Bieniawski 1987). Some advantages of rock bolts over other supporting systems significantly enhanced the application as discussed by Luo (1999):

- Reducing storage and material handling requirements compared to traditional support systems, such as, the timber support system;

- Decreasing the size of the opening that is needed to achieve the same given clearance by other supporting systems;

- Preventing roof deformations by a quick installation after opening is excavated;

- Improving ventilation by lowering the resistance to the air via the elimination of obstructions;

- Providing greater freedom for trackless vehicles without risk of dislodging supports; and

- Providing natural supports for hanging pipes, tubes, and electrical cables.

Millions of rock bolts have been installed each year for the purpose of supporting subsurface excavations in mining and tunneling engineering. A lot of rock bolts are grouted with cement or resin to develop a bond between the bolt and the surrounding rock.

Pull-out test and over-coring are conventional methods to test the grout quality, which are destructive and time consuming. Searching for a non-destructive test method, for example the ultrasonic wave method, has become an attractive topic to many researchers.

It has been shown by Beard et al (2003) that ultrasonic guided wave is promising as a non-destructive method to test the grout quality. In recent years, some significant progresses have been achieved in the use of this method and parameters of attenuation and wave group velocity of ultrasonic guided waves are found to be good indicators of grout length of rock bolts (Madenga 2004, Cui 2005, Zou et al 2007 and Han 2009).

In this chapter, the application and mechanics of rock bolts, and traditional and non-destructive test methods are reviewed. Previous achievements regarding traditional and non-destructive tests, including the ultrasonic guided wave method, are summarized.

2.1 MECHANICS OF ROCK BOLTS

Today, rock bolts are widely used in underground mining, tunneling, slope stability and other ground stability applications. Rock bolts installed in different grounds have varied purposes, such as roof supporting, preventing wedge falling, fractured rock slope stability, and the theories used to explain the bolting mechanisms vary from place to place.

2.1.1 Roof-supporting

The most common application of rock bolts in mining industry, especially coal mine, is roof supporting. Weigel (1943) explained the fundamental concepts of rock bolts as a roof-supporting method. He stated that the contributions of rock bolts could be in supporting weakened rock below the natural arch line; bolting weak, thin strata together to create thicker, stronger strata; and providing early support in the mining cycle.

Peng (1984) considered that the main function of roof supporting is to bind together stratified or broken rocks consisting of natural joints and fractures, or rocks with artificial fractures and cracks caused by explosions. It is broadly believed that bolt binding effects are accomplished by one or a combination of the following three basic mechanisms: suspension, beam building, and prevention of fissure movement in fractured grounds (Choquet 1991 and Luo 1999).

Suspension

When an opening is made, the strata directly overhead tend to sag. The laminated immediate roof could separate from the main roof and fall out. Rock bolts can be used to suspend the immediate roof to the self-supporting main roof by the tension applied to the bolt. The rock bolts used as a suspension of a laminated layer to upper layers with good holding power is illustrated in Figure 2-1.

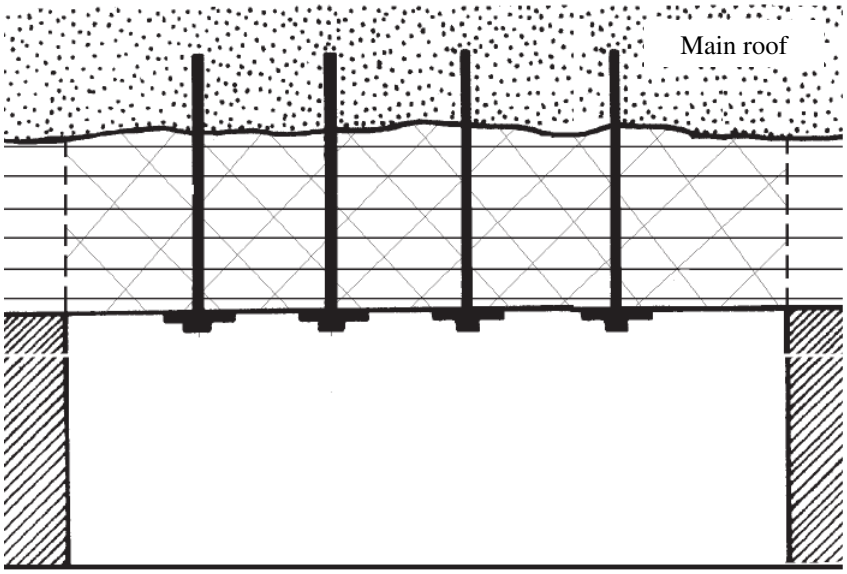

Figure 2-1 Suspension of fissured layers

Beam Building

Rock bolts clamp the layers together as a support of the bedded grounds to form a thick and self-stable roof as shown in Figure 2-2. This bolting pattern is similar to clamping a number of thin, weak layers into a thicker, stone beam.

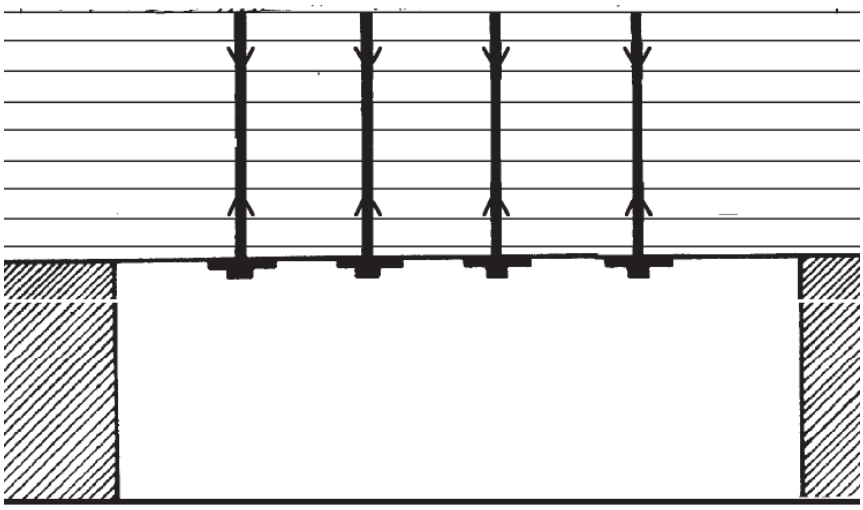

Figure 2-2 Beam building support of bedded grounds

Prevention of Fissure Movement in Fractured Grounds

When the roof strata are highly fractured and blocky, or the immediate roof contains one or several set of joints with different orientations to the roofline, rock bolts provide significant frictional forces along fractures, cracks, and weak planes. The rock bolts used as a prevention of the fissure movement in fractured grounds to stabilize the roof with joints as demonstrated in Figure 2-3.

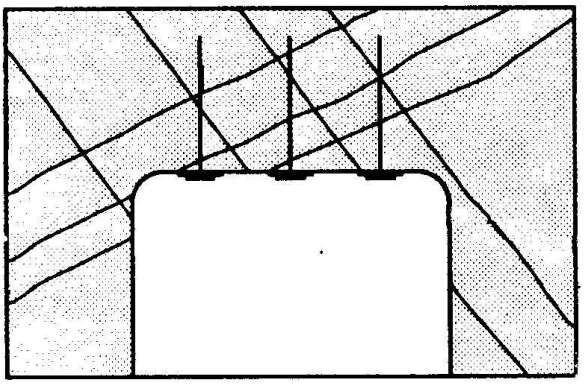

Figure 2-3 Prevention of fissure movement in fractured grounds (Modified from Choquet 1991)

2.1.2 Preventing Wedge Falling

The excavation of underground tunnels, drifts and caverns may cause considerable changes in the state of stress with associated strains and deformations (Xanthako 1991). In tunnels excavated in jointed rock masses, the most common types of failure involve wedges falling from the roof or sliding out of the side walls of the openings (Hoek et al 2000). These wedges are formed by intersecting structural features such as bedding planes and joints, which separate the rock mass into discrete but interlocked pieces. Rock bolts installed to prevent roof and sidewall wedge falling are shown in Figure 2-4.

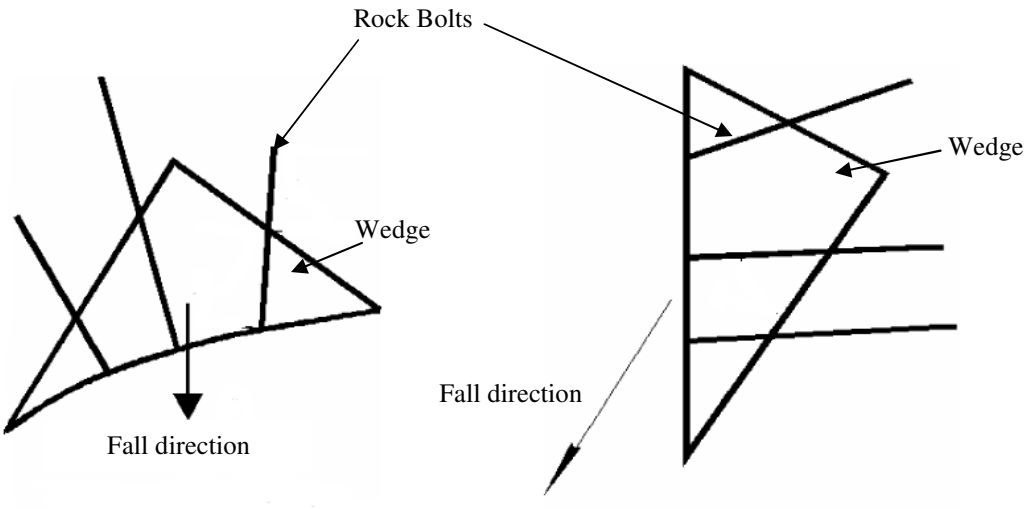

Figure 2-4 Rock bolt preventing wedge falling (Modified from Hoek et al 2000)

2.1.3 Rock Slope Stability

In many cases, engineered slopes require stabilization to ensure their long-term viability and reduce localized slope failure (FHWA 2011) as shown in Figure 2-5. Rock bolts

installed in an unstable slope can increase the normal force friction and shear resistance along discontinuities and failure surfaces (Xanthako 1991).

Rock bolts for slope stability can be tensioned or untensioned. Untensioned rock bolts can provide reinforcement through the shear strength of the steel, which increases friction along the potential failure plane. Once rock block movement occurs, the tensile strength of the rock bolt is engaged and the normal force between opposing discontinuities is increased. The tension bolts are used to add compressive stress to joints within a rock mass. This force increases the friction along the fracture planes and helps to reduce block movement.

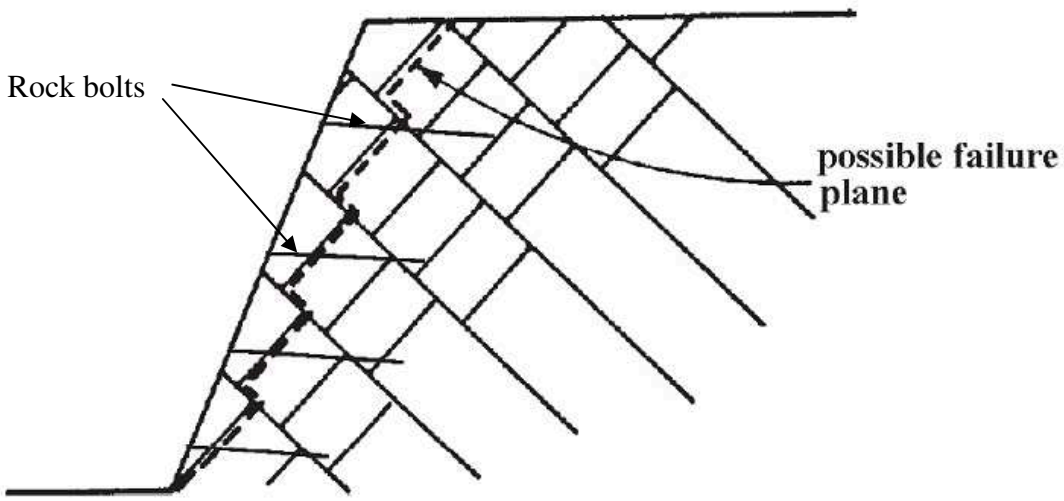

Figure 2-5 Rock bolts for slope stability (Modified from Luo 1999)

2.2 TYPES OF ROCK BOLTS

Based on the anchoring mechanism, rock bolts can be divided into three types, point anchored, partially or fully grouted and friction anchored. Point anchored rock bolts are usually mechanically anchored bolts. Partially or fully grouted rock bolts are anchored by

cement or resin. Friction anchored rock bolts are anchored by friction between the bolt bar and the surrounding rock.

Whether the rock bolt is tensioned is another way to categorize rock bolts. Traditionally, the majority of mechanically anchored bolts are tensioned at installation to provide initial resistance to ground movement. Many fully grouted bolts are un-tensioned, unless tension is applied before grouting. Some of partially grouted rock bolts are tensioned. Whether a rock bolt is to be tensioned or not is a decision based on rock mechanics for the particularly ground and stress condition.

The description of several traditional types of rock bolts, mechanically anchored bolts, rock bolts grouted with resin or cement, friction bolts and cable bolts are illustrated in the following sections.

Mechanically anchored bolts

This kind of rock bolts as shown in Figure 2-6 has a bolt with one threaded end to fit a shell in the ground end and another threaded end to fit a plate and a nut at the collar.

The steel bar of rock bolts is usually made of high strength steel. The objective of the plate is to keep the steel bolt bar in tension. A shell exists to satisfy the diameter of the hole. The type of shell used in practice is usually decided according to the diameter of the bolt bar and the drill hole, and the rock matrix condition. The size of the plates is different in practice.

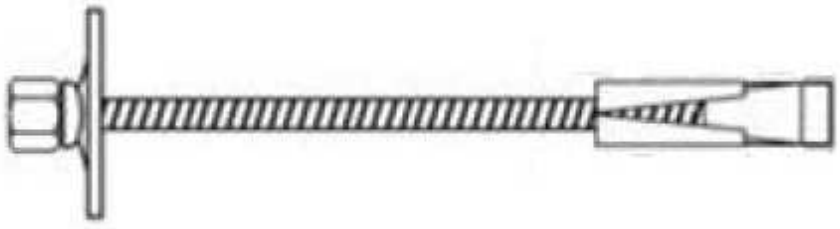

Figure 2-6 Mechanical bolt (Modified from DSI 2010)

Rock bolts grouted with resin or cement

The rock bolt is installed in the rock and partially or fully grouted with cement or resin. A plate is typically installed at the external end if it is a partially grouted bolt. Typical partially grouted and fully grouted rock bolts are illustrated in Figures 2-7 and 2-8, respectively. The primary function of the grout material is to transfer load from the bolt stem to the surrounding rock mass during the rock movement (Madenga 2004). The ultrasonic wave method studied in this thesis is for the use of this type of grouted rock bolts.

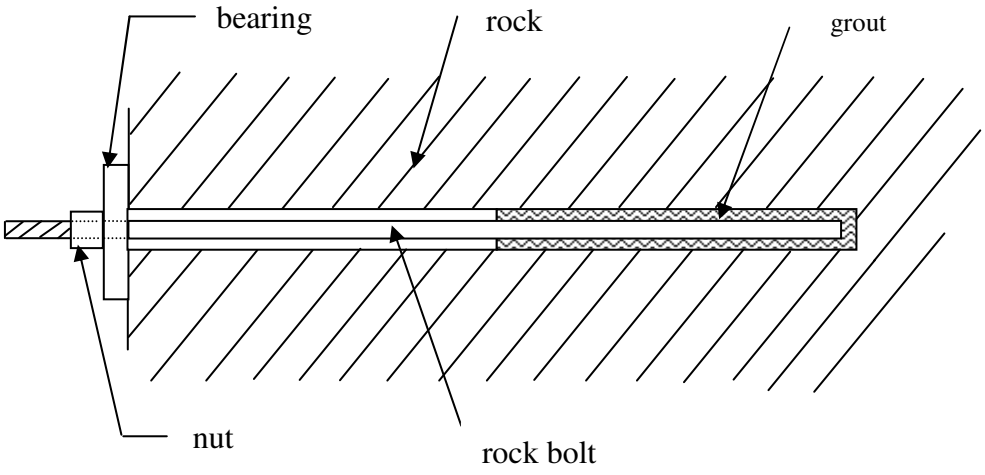

Figure 2-7 Partially grouted rock bolt

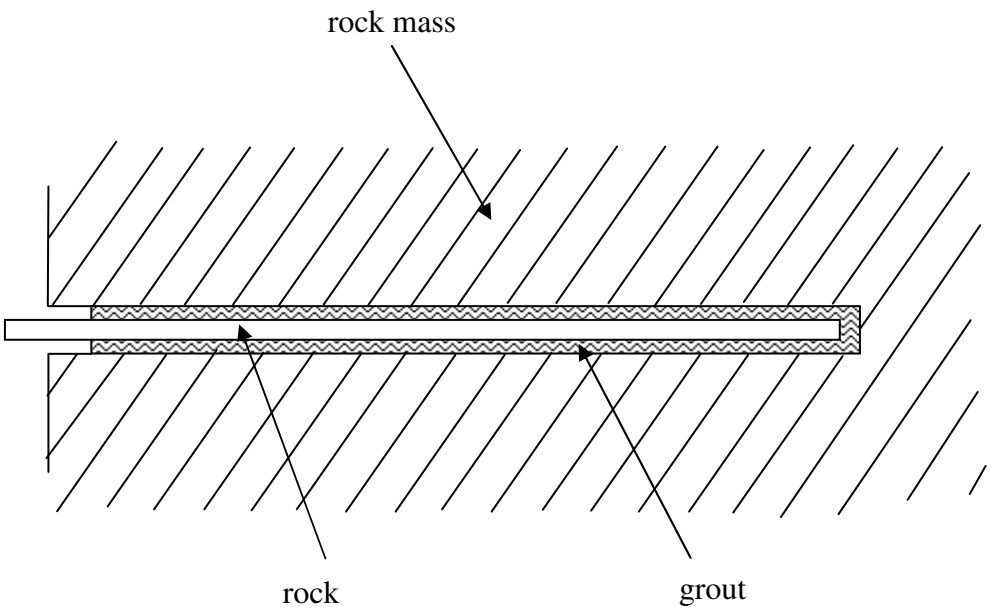

Figure 2-8 Fully grouted rock bolt

Frictional bolts

There are two kinds of friction bolts. One kind friction bolt is a closed steel tube. After fitting into a pre-drilled hole in the rock mass, the tube is inflated by hydraulic pressure to provide friction against the borehole wall. Another kind friction bolt called split set friction bolt is an open steel tube, which is larger than the drilled hole and has to be driven into the rock mass by force as shown in Figure 2-9.

Figure 2-9 Split set friction bolt (Modified from DSI 2010)

Cable bolts

The cable bolts use stranded steel cables rather than steel bars as a load bearing element. The cable bolt is not limited by its length and can be installed in conditions where the use of other type rock bolts is constrained by the geometry of opening. Cable is relatively flexible in comparison with rebar. Typical cable bolt is illustrated in Figure 2-10.

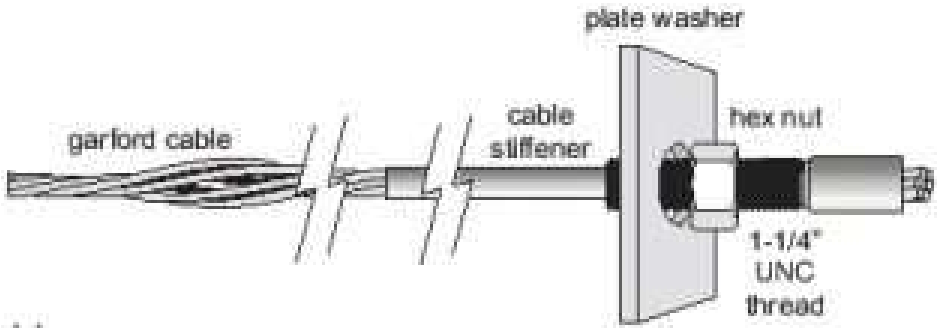

Figure 2-10 A typical cable bolt

In longwall mining, cable bolts are now widely used as secondary supports, supplementing or replacing traditional secondary support systems, such as wood cribs and posts, hydraulic jacks, or spot roof bolts (Tadolini and Koch, 1993).

2.3 BOLT FAILURES AND MOBILIZED ANCHORAGE STRENGTH ALONG ROCK BOLTS

A rock bolt may fail in the bolt, the collar plate, the rock and the anchorage. Bolt failure is a design issue and can be avoid during the design of the support system. The following discussion only focuses on the failure of the anchorage, which is related to this research.

It is understood (Zou 2004) that the anchorage is the mechanism that bonds the bolt and the rock mass together. For grouted rock bolts, the anchorage is the combination of the grout, the interface between the bolt and the grout, and the interface between the grout

and the rock. Zou (2004) also analyzed in details on the mobilized anchorage strength for different bolt types, such as fully grouted, partly grouted, with bearing plate and without bearing plate.

Figure 2-11 shows a fully grouted rock bolt across a weak joint. If a weak joint exists in the grouted segment, the associated ground movement is likely the largest at the joint location. As a tension is generated due to ground development, part of the anchorage strength is mobilized near the weak joint and distributed in both sides of the joint (curve 1 in Figure 2-11). As the tension further developed when ground moved along the joint, the mobilized anchorage strength developed until reaching the maximum strength (curve 2 in Figure 2-11), which depends on the grout strength, the interface strength between the bolt and grout and the interface strength between the grout and the adjacent rock. When the maximum strength is reached, the mobilized anchorage strength will not increase in magnitude further but horizontally extends along the bolt further (curve 3 in Figure 2-11).

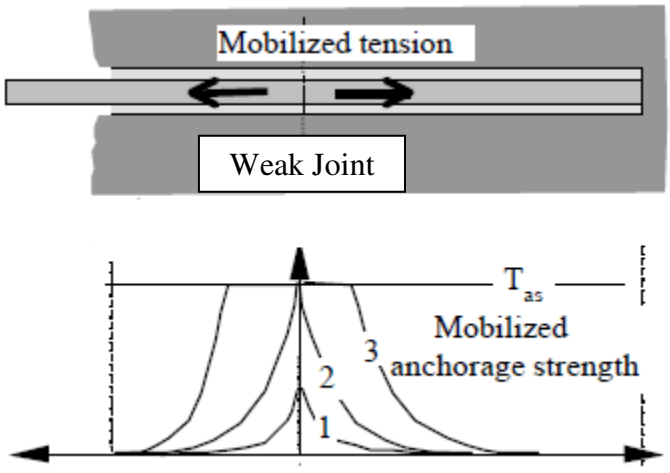

Figure 2-11 Fully grouted rock bolt cross a joint (modified from Zou 2004)

The bond resistance is directly proportional to the grout length and grout quality. Field test methods to determine the grout length and quality are important to estimate the loading capacity of rock bolts. It should be noted that the modified anchorage strength distribution in the field is not the same as the bond resistance during the pull-out test, which will be discussed later in this thesis. The results obtained from the pull-out test are

not fully representative to be used to estimate the modified anchorage strength in rock bolts in the field.

2.4 GROUTED BOLT INSTALLATION PROCEDURES AND DEFECTS

The installation of grouted rock bolts starts with the drilling of a borehole. Cement grout or epoxy resins are typically used for bonding the bolt to the rock mass (FHWA 2011).

Resin or cement capsules are placed into the borehole manually or by a compressed air gun (Kelly and Jager 1996). The bolt is then spun or hammered into the borehole to puncture the capsules and let the grout filling the annular space between the bolt and the surrounding rock.

Another commonly used method to install rock bolts is pumping grouting fluid into the borehole. For bolts installed upwards, pumping the grouting material into the space between the bolt and the surrounding rock starts from the collar, progressively filling up the hole towards the bottom (Choquet 1991 and Kelly and Jager 1996). An air tube is installed to the bottom to provide a return way for the air in the hole. This air return tube is not always necessary for bolts installed downwards, if the grouting process starting from the bottom to the collar.

Based on the installation methods, it can be concluded that if the grouting process is not carefully carried out, air voids or gaps may occur in the grouting. Poor grouting may also be encountered where joints exist in the formation of the surrounding rock. Kelly and Jager (1996) reported that up to 50% of grouted rock bolts installed in South African platinum and gold mines were not effectively grouted. Thurner (1988) reported that a similar high proportion of poorly grouted rock bolts in Sweden. Common quality defects in grouting are summarized as follows:

- Missing grout in certain portions of the bolt due to inadequate installation such as using fewer grout capsules than required, bigger borehole diameter (Kelly and Jager 1996) and stopping of grouting before the required grout length is achieved (Vrkljan et al 1999);

- Grouting strength is lower than desired (Choquet 1991);

- Presence of air voids due to poor installation procedures (Sundholm 1988); and

- Loss of grout into fissures in the surrounding rock mass (Sundholm 1988).

Kelly and Jager (1996) and Thurner (1988) considered that the inadequate reinforcement is chiefly due to poor grout quality. Kilic et al (2002) found in pull-out tests that the failure occurred between the bolt and cement grout. This means that the defection of the grout usually causes a change of the bolt capacity.

2.5 TRADITIONAL GROUT QUALITY MEASUREMENT METHODS

The grout quality is a critical concern in the field. Traditionally, there are several methods available in practice, for example, pull-out test and over-coring.

2.5.1 Pull-out Tests

Pull-out tests involve the application of an increasing pull-out force, using a hydraulic jack, at the protruding end of a rock bolt until the bolt ruptures, the anchorage failure at the interface between the bolt and grout or between the bolt and the surrounding rock mass. Typical pull-out test equipment is shown in Figure 2-12.

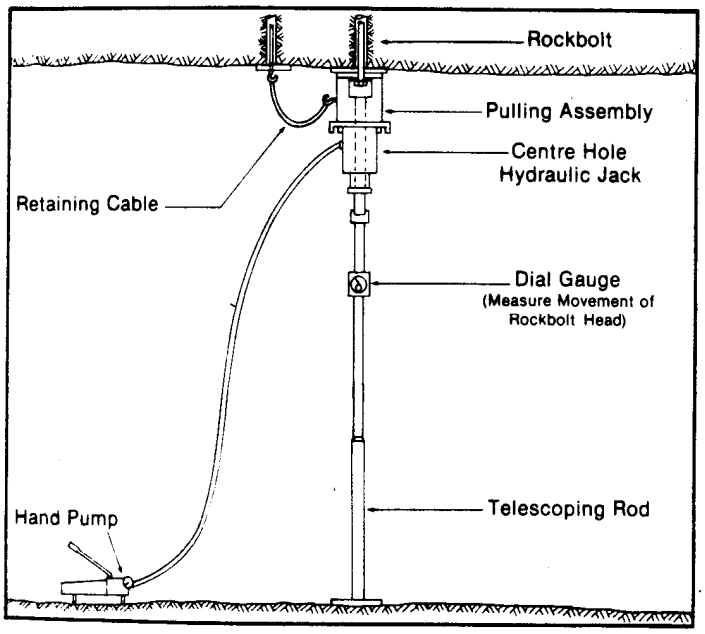

Figure 2-12 Rock bolt pull-out test (Modified from Choquet 1991)

The stress distribution along a rock bolt during a pull-out test is not the same as in the field shown in Figure 2-11. Figure 2-13 shows the bond distribution at stages of pull-out tests (Gilkey et al. 1956 and Hawkes and Evans 1951). Phillips (1970) recommends that the bond distribution should be expressed by an exponential function.

Xanthakos (1991) considered that the bond distribution is developed under the following mechanisms:

- Bond resistance is first developed as cohesion near the exposed end. Only as slight slip occurs are tension and bond stress progressively transferred distally;

- As the pull increases, the bulk of bond resistance begins to move toward the ground end. Between the exposed end and the region of the maximum bond concentration, there is a fairly uniform friction drag of moderate intensity;

- First slip occurs only after the bulk of bond resistance has migrated along almost the entire bond length and is near the ground end; and

- After appreciable slip, the primary adhesion disappears and the force is counteracted solely by friction.

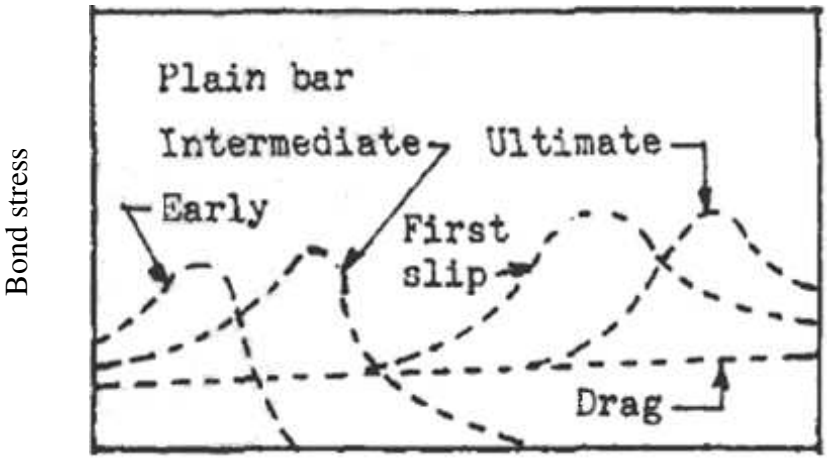

Figure 2-13 Bond distribution during pull-out test (Modified from Gilkey et al 1956)

It can be concluded that the bond resistance obtained from pull-out tests are not the same as mobilized anchorage strength in a rock bolt in the field. This method cannot provide all the information required (Zou 2004). In addition to the destructive nature, the high cost involved and the time-consumed by pull-out tests have been identified as the factors limiting the use of these tests to a very small proportion of installed rock bolts (Kelly and Jager 1996).

2.5.2 Over-coring Tests

Over-coring of installed rock bolts involves diamond drilling to obtain an intact core concentric with the rock bolt for the purpose of visual inspection of the in-situ conditions of the grout quality, the rock bolt and the embedding rock mass (Thurner 1988 and Sundholm 1987). An over-coring sample is shown in Figure 2-14.

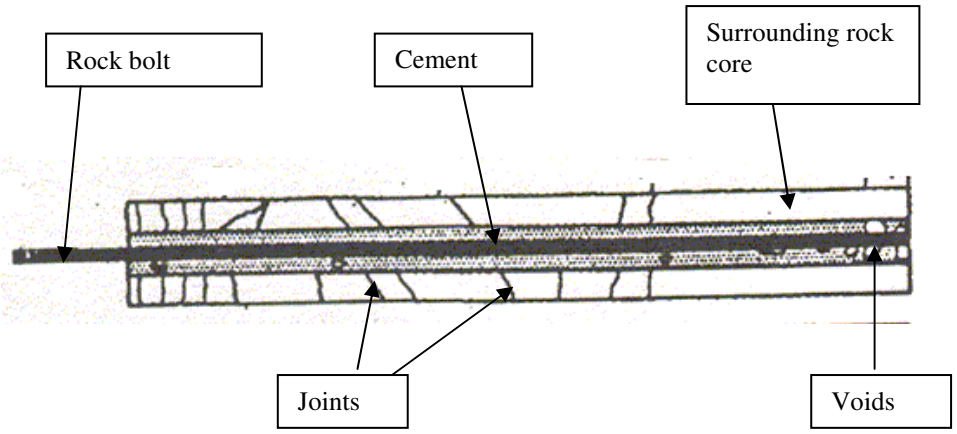

Figure 2-14 Typical over-cored rock bolt (Modified from Sundolm 1988)

While the over-coring test of an installed rock bolt is the only method allowing the undisturbed in-situ conditions of grouted rock bolts to be studied, it's use is limited to a research tool as opposed to a method for the day-to-day testing of the grout quality of rock bolts in the field due to the following factors (Sundholm 1987):

- The method is inherently destructive;
- The procedure is cumbersome; and
- Over-coring is expensive.

2.5.3 Other Traditional Methods

There are several other traditional methods used in field tests of rock bolts; for example, torque wrench technique, load cells, and strain gauge techniques. Because such methods are less relevant to this research, descriptions about those methods are not included in this thesis.

2.6 NON-DESTRUCTIVE TESTS USED IN INDUSTRY

Because traditional testing methods, such as the pull-out test, are destructive or time

consuming and may not be able to provide all required information, researchers are trying to find non-destructive testing methods, such as the ultrasonic guided wave method.

Non-destructive testing includes various methods, each based on a particular scientific principle. The various methods and techniques, due to their particular natures, may work well for certain applications and be of little or no value for others.

The initial idea of ultrasonic waves used in non-destructive test is based on the theory of the bulk wave propagating in solid. The group velocity of ultrasonic or sound waves in an infinitely large solid medium can be expressed as a function of the physical properties of the solid medium. In many applications, the dynamic Young's modulus, density and etc., can be interpreted from measurements of the bulk wave velocity (Levy 2001).

The point-source/point-receiver method is the most commonly used ultrasonic bulk wave technique of ultrasonic wave test. One of the advantages of this method is that the point source generates both longitudinal and shear waves in a medium. Information about both types of waves can be extracted from a received single waveform. Furthermore, signals of this method are simultaneously propagated in all directions in a medium, and thus, we can use an array of sensors or scan either the source or the receiver over the medium surface to determine the directional dependence of the propagating velocity and amplitudes of various wave modes in a material (Kim and Sachse 2001).

Another well studied bulk wave method is the microseimic monitoring technique, which is widely used in mining industry. Energy imbalances created by mining often lead to microseismic activities that may, under extreme stress conditions, lead to rock bursts or seismically induced falls of ground (Ge and Kairser 1992). The microseismic monitoring technique utilizes the signals generated by the materials itself to study the fracture/failure process (Ge and et al. 2009).

Although the bulk wave method is widely used in a lot of areas, in a rock bolt, as illustrated later, ultrasonic guided waves occur and bulk wave cannot be applied.

Some non-destructive test techniques are presented in the following sections.

2.6.1 Acoustic Emission

Acoustic emission as shown in Figure 2-15 refers to the generation of transient elastic waves during the rapid release of energy from localized sources (ASTM 1982). The source of these emissions is closely associated with displacements accompanying the initiation and extension of cracks in a structure under stress. The acoustic emission technique is based on the detection and conversion of these elastic waves to electrical signals.

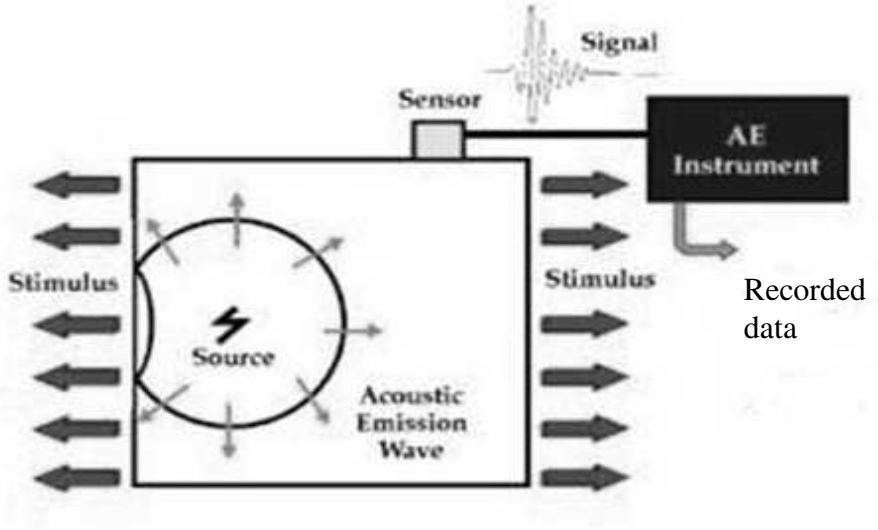

Figure 2-15 Acoustic emission (Modified from ASTM E610-82)

Acoustic emission tests are conducted by installing piezoelectric transducers on the surface of the structure and then loading the structure. The obtained signals from sensors are amplified and filtered to remove noises. Based on the obtained signal, the location of the cracks can be estimated. This method is widely used to study the formation of cracks during the welding process (Biltz and Simpson 1991).

This method is not suitable to evaluate the effective grout length and grout quality of rock bolts due to no suitable locations to install instruments after rock bolts grouted in the rock mass.

2.6.2 Borehole Acoustic Logging for Oil and Gas

The borehole acoustic logging is commonly used in the petroleum reservoir exploration, reserve estimation, well completion and hydrocarbon production. Because velocity and attenuation of an acoustic wave are related to the rock type and formation fluid, measuring these properties can provide information for formation evaluation (Tang and Cheng 2004).

In acoustic logging as shown in Figure 2-16, a logging tool is lowered into the drilled borehole and an acoustic wave is generated by a transmitter. The wave travels along the borehole and interacts with the formation, and the signals received by a series of receivers located on the probe in the borehole. The measurement is usually performed continuously as the tool is pulled up or lowered down along the borehole. Analysis of the acquired acoustic data can produce a log of the acoustic properties of the formation around the borehole.

The obtained data can be used to estimate the porosity in permeable rocks. Based on the wave velocity, the formation mechanic properties, such as modulus, passion's ratio and density, can be evaluated (Tang and Cheng 2004).

This method is widely used in the petroleum industry, but not suitable for the rock bolt tests due to no open hole for the installation of the transmitter and transducer.

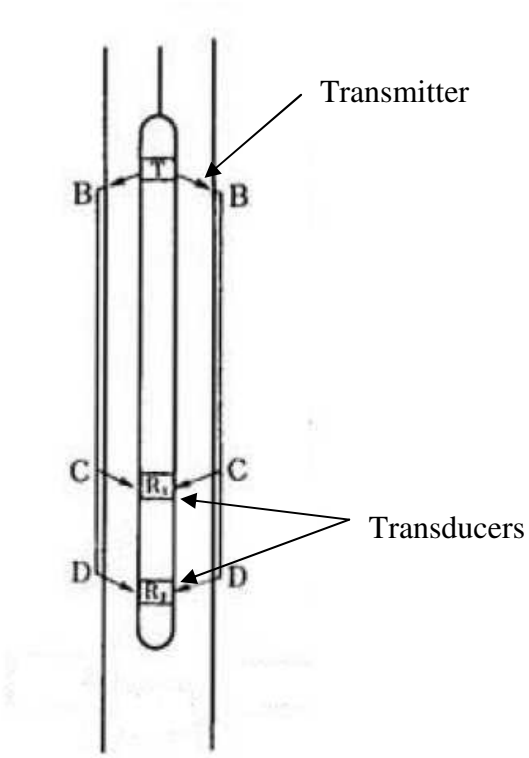

Figure 2-16 Acoustic logging

2.6.3 Dynamic Testing for Pile Capacity

Dynamic testing has been used to estimate pile capacities since 1888. In the late 1960's, research focused on predicting stresses and pile capacities based on wave mechanics (McVay et al 2002).

Dynamic testing for pile capacity is an impact-echo method. It is an iterative curve-fitting technique to the measured response of the actual pile for a single hammer blow. It is performed by attaching sensors to the pile wall and monitoring the response in terms of force and velocity of a stress wave, which is imparted into the pile head by a falling weight as shown in Figure 2-17 (Bowels 1997).

Data is collected and stored automatically on a blow-by-blow basis to aid decisions during pile driving. If the recorded curves fit the finite element analysis results, the

designed pile capacity is considered to be achieved. A description of the fundamentals of dynamic testing is presented in Design and Construction of Driven Pile Foundations (Federal Highway Administration report no. FHWA-HI-97-013). In recent years, some software such as GRLWEAP (PDI 2005), PDA (Widjaja 2006) and CAPWAP (PDI 2006) were developed for the dynamic testing of the pile capacity.

Both the rock bolt and pile are cylindrical structures. The successful application of the wave equation method for the pile capacity estimation initialized the exploration of the method for rock bolt tests, such as the Boltometer method.

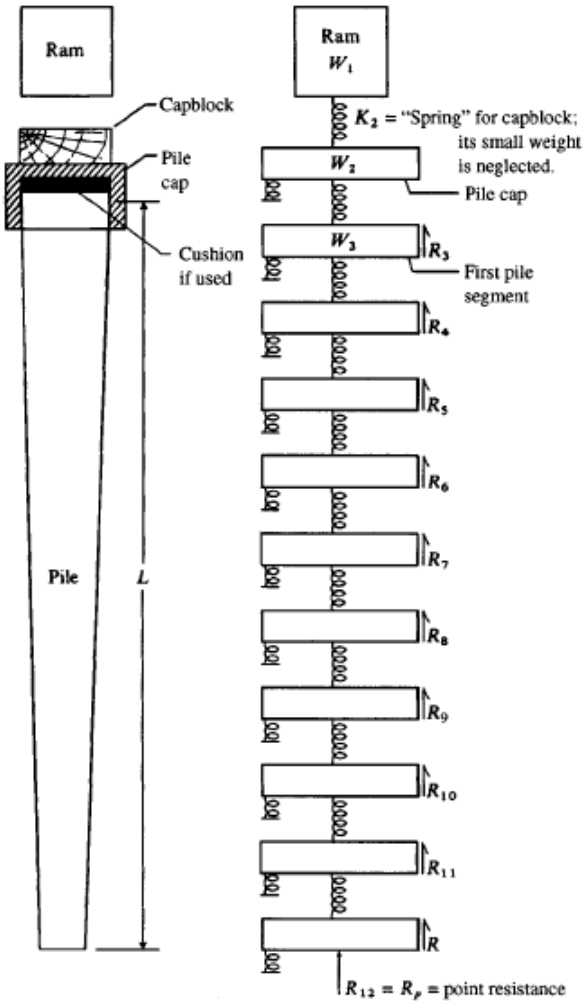

Figure 2-17 Dynamic tests for pile capacity (Modified from Bowles 1997)

2.7 NON-DESTRUCTIVE TESTS ON ROCK BOLTS

2.7.1 Bolt Natural Frequency Method

The natural frequency method, for example, the GRANIT system, operates by applying a measurable and repeatable impact using an air hammer. The signals obtained are transformed from the time to the frequency domain where the main natural frequencies are obtained. The natural frequency of vibration modes of the free part of a bolt is used to determine the load in the free part of bolts and anchors (Ivanovic et al 2001).

Milne (1999) showed that an increase in the main frequency and a reduction in amplitude were noted with increasing the level of stresses in rock bolts. Tests regarding changes in the prestress level have been undertaken on a full-scale laboratory rock bolt anchorage (Starkey 2000), and influence of prestress on the dynamic response of ground anchorages has been studied using this system (Ivanovic et al 2001).

This method is useful for assessing the tension in the free length of rock, but not suitable to test the grout quality and grout length of grouted rock bolts.

2.7.2 Boltometer

Thurner (1988) introduced non-destructive tests using the Boltometer. A piezo-eletric transducer transfers bulk waves to the bolt. These waves propagate down along the bolt at different velocities, and then are reflected back to the sensor. Through the signal history in the time domain, the Boltometer is expected to be able to determine the bolt length and the quality of the grout.

Theoretically, poor grout would cause low attenuation of the pulses, and is therefore indicated by corresponding higher amplitudes of echoes of the reflected pulses. On the other hand, good grout could be indicated by lower amplitudes of the echoes received by the transducer (Thurner 1988).

The Boltometer is mainly designed to discover rock bolts with poor grout quality. However, the attenuation in grout limits the penetration range of the wave signals (Thurner 1988). Additionally, the Boltometer method does not consider the characters of ultrasonic guided waves, the actual waves in the rock bolt. Therefore, the method could not provide a quantitative result for grout quality estimation.

2.7.3 Ultrasonic Pulse Attenuation Method

Kelly and Jager (1996) reported a method that using a transducer to launch ultrasonic pulses and another piezo-electric transducer to receive the reflection. This method is used to measure the grout quality by measuring the attenuation of grouted bolt.

The field application of this method had very little success, chiefly due to the fact that the penetration depth is limited because the transducer could not transmit sufficient ultrasonic energy into the bolt. In addition, the amplitudes of reflected waves may be affected by coupling conditions at the transducer-bolt interface.

Same as the Boltometer, because this method does not consider the characters of the ultrasonic guided waves, it cannot provide a quantitative result for rock bolt grout quality estimation.

2.7.4 Ultrasonic guided wave Method

Beard et al (2003) argued that conventional bulk ultrasonic waves could only propagate in an infinite expanse of material, while ultrasonic guided waves would propagate in the cylindrical structure of a rock bolt. The ultrasonic guided waves in the bolt are different from conventional bulk compression and shear waves (Beard et al 2003).

Theoretically, accurate knowledge of the wave velocity dispersion curves allows the position of defects or the bolt length to be calculated from the reflection arrival time

(Beard et al 2002). Using the ultrasonic guided wave method, the grout length of the bolt may be measured. Beard and his co-workers did not perform tests in the field. In addition, the detection of discontinuities in the grout may be hampered by the presence of unwanted echoes emanating from geological discontinuities in the rock mass (Beard and Lowe 2003).

Previous Researches in Dalhousie University

The Geomechanics and Mining Innovations (GMI) research group led by Professor D.H. Zou in Mineral Resource Engineering at Dalhousie University is actively pursuing research in recent years in this area.

Experiments were conducted by Madenga (2004) to examine the characteristics of ultrasonic guided waves in grouted rock bolts. Effects of the curing time of grout and wave frequency on the ultrasonic wave velocity in grouted rock bolts were studied and satisfactory results were achieved.

The equipment set-up used on the experiments conducted by Madenga (2004) is shown in Figure 2-18. A transmitter was used to launch ultrasonic wave pulses into one end of the rock bolt sample. A receiving transducer was used to receive waveforms arriving at the other end of the test sample.

Based on the results from experiments, group velocity in the free bolt was analyzed and effects of frequency on wave velocity in grouted rock bolts were researched by Madenga (2004). Observations on obtained waveforms showed that, with input signal frequencies lower than 100 kHz, clearer waveforms in both free bolts and grouted bolts can be achieved. This result, together with the high sensitivity of low frequencies to the material properties surrounding the rock bolt rebar, suggested that signals with frequencies lower than 100 kHz should be used on ultrasonic methods to test the grout quality in rock bolts (Madenga 2004).

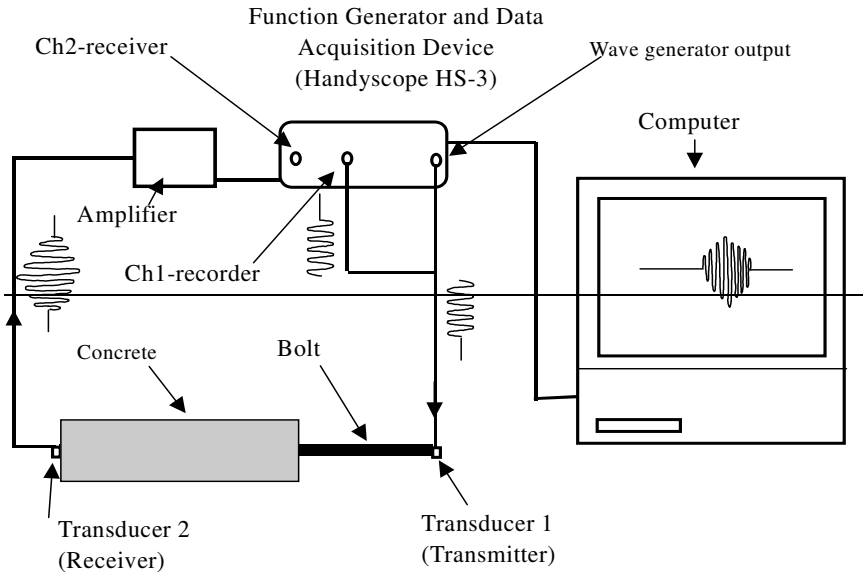

Figure 2-18 Transmission-through set-up used in experiments

Zhang et al. (2006), using LS-DYNA (Livermore Software Technology 2001) simulated the ultrasonic guided wave propagating in rock bolts. Cylindrical models were created for free and grouted bolts. Dynamic input signals with controlled frequencies were used for excitation. The effects of the mesh density on the accuracy of the simulation and the effects of the wave frequency on the wave velocity and attenuation in grouted bolts were analyzed. The results showed that the element size in the radial and axial direction has significant effects on the accuracy of ultrasonic guided wave simulation.

The most important achievement of Zhang's work is the quantification of the effects of the element size on the accuracy in the simulation on ultrasonic guided waves in grouted rock bolts, which can be used as criteria when approaching the finite element modeling for ultrasonic guided waves in grouted rock bolts. The suggested (Zhang et al 2006) element sizes used in simulating the behaviour of ultrasonic guided wave in grouted rock bolts are summarized in Table 2-1.

Table 2-1 Suggested element sizes used in simulation (Zhang 2006)

	50kHz		75kHz		100kHz	
	Radial (mm)	Axial (mm)	Radial (mm)	Axial (mm)	Radial (mm)	Axial (mm)
Steel bolt (Φ20mm)	≤5	≤5	≤3	≤3	≤1.3	≤2
Concrete	≤3.5	≤3.5	≤2.1	≤2.1	≤1	≤1.5

In the simulation study completed by Zhang (2006), a series of numerical models were created to simulate laboratory tests. The properties of those numerical models were adjusted until waveforms obtained from numerical models were similar as those obtained from laboratory tests. In this study, the same rebar and cement are used to make laboratory test samples. As the laboratory tests are to verify the numerical results, the numerical input properties used in this study is the same as Zhang (2006).

Recent research in rock bolt tests using guided ultrasonic waves has made significant progresses and there have been a number of new findings. The group wave velocity of the ultrasonic guided wave was found to be dependent on the material properties and the wave frequency (Madenga et al 2006, Zhang et al 2006 and Zou et al 2007).

The wave attenuation is another important parameter and has been extensively studied. It is known that the attenuation in a rock bolt is inversely proportional to the travel distance and is directly related to the amplitude ratio (O'connell and Budiansky 1974, Tavakoli et al 1992, Klimentos et al 1990 and Cui and Zou 2006) in the following format:

$$\ln \frac{A_b}{A_a} = \ln(R) = -\alpha L \qquad [2\text{-}1]$$

where A_a and A_b are the amplitudes at locations *a* and *b* respectively, R is the amplitude ratio, α is the attenuation coefficient and *L* is the distance from locations *a* to *b*.

Researches completed by Zhang et al (2006), Cui and Zou (2006) and Zou et al (2007) have led to the understanding of the effects of frequency and grout length on wave attenuation.

A wave would travel back by reflection along a rock bolt once it has reached the end of the bolt. The amplitudes of two consecutive waveforms recorded at the same location of a bolt are used to calculate the amplitude ratio. Cui and Zou (2006) indicated that the attenuation in a short (less than 2 m) free bolt is negligible. The boundary effect on the attenuation at the reflection point is significant in a grout bolt. Equation [2-1] is thus modified for attenuation calculation along the axis of a rock bolt by introducing a boundary correction factor, K_b, as follows:

$$-\alpha L = \ln(R) - \ln(K_b) = \ln(R / K_b) \qquad [2\text{-}2]$$

Zou et al (2007) observed a fixed energy loss at the contact interface between the transducers and bolts as wave reflecting. Therefore, the sensor recorded amplitude ratio during a test is typically lower than the attenuation amplitude ratio (R) in Equation [2-2]. This part of the energy loss is constant for a specific test set-up and is accounted by a fixed energy loss factor, K_f. The formula of the total attenuation in the whole bolt (grout and free part) is then modified as:

$$-\alpha L = \ln(RK_f / K_b) \qquad [2\text{-}3]$$

Theoretically, with the measured amplitude ratio, $R_m = RK_f$, the value of attenuation coefficient, α and correction factors, K_b and K_f, the grout length of the rock bolts can be calculated using Equation [2-3].

Zhang et al (2009) studied wave propagation characteristics in a grouted rock bolt using numerical and experimental method. It is concluded that the ultrasonic guided wave group velocity and attenuation are frequency dependent. There is an optimum excitation

signal with which the ultrasonic guided wave has longest propagating distance for the experimental grouted bolt samples.

Other recent achievements of the ultrasonic guided wave method

Wang et al (2009) reported a study for the propagating properties of ultrasonic guided wave in the anchorage structure of rock bolts using numerical and experimental methods. The ultrasonic guided wave was used to study rock bolts with different grouting strength and bonding lengths.

Lee et al (2007) studied the group velocity in a rock bolts using numerical and experimental methods. It has been shown that the ultrasonic guided wave method may be a valuable technique to evaluate the rock bolt integrity.

Han et al (2009) installed full scale rock bolts in a concrete and in a rock mass and then performed ultrasonic guided wave tests to verify their numerical solution. The input transmitter was installed on the exposed end of the bolt and the output transducer was on the other end embedded in the concrete or rock mass. The results of their tests showed that the waveforms obtained in the field were analyzable and could be used for testing rock bolt grouting defects. This is an important step to proof that the ultrasonic guided wave method may be used for rock bolts installed in a rock mass. However, the equipment set-up used in their research is not practical due to one end of the rock bolt has to be installed in the rock mass in field. Embedding output transducer in the rock mass is suitable for research purposes, but not practical for routine field tests.

2.8 DISCUSSIONS ON PREVIOUS RESEARCHES

Based on above discussions, it can be concluded that the ultrasonic guided wave method is promising to be a valuable technique to evaluate the grout quality of rock bolts. However, previous researches were performed with an equipment set-up that the input transducer was installed at one end of rock bolt and the receiving signal was obtained by

another transducer at the other end. This equipment set-up is suitable to study the rock bolts in laboratory, but not practical in field tests due to the fact that most of rock bolts have to be installed into the ground in the field. A practical testing method is required before the ultrasonic guided wave method can be used. The first step to apply the ultrasonic guided wave method to field practice is to find a suitable installation location for the installation of the receiving transducer in the field environment.

Previous researches have mainly focused on the feasibility of the ultrasonic guided wave method used for rock bolt tests. However, one of the purposes of the tests is to identify defects in grouted rock bolts. The understanding of the ultrasonic guided wave behaviours in rock bolts with defects is necessary before this method can be used in field practice.

CHAPTER 3 THEORETICAL BACKGROUND

Ultrasonic guided waves propagate differently than the longitudinal and shear bulk waves. The ultrasonic guided wave velocity depends not only on the material properties, but also on the thickness of the material and the wave frequency (Rose 1999). Even in an infinite length steel rod (free bolt), the group velocity of the wave is a function of the diameter of bolt and the frequency.

Attenuation is another important character of waves, which is a general term that refers to the reduction of the strength of a wave signal. Attenuation occurs with any type of signals. It is a natural consequence of signal propagating over a distance because of the wave energy loss.

The understanding of the theoretical behaviour of ultrasonic guided waves is essential to the study of ultrasonic guided wave propagating in rock bolts. In this chapter, the fundamentals of ultrasonic guided waves are summarized.

3.1 GROUP VELOCITY

When ultrasonic waves propagate in a rock bolt, the incident wave interacts with the cylindrical surface bounding the rod and keeps getting reflected and bouncing back and forth within this surface (Achenbach 1973) as shown in Figure 3-1. As a result, various constructive interference patterns can be derived from the interaction among the reflected waves. The wave propagating velocity depends on the frequency, the type of wave (longitudinal or shear), and the diameter of the rod.

The propagation of a wave packet is illustrated graphically in Figure 3-2. Such a wave packet is made up of a band of superimposed frequency components, and the group velocity is the speed at which the 'envelope' of the packet moves along. In the kinematic

argument one can infer that the rate of transfer of energy is identical with the group velocity (Achenbach 1973).

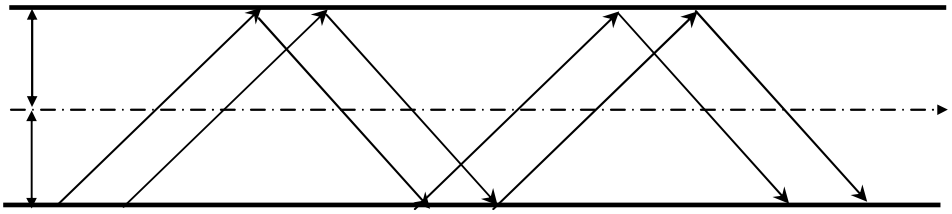

Figure 3-1 Two-dimensional illustration of incident and reflected waves in a cylindrical structure giving rise to ultrasonic guided waves (Modified from Madenga 2004)

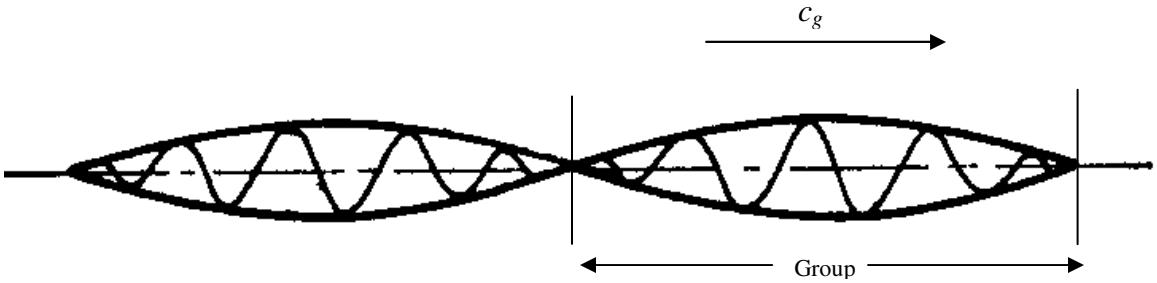

Figure 3-2 Wave packet as group (Modified from Achenbach 1973)

Although the behaviour of ultrasonic guided waves in a rod (free rock bolt) is complicated, the analytical solution without the consideration of the attenuation is available. It ends up with solutions for velocity versus frequency. These values could be plotted on engineering dispersion curves (Rose 1999). However, for grouted rock bolt, no analytical solution is available.

Cui (2005) concluded that the group velocity in the free bolt is frequency dependent and not affected by the length of the free bolt. When wave propagates in a grouted rock bolt, the group velocity of the wave is uniform along the grout portion.

3.2 ATTENUATION

Attenuation is a general term that refers to the reduction of the strength of a signal. Attenuation occurs for any type of signals. It is a natural consequence of signal transmission over a distance because of the wave energy loss.

Many researchers are involved in the study of the attenuation in solid medium (Tavakoli and Evans 1992, Klimentos and McCann 1990, O'Connell and Budiansky 1974, Boadu 1994 and Berkhout 1987). The wave attenuation is measured by an attenuation coefficient. For a wave in an infinite length rod, the amplitude decay can be express by Equation [3-1].

$$\sum_{i=1}^{n} \alpha_i L_i = -\sum_{i=1}^{n} \ln(R_i) = -\ln\left(\prod_{i=1}^{n} R_i\right) \qquad [3\text{-}1]$$

where: α_i is the attenuation coefficient of the *i*th component,

L_i is the travel distance affected by the *i*th factor,

R_i is the amplitude ratio after attenuation of the *i*th component

Some studies were conducted to research the ultrasonic guided wave attenuation in grouted rock bolts. The attenuation is a more complicated and more sensitive parameter than the group velocity. It is known that the ultrasonic guided wave attenuation is affected by parameters of the grout material properties, grout lengths, grout quality, and grout defects.

In general, the observed wave attenuation may have several components, some of which are frequency independent and some are frequency dependent. The frequency dependent components are characterized by a phenomenon that the high frequency has high rate of attenuation (Yilmaz 1987).

The total attenuation is the sum of the contributions of all influencing factors (Gibowicz and Kidjko 1994) and this relationship applies to both bulk waves and ultrasonic guided waves.

If L_i is the same for all factors, Equation [3-1] can be rewritten as:

$$\sum_{i=1}^{n} \alpha_i L = \alpha_t L \qquad [3\text{-}2]$$

or $$\alpha_t = \sum_{i=1}^{n} \alpha_i$$

where α_t is the total attenuation coefficient.

The following is a summary of findings on ultrasonic guided wave attenuation in grouted rock bolts:

- The dissipative attenuation is an energy loss due to the non-elastic resistance of the medium. It increases with the wave travel distance and is more profound over a long distance. This component of attenuation can be ignored in practice for ultrasonic guided waves traveling in rock bolts due to the relatively short wave travel distance.

- The dispersive attenuation is an energy loss due to deformation of waveforms during wave propagation, a characteristic that is very serious in ultrasonic guided

waves comparing to bulk waves. The phenomenon of the wave deformation is called dispersion.

- The spreading attenuation is an energy loss occurs at the interface between the bolt and the grout materials. As ultrasonic guided wave reaches the interface, not all of the wave energy can be reflected at the interface. Part of the energy passes through the interface and is transmitted into the grout material, a phenomenon called energy leakage.

It can be assumed that the attenuation in grouted rock bolt consists of two major components: the dispersive and the spreading attenuation, both of which are frequency dependent (Zhang 2006). The total attenuation in grouted rock bolt should thus be the sum of these two components.

Theoretically, when a wave reaches an interface adjoining a medium, which does not transmit mechanical waves (e.g., vacuum or air), no refraction occurs and all energy is reflected back (Achenbach, 1973). In rock bolt test, the bolt sample must be connected with transmitter and transducer to input and receive signals, creating contact surfaces. It is at these interfaces that some energy is inevitably refracted causing energy loss. This type of energy loss is expected to be a constant and has a fixed amount for a specific type of equipment set-up. As a result, the recorded amplitude decay and energy loss during rock bolt tests will be greater than what is actually caused by the dispersive and spreading attenuation as illustrated in Equation [2-2]. Zou et al (2007) considered that this part of energy loss is a constant for a specific test set-up and may be accounted by a fixed energy loss factor, K_f, as shown in Equation [2-3]

CHAPTER 4 RESEARCH METHODOLOGIES

It can be concluded that the most promising non-destructive rock bolt test method is the guided wave method (Beard et al 2003 and Madenga 2004). The attenuation and group velocity along the bolt have been studied (Madenga et al 2006, Zhang 2006, Cui and Zou 2006 and Zou et al 2007) by numerical modeling and laboratory experiments. Han et al (2009) verified that analyzable guided wave signals can be obtained for rock bolts installed in a rock mass.

Previous researches were completed with an equipment set-up as shown in Figure 1-1, in which the input transducer was installed at the exposed end of the rock bolt and the receiving signal was obtained by another transducer installed at the other end. This equipment set-up is not practical for field tests.

A rock bolt installed in the field for ground support has only one short exposed end on the rock surface. This condition has posed challenges in field instrumentation. The input transducer is typically installed at the exposed end of bolt, but the receiving transducer is usually difficult to be installed at a suitable location for receiving valid data. For a rock bolt in the field, both input and output transducers have to be installed at the input end of the rock bolt. The first task of this thesis is to find a practical method for field testing.

Theoretically, the grout near the rebar will vibrate with the rebar and the wave behaviours along the rebar should relate to this vibration. Cui (2005) stated that the receiving transducer may be installed on the grout surface at the input end as shown in Figure 1-2 to test this vibration. However, no further details of this method were discussed. It is reasonably believed that the test results obtained at various locations on the grout surface should be different. In this thesis, the effect of the receiving transducer location is studied to make this method possible.

One of the purposes of the rock bolt test is to identify grout defects (missing grout portion, insufficient rebar length, voids in grout and etc.). The guided wave behaviours in rock bolts with grout defects have to be studied before this method can be used in field.

Cui and Zou (2006) reported a successful numerical simulation. The accuracy of that simulation has been verified by comparing the results of simulation and laboratory tests. The study reported in this thesis is a numerical study based on that simulation model.

To achieve the objectives of this research, which have been discussed in Section 1.1, the following topics are studied in this thesis:

- effects of transducer installation locations on the attenuation and wave travel time in fully grouted rock bolt samples as shown in Figure 1-2;

- guided wave's behaviours in rock bolts with a missing grout portion at the ground end;

- guided wave's behaviours in rock bolts with an insufficient rebar length at the ground end; and

- guided wave's behaviours in rock bolts with a void in grout. To simplify this problem, the void surface is assumed to be perpendicular to the rebar.

In this research, numerical modeling is used to study the effects of the measurement location of the receiving transducer on the attenuation and group velocity for fully grouted rock bolt samples. Numerical modeling is also performed for rock bolts samples with typical defects in grout (a missing grout portion, an insufficient rebar length and a void in grout). Laboratory tests are conducted to verify the numerical modeling results.

4.1 NUMERICAL MODELING

Fully grouted rock bolts as shown in Figure 1-2 are generated in this study. The effects of the receiving transducer location are studied by comparing the wave signals obtained from various locations of Point C in Figure 1-2. Grouted rock bolt models with some typical defects (a missing grout portion, an insufficient rebar length and a void in grout) are also created in this study. The effects of grout defects are evaluated by comparing the wave signals obtained from rock bolts with defects and signals obtained from fully grouted rock bolts,

Finite element analysis platform, LS-DYNA (Livermore Software Technology, 2001), is used to perform this study. The numerical study is a transient dynamic analysis to determine the dynamic response of the rock bolt under a time-varying (transient) pressure load. All models in this study consist of a steel bar embedded into a cylindrical concrete block.

4.1.1 Material Parameters and Element Sizes

Using LS-DYNA, Zhang (2006) and Cui and Zou (2006) performed successful numerical simulation studies on rock bolt tests using ultrasonic guided waves. The numerical simulation results were verified using experimental tests. Material properties and element sizes used in those studies are shown in Table 4-1 and Table 4-2, respectively. The same parameters and element sizes are used on numerical models in this thesis.

Table 4-1 Material properties used in numerical modeling

	Density (g/cm3)	Young's Modulus (GPa)	Poisson's ratio
Rock bolt	7.84	210	0.3
Concrete	2.405	38	0.25

Table 4-2 Element size in model mesh

	Radial (mm)	Axial (mm)
Steel bolt (diameter 20mm)	≤3.5	≤.35
Concrete	≤3.5	≤3.5

4.1.2 Numerical Model Input Signal

The input signals in experiments are generally electrical signal created by a function generator (Figure 2-18) or a similar device. This electrical signal is transformed to mechanical signal by the transmitter installed at the exposed end of samples. However, the waveform of the input electrical signal is recorded before it transformed to a mechanical signal. Therefore, the recorded signal is not the same as that of the excited mechanical vibration of the input transducer, although the initial time of the recorded electrical signal and the mechanical vibration occur at the same time. The recorded input electrical waveform in experiments cannot directly be used to numerically simulate the input signal at the input end of the sample.

For a free bolt with a short length, if the input and output transducers are installed at each end of the rock bolts as shown in Figure 2-18, the received waveform at receiver (Transducer 2) in experiments seems similar to the mechanical vibration that is transferred from Transducer 1 (Zhang et al 2006). Theoretically this received waveform at receiver (Transducer 2) is the same as that at the input location (Transducer 1) of the sample with some dispersion, which is affected by the length of the free bolt. For a long free bolt, the dispersion is serious, while for a too short free bolt the received waveform is affected by the reflected signals (echo).

It was found (Cui 2005) that the best input signal as shown in Figure 4-1 could be derived by testing a 1000 mm long free bolt using the transmission-through equipment set-up. Using this waveform as the numerical input signal, the simulated waveform is the most similar to that of experimental ones. It should be noted that, using the transmission-

through set-up, the obtained mechanical signal at receiver (Transducer 2) is recorded as electrical signals in experiments. Zhang (2006) suggested that this recorded electrical signal could be applied as pressure (keep the numerical data but change the unit from Voltage to MPa) in numerical modeling to simulate the mechanical vibration generated in experiments.

In this study, the same method is used to obtain the numerical input signal, which is applied on the surface of the input end (Point A of Figure 1-2) in all models of this study.

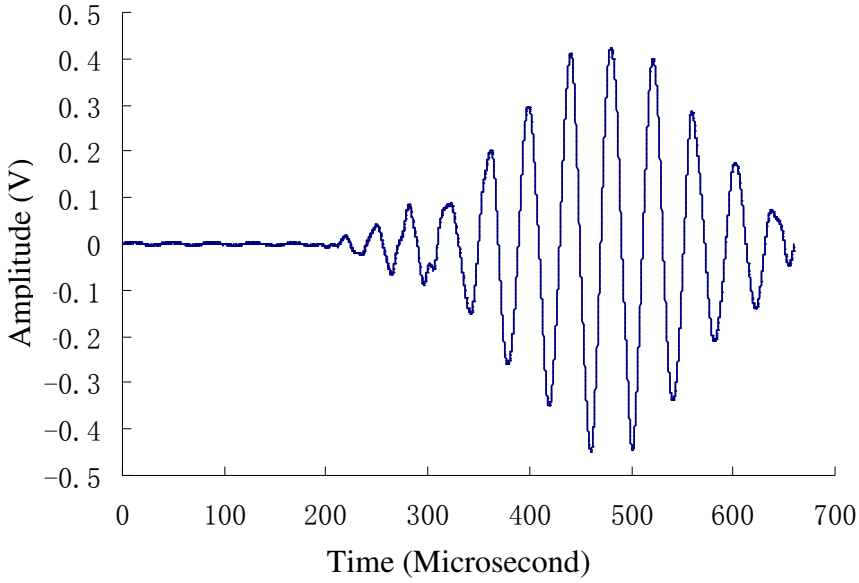

Figure 4-1 Input signal used for numerical studies

4.1.3 Model Boundary Conditions and Symmetry Conditions

To save computing time, the symmetry condition of models is considered and only one quarter of samples is created to study the following topics:

- effects of transducer installation locations on the attenuation and wave travel time in fully grouted rock bolt samples (Chapter 5);

- guided wave behaviours in rock bolts with a missing grout at the ground end (Chapter 6); and

- guided wave behaviours in rock bolts with an insufficient rebar length at the ground end (Chapter 7).

The boundary conditions of these models are shown in Figure 4-2. Because of symmetric geometry and boundary conditions of these models, the results from these one quarter models are expected to be the same as those from full models.

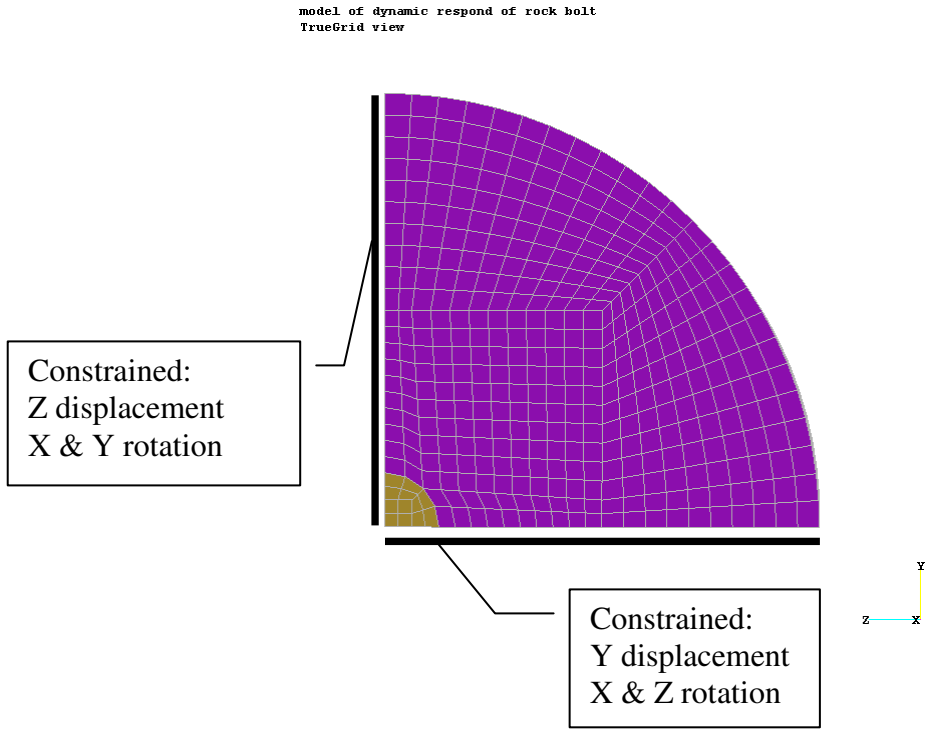

Figure 4-2 Model boundary conditions (quarter size)

The one quarter model however cannot be used to study the rock bolts with a void in the grout. To simplify the models used for this problem, the void surface is assumed to be smooth and perpendicular to the rebar as shown in Figure 4-3. A symmetry condition of the sample may be considered based on an axisymmetric axis shown in Figure 4-3 and a half of the sample is used to study this topic as shown in Figure 4-4.

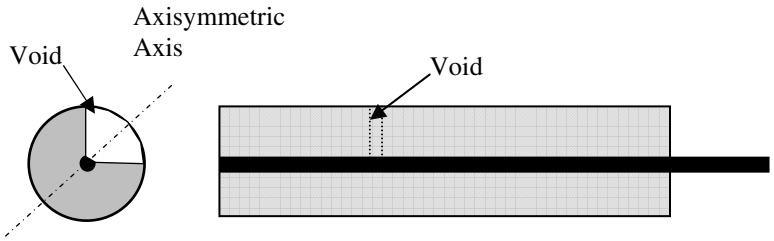

Figure 4-3 Grouted rock bolts with a void

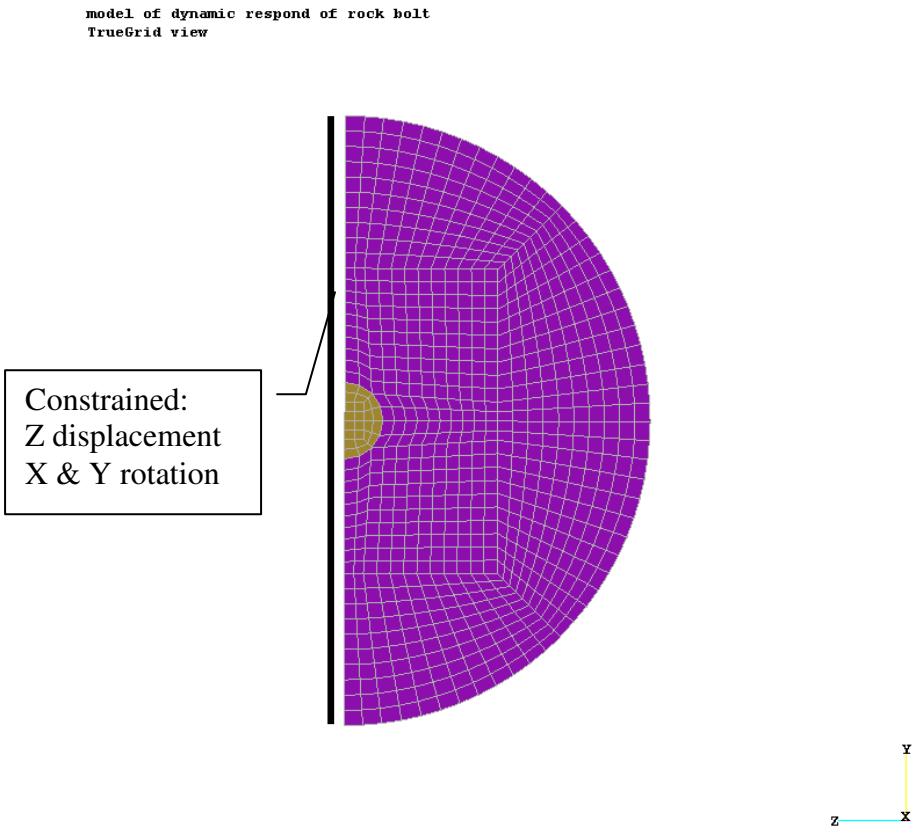

Figure 4-4 Model boundary conditions (half size)

Cement is used as grout material in this study. Zou et al. (2010) commented that "resin grout forms better anchorage and increases the holding capacity, and its behavior is expected to follow similar trend as the cement grout". Therefore, resin grout rock bolts are expected to have similar behavious as cement grout rock bolts.

The dimension of the rock mass in the field could be considered as infinite compared to the diameter (160 mm) of the numerical samples used in this study. Beard and Lowe (2003) and Han et al. (2009) performed tests for resin grouted rock bolts installed in laboratory and in field rock mass, and valid results were obtained. Others (Beard and Lowe, 2003; Madenga, 2004 and Zou et al., 2010) performed research on bolts with grout diameters ranged from 50 mm to infinite (rock mass) and valid results were achieved, although all those studies were conducted using the previous transmission-through equipment set-up. With the proposed transmission-echo-off-path equipment set-up used in this study, rock bolts installed in the field are expected to have similar behaviour as numerical models and laboratory tests performed in this study. However the rock mass properties may affect the wave behaviours, the results obtained in this study may not be directly used for field tests without field verification.

4.2 EXPERIMENTAL VERIFICATION METHODS

All results obtained from numerical studies in this thesis are verified by experiments. The equipment and input signals used for the experimental verification are summarized as follows.

4.2.1 Laboratory Equipment

The laboratorial study is completed with instruments similar to that used by Madenga (2004). The system includes a data acquisition device with a wave generator, an amplifier, transducers and a computer.

The equipment set-up is illustrated in Figure 4-5. The Handyscope HS-3 unit has the capability of generating ultrasonic signals with varying frequency and receiving and digitizing waveforms. The sinusoidal ultrasonic input signal is employed to excite the transmitter at the free end of the bolt sample. The received signal at the receiving location is amplified before being displayed and recorded. The computer is used to record and display signals. The following is a description of the instrument:

The Handyscope HS-3 is a computer controlled USB measuring instrument that consists of six measuring instruments: a USB Multimeter, a USB Oscilloscope, a USB Spectrum analyzer, a USB Data logger/Transient recorder, a Protocol analyzer and an Arbitrary Waveform Generator (TiePie engineering 2012).

The experiments were conducted by exciting the input transducer (R3) with input signals at different frequencies into the input end of bolt samples. The arrived signal at the receiving location was picked up by a transducer (R3) and recorded digitally by associated software.

Cui and Zou (2006) suggested that transducers used for testing rock bolts should be selected with low frequency (<50 kHz). In this study, clear and analyzable signals could only be received for tests with input signals having a narrow range of frequencies. It was found in this study that the suitable frequency was affected by sample diameters (160 mm), and transducer used in laboratory tests was selected based on trial tests on rock bolt samples.

To enhance the received waveforms, sometimes it is necessary to amplify the received signal before it is displaced. For this purpose, a wide bandwidth (10 kHz-5 MHz) AE5A Amplifier with a variable gain (0-41dB) and a fixed internal gain of 40dB was employed to amplify the signals received from the test samples.

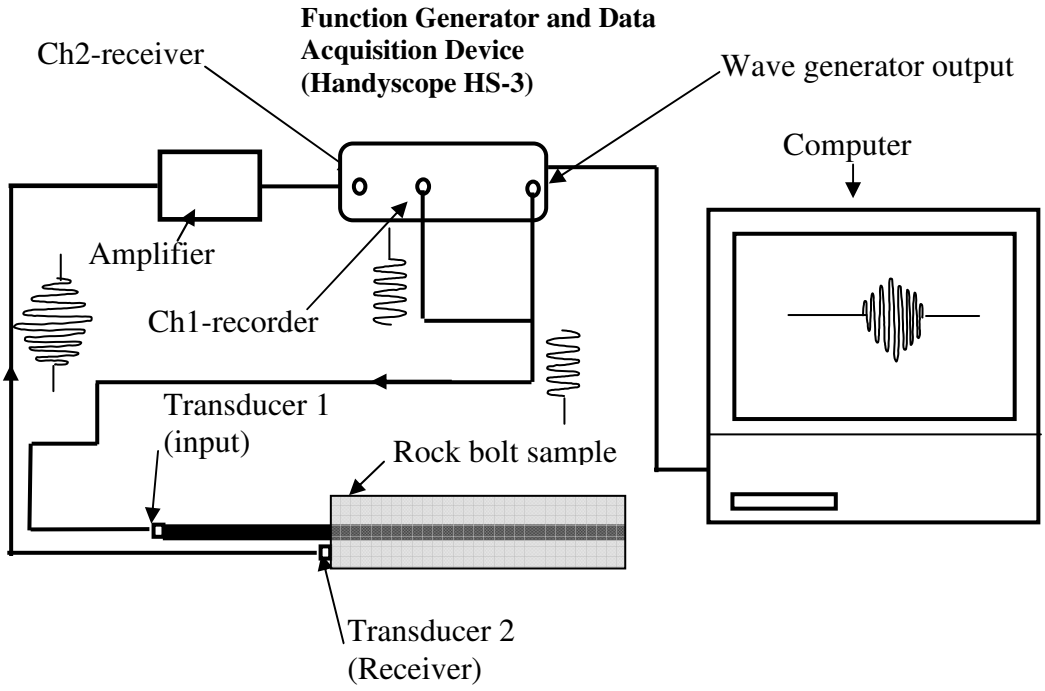

Figure 4-5 Equipment set-up for rock bolt tests

4.2.2 Experimental Input Signal

If the received waveforms include a wide range of frequency components, it would be difficult to interpret the data. The received waveform will be too weak to analyze and will be difficult to find the location where the maximum energy is included in the waveform.

In practice, it is possible to enforce the majority energy in a narrow range of frequency by inputting the signal with a specific frequency. In this research, sinusoidal signals are used to excite the ultrasonic wave. Madenga (2004) found that the more the number of cycles of the input signal is used; the stronger the output signal can be received. However, if the input signal continues too long, it is difficult to identify the boundary of wave packets of the input group and the echo.

Based on results of previous researches (Madenga 2004, Zou et al 2007, Zou et al 2010 and Zou and Cui 2011), rock bolt samples are excited by sinusoidal signals with five cycles. For input signals in this range, the majority energy of the received waveform concentrated in a narrow range of frequency centered at the frequency of the input signals, and the input group and echo are easy to identify (Cui 2005). A typical experimental input signal is shown in Figure 4-6.

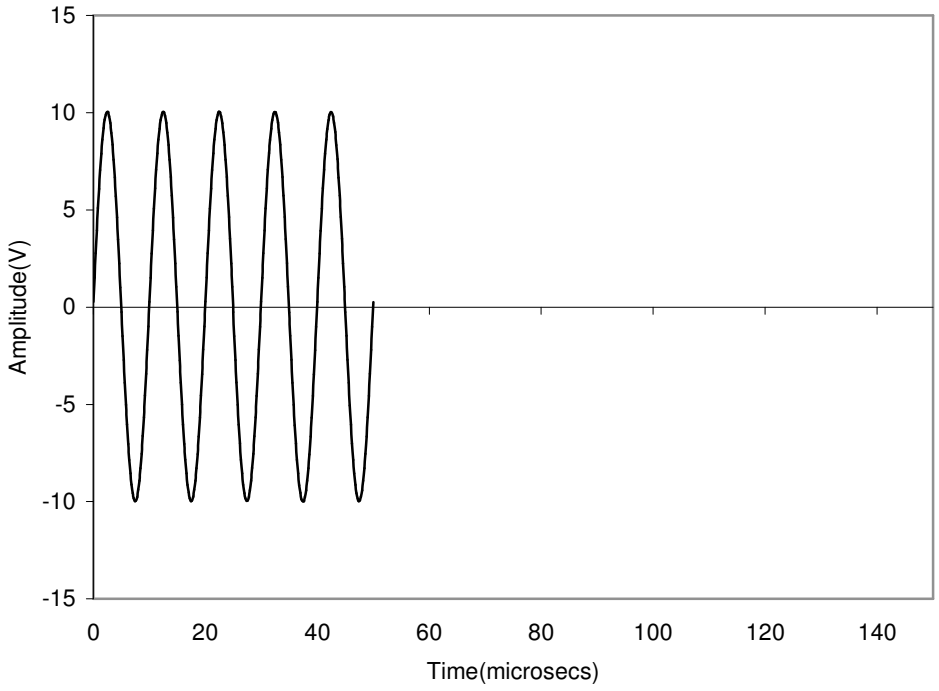

Figure 4-6 Typical Input Signal

4.3 DATA ANALYSIS METHODS

The recorded waveforms in experiments are usually difficult to be analyzed because of the dispersion of ultrasonic guided waves. In addition, ultrasonic wave test is affected by the noises around the testing environment. It is necessary to develop proper data analysis methods. The methods for calculating wave travel time and amplitude ratio used in this research are illustrated in this section. It should be noted that the purpose of the experiments in this study is to verify the numerical results, by comparing the

experimental results with the numerical ones. Therefore, the following data analysis methods are also applied to the data obtained from numerical modeling for consistency.

4.3.1 Wave Filter

A typical received waveform is shown in Figure 4-7, where the location of the input group and echo are also shown.

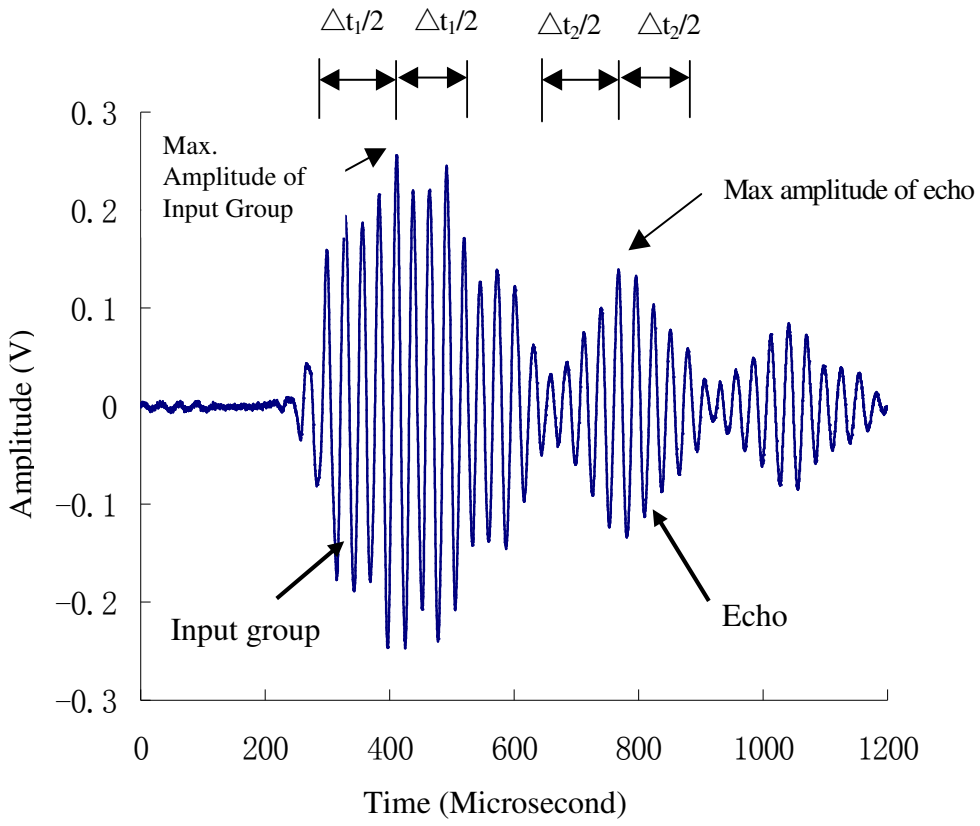

Figure 4-7 Typical received waveform

The recorded raw waveforms have to be filtered first by a band filter to narrow the frequency band around each testing frequency (Madenga et al 2006). This is achieved using a filtering program written in MATLAB.

All raw waveforms from experiments and numerical modeling are filtered using this program. For each waveform, the filter is centered at the input frequency with a band of ±5 kHz as suggested by Madenga et al (2006). The input file of the Filter is presented in Appendix A.

4.3.2 Wave Travel Time along the Bolt

The ultrasonic guided wave group velocity is typically based on the ratio between the wave travel distance and wave travel time. In guided wave researches completed before, the travel time was typically determined by the time gap between the input group and the echo, which correspond the distance of wave traveling from the transducer installation location to the first reflection point and reflecting back from the first reflection point to the transducer installation location. As the wave travel distance in experimental samples is known, the group velocity can be calculated by the wave travel distance divided by the wave travel time between the input group and the echo.

In this study, the recorded waveform is filtered first as discussed before. The time interval is determined by the time gap between the maximum amplitudes of input group and the echo, which are recorded at the transducer installation location. It should be noted that identification of the maximum amplitude of the input group and echo is often complicated due to the dispersion character of ultrasonic guided waves. The wave travel time cannot always provide accurate estimation of the grout length of the rock bolt. Other factors, such as wave attenuation, have to be considered to obtain more accurate results.

4.3.3 Amplitude Ratio Estimation

Attenuation is known to be inversely proportional to the amplitude ratio, the higher the attenuation, the more the energy loss and the lower the amplitude ratio. In this thesis, the attenuation is estimated by investigating the amplitude ratio between the reflected echo and input group picked up by the receiving transducer as Equation [4-1]. Because they

received at the same location using the same transducer, the amplitude ratio obtained is considered to be the suitable measurement for wave travel attenuation.

$$R = \frac{A_e}{A_f} \qquad [4\text{-}1]$$

where, A_f is the amplitude of input group, and A_e is the amplitude of echo

Theoretically, the location of the maximum amplitude should be at the centre of the input group and echo pockets, and may be used for the calculation of the Equation [4-1]. However, due to the dispersion of the wave and the existence of the noises, the maximum amplitude obtained from experiments may be not at the center of the pockets as shown in Figure 4-7. Errors may exist if the waveforms obtained from tests are directly used for the calculation of amplitude ratio. Cui (2005) suggested a method by using the average amplitude over a time interval to calculate the amplitude, as shown below:

$$A_i = \sqrt{\frac{\int_{t_{i1}}^{t_{i2}} k v_i^2(t)dt}{\frac{1}{2}k(t_{i2}-t_{i1})}} = \sqrt{\frac{2}{(t_{i2}-t_{i1})}\int_{t_{i1}}^{t_{i2}} v_i^2(t)dt}, \quad i = 1,2 \qquad [4\text{-}2]$$

where: A_i is A_f or A_e in Equation [4-1]

$\Delta t_i = t_{i2} - t_{i1}$ is the time interval contented with a wave pocket.

$v_i(t)$ is the recorded wave amplitude.

$i = 1$ is the input group, and $i = 2$ is the echo waveform.

k is a constant.

Parameters Δt_1 and Δt_2 are illustrated in Figure 4-7.

Because this method considers the average amplitude in the same length of time intervals for both the input group and the echo, the effects of errors and noises on the maximum amplitude can be minimized. Because the purpose of the experiments in this thesis is to verify the numerical results, the waveforms obtained from numerical data are also calculated using Equation [4-2] for consistency.

It is found (Cui 2005) that if the time interval is small (e.g. $\leq 25\%$ of the whole waveform), the calculated amplitude ratio might not represent accurately the ratio derived from the whole waveforms, resulting an error. The error decreases as the time interval increases. When the time interval is more than 25% of the whole waveform, the error is negligible.

In this study, $\Delta t_1 = \Delta t_2 = 100$ microseconds are used in calculation of the average amplitude for both the free and the grouted rock bolts as suggested by Cui (2005), which is much greater than 25 percent of all waveforms.

The test instrument can display and record electrical signals. The unit of the input and received amplitude in experiments is Voltage. However, the generated waveforms in finite element simulations are acceleration, which can be integrated as displacements. Thus, the simulated amplitude cannot be directly compared with the experimental ones. The method to verify the accuracy of the simulation is comparing the simulated waveforms and amplitude ratio with the experimental ones.

CHAPTER 5 EFFECTS OF THE RECEIVING TRANSDUCER LOCATION

As discussed in Chapter 4, previous experiments and tests were conducted with a transmission-through set-up as illustrated in Figure 1-1. This equipment set-up is not practical in the field due to the fact that a rock bolt has only one short exposed end on the rock surface.

Efforts were made in our research to search for various solutions to field application. A single transducer with dual elements was first considered. However there was only one such transducer available on the market and it was designed for frequencies above 1000 kHz, far beyond the frequency range used in this research.

Consideration was then given to modifying the data acquisition device. A customized system was designed to send and receive signals using a single transducer with delayed receiving. The system was tested and a new problem was encountered. The transducer after transmitting the input signal continued vibrating when the reflected signal has returned.

Among other ideas to solve the problem, one option is to use two transducers at the same end of the bolt, which has shown high potential. The initial idea (Cui 2005) was to locate the receiving transducer near the input transmitter on the bolt or on a mechanical attachment of the bolt. That seemed to introduce more noises due to multiple interfaces and some difficulties for field application as well. Further thoughts led to the current idea that the receiving transducer was directly located on the grout surface at point C, a transmission-echo-off-path set-up, as shown in Figure 1-2. Experiments and numerical modeling were conducted with this method and the results were satisfactory.

With the transmission-echo-off-path set-up shown in Figure 1-2, the next question is how close the location C should be to the rebar (i.e., point B in Figure 1-2) to get meaningful

data. It is expected that the distance between Points B and C will affect the measurement results.

In this chapter, the effects of the receiver location on the wave attenuation and the time interval between the input group and echo are evaluated using numerical models. The numerical results are verified by experimental tests for rock bolt samples.

5.1 MODEL AND INPUT PARAMETERS

The numerical model geometries are specified in Table 5-1 (Samples FG750 and FG1000). The sample IDs of FG stands for fully grouted rock bolts as shown in Figure 1-2. The input parameters and element sizes of these models are the same as those used in Chapter 4 shown in Table 4-1 and Table 4-2. The LS-DYNA input file for modeling a typical fully grouted rock bolt (FG750) is provided in Appendix B.

To save computing time, the symmetry condition of the sample is considered and only one quarter of the sample is created. The boundary conditions of the model are shown in Figure 4-2. One typical finite element model is shown in Figure 5-1. For Sample FG750, a total of 3192 elasto-plastic elements are used to simulate the rock bolt, 112750 elastic elements to simulate the concrete cylinder, and 126557 nodes with 6 degrees to connect all the elements. For Sample FG1000, a total of 4188 elements are used to simulate the rock bolt, 150183 elements to simulate the concrete cylinder, and 168306 nodes with 6 degrees to connect all the elements.

It was found in our earlier research (Cui 2005) that when a receiver was installed on the grout surface, clear and analyzable signals could only be received for the input signals within a narrow range of frequencies, which depended on the sample physical properties and sample geometries. A trial and error method is used in numerical modeling and laboratory tests to search for the most suitable frequency range. It is found that clear

waveforms can be obtained using input signals within a frequency range from 28 kHz to 32 kHz. Therefore, the input wave frequency used in this study is limited to this range.

In numerical simulation, the input signals are applied as pressure at Point A shown in Figure 1-2. A typical input signal used in this study is shown in Figure 4-1. Typical waveforms obtained on Sample FG750 are shown in Figure 5-2. The waveforms are obtained on the grout surface at Point C (Figure 1-2) with a lateral distance of 15.5 mm, 31.8 mm and 40.0 mm, respectively, measured from the rebar axis (Point B in Figure 1-2). As expected, the waveforms obtained at different locations are not the same, indicating a significant effect of the receiver installation location.

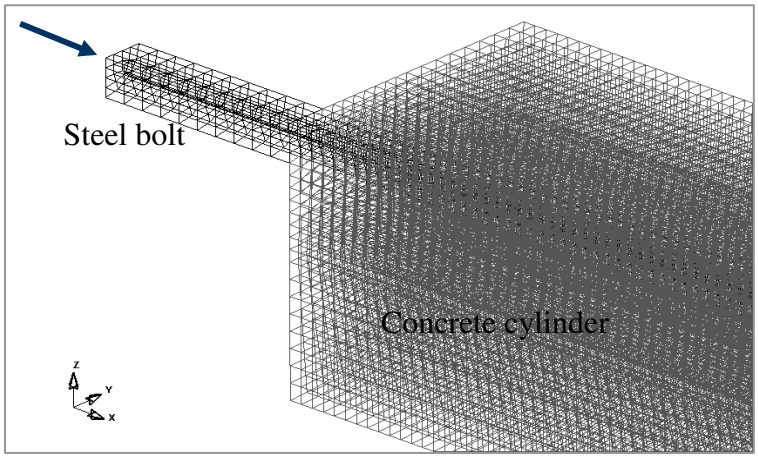

Figure 5-1 Typical fully grouted rock bolt model (quarter size)

Table 5-1 Chapter 5 model geometries

Sample ID	Free Length		Bolt diameter (mm)	Grouted Rebar length (mm)	Total Grout length (mm)	Total Rebar length (mm)	Diameter of concrete cylinder (mm)
	at input end (mm)	at ground end (mm)					
Sample FG750	50	0	20	750	750	800	160
Sample FG1000	50	0	20	1000	1000	1050	160
Sample LFG500	300	0	20	500	500	800	160

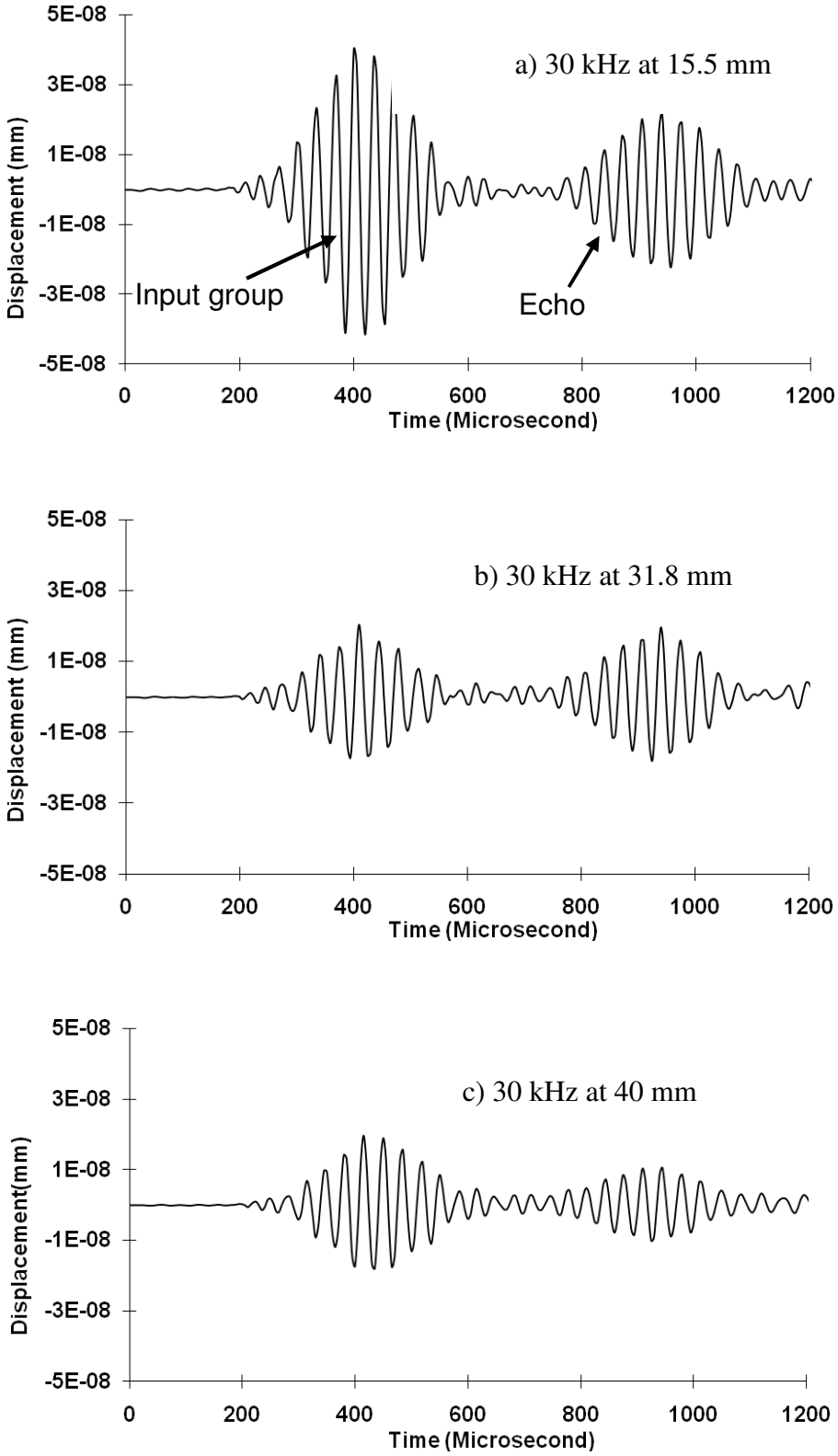

Figure 5-2 Typical waveforms - Sample FG750 at different receiving locations

The waveforms obtained at a lateral distance (between Points B and C) less than 15 mm are not clear due to the effects of the complicated boundary conditions at the interface between the grout and rebar. The echo at a lateral distance greater than 40 mm gradually becomes weak and unclear due to the boundary effects and attenuation. The limited size of the concrete model (80 mm in radius) may also affect the data. Therefore, only the data obtained at a receiver location (Point C in Figure 1-2) with a distance between 15 mm and 40 mm measured from the rebar axis (Point B in Figure 1-2) are analyzed.

It is observed in all models that the waveforms after the echo pocket are difficult to analyze. Therefore, only the input group and echo are analyzed.

5.2 ANALYSIS OF LATERAL TRAVEL TIME

Theoretically, if a wave travels along a line path and back from a reflecting point, the travel time can be determined by the time gap between the maximum amplitudes of the input group and the echo. All previous research results were based on wave travel time along the rebar of a rock bolt. However, in the proposed measurement method, the receiving transducer is installed at Point C (Figure 1-2) with a lateral distance from the shortest line path of the signal along the rebar (Point B in Figure 1-2). Point B is here used as a base point for comparison.

As the input signal travels from A to B, it continually travels to C and the ground end of the bolt simultaneously. After a time period, Δt, the wave has reached Point C and has also traveled some distance along the bolt. Therefore, the input signal recorded at C is expected to be Δt later than that at B. The lateral travel time Δt from B to C needs to be considered in calculating the wave travel time along the rebar when waveforms recorded at Point C are used for analyses.

In a fully grouted bolt, the wave velocity in the grouted steel bar is the same as that in the grout (Cui and Zou 2006, Madenga et al 2006, Zou et al 2007). Therefore the signals

reflected back from the ground end will travel at the same speed to Points B and C. It can be demonstrated that the travel time difference of the echo to B and C is negligible because the time of the waves arrived are very close to each other.

It is considered that the input group recorded at Point C is Δt later than at Point B, but the echo at Point C arrived at the same time as Point B. Therefore, if travel time is to be calculated based on the signals recorded at Point C, the measured travel time will be shorter by Δt than that measured at B. The lateral travel time Δt should be added to the recorded travel time.

Figure 5-3 shows the lateral travel time Δt for Sample FG750 based on time gaps between the maximum amplitudes of the input group at the central point (Point B) and at a location (Point C) on the grout surface. The location shown in Figure 5-3 is the lateral distance between Point C and Point B. The results indicate that the lateral travel time increases with the lateral distance and the variation due to wave frequency is minimal for frequency from 28 kHz to 32 kHz. Similar results are obtained for Sample FG1000.

After adjustment by Δt, the wave group velocities along the rebar calculated from waveforms obtained at Point C of Samples FG750 and FG1000 are in the range of 2730 m/s and 2850 m/s. These results are the same as those calculated using data obtained at point B for samples excited with input signal frequencies ranged between 28 kHz and 32 kHz. The results are comparable with previous experimental results reported by Madenga et al (2006).

Theoretically, wave travel time can be used to evaluate the fully grouted rebar length based on group velocity. However, as discussed by Cui and Zou (2006), the maximum amplitude of the input group and echo is not always at the central of a wave pocket. The grouted bolt length estimated based on wave travel time may not be accurate. Other factors, such as wave attenuation, needs to be considered as well.

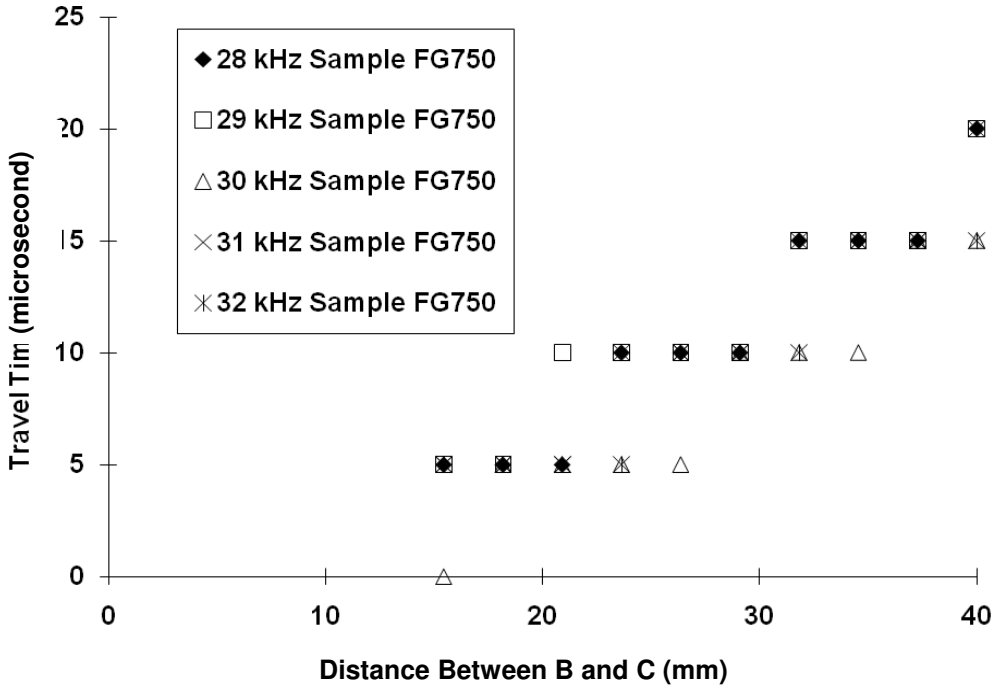

Figure 5-3 Lateral travel time Δt vs. lateral distance of receiving location

5.3 ANALYSIS OF WAVE ATTENUATION AT A LATERAL LOCATION

Wave attenuation is usually measured by a coefficient, α, as shown in Equation [2-1], which has an inverse logarithm relationship with the amplitude ratio. The amplitude ratio can be calculated using the waveforms recorded along the rebar of the bolt. As mentioned earlier, two consecutive waveforms (the input group and the echo) are used to calculate the amplitude ratio.

As shown in Figures 5-2, the amplitudes recorded at different locations on the grout surface (Point C in Figure 1-2) are not the same. In this study, the receiver location (Point C in Figure 1-2) is off the wave path of the wave signals and this effect has to be considered. If a relationship between the amplitude at the central point of the rebar (Point B in Figure 1-2) and that at a location on the grout surface (Point C) is established, the amplitude recorded at the grout surface can be correlated to the amplitude along the axis

of the rebar, and the wave attenuation along the rock bolt can be estimated using the data recorded at C, accordingly. The problem is that the echo obtained at Point B from the numerical study is not adequately clear to perform detailed analyses due to the complicated boundary condition.

Our previous research indicated (Cui and Zou 2006) that the attenuation along a free bolt (un-grouted) was negligible. This implies that the wave energy at the excitation end is nearly the same as that at any point along the un-grouted portion of a bolt. Numerical study makes it possible to record the waveforms at any location in the model. Therefore, the amplitudes of the input signal and the echo at the excitation end (Point A in Figure 1-2) can be considered approximately equal to those at Point B. The waveform data at Point A are used to represent the data at Point B for this study.

During the analysis, the input signal and the echo are considered separately to evaluate the off-path effects of the receiver location. Two parameters are introduced here. R_f, the input-amplitude ratio of the input waveforms at Point C and Point B, and R_e, the echo-amplitude ratio of the echo waveforms at Point C and Point B are defined as follows:

$$R_f = \frac{A_{fC}}{A_{fB}} \qquad [5\text{-}1]$$

$$R_e = \frac{A_{eC}}{A_{eB}} \qquad [5\text{-}2]$$

In Equations [5-1] and [5-2], A_{fC} is the average amplitude of the input group at Point C on the grout surface, A_{fB} is the average amplitude of the input group at Point B, A_{eC} is the average amplitude of the echo at Point C on the grout surface and A_{eB} is the average amplitude of the echo at Point B. The average amplitude ratios are estimated using the method presented in Equation [4-2].

The results of the input- and echo- amplitude ratios are shown in Figures 5-4 and 5-5, respectively.

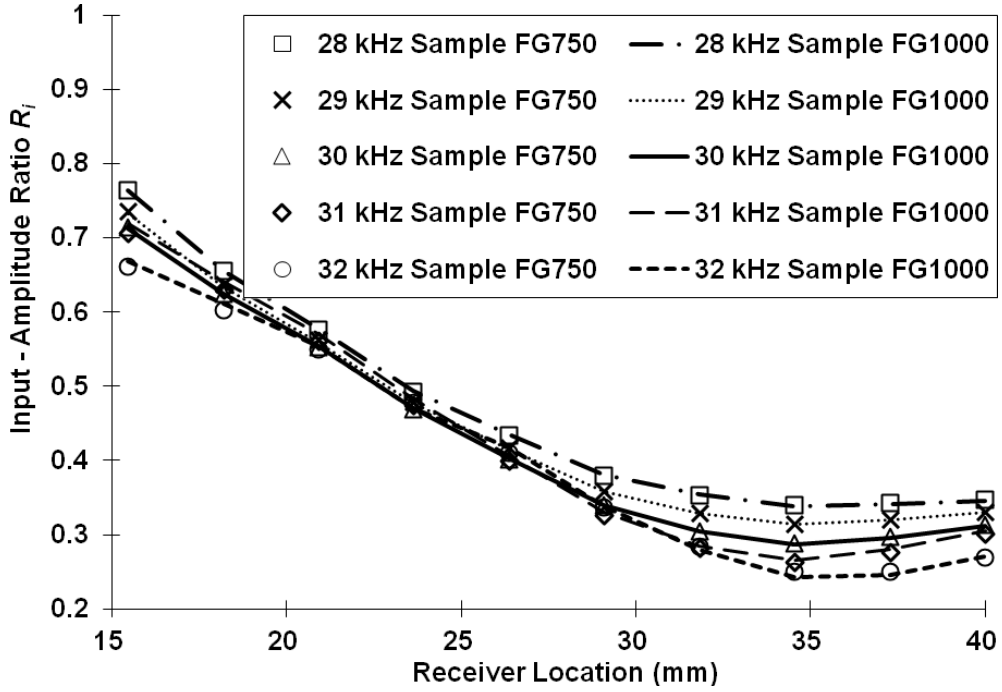

Figure 5-4 Input - amplitude ratio R_f vs. lateral distance of receiving location

The results in Figures 5-4 and 5-5 indicate that R_f and R_e both vary with the receiving locations. In general, the further away of Point C from the bolt axis, the more reduction in wave amplitude. However the input amplitude ratio seems to follow a different pattern from the echo amplitude ratio. The former has more changes when the receiver location is up to 30 mm from the bolt axis while the latter has more changes when the receiver location is 25 mm or further away.

Analyses indicate that the input amplitude ratio is a measurement of the true attenuation of wave propagation along its path as defined in Equation [2-1]. At locations further away than 32 mm (from Point B to Point C), the results could be affected by the weakened signal and the boundary condition of the model. The echo amplitude ratio, on the other hand, does not really measure the attenuation along a wave path. It simply compares the wave magnitudes of the echo at two different locations on two separate

paths. When the receiver location (Pint C in Figure 1-2) is very close to the bolt axis (Point B), the echo wave energy is expected to be similar at both locations, implying a larger amplitude ratio. When they are further apart to a certain distance, the effect of attenuation will show up.

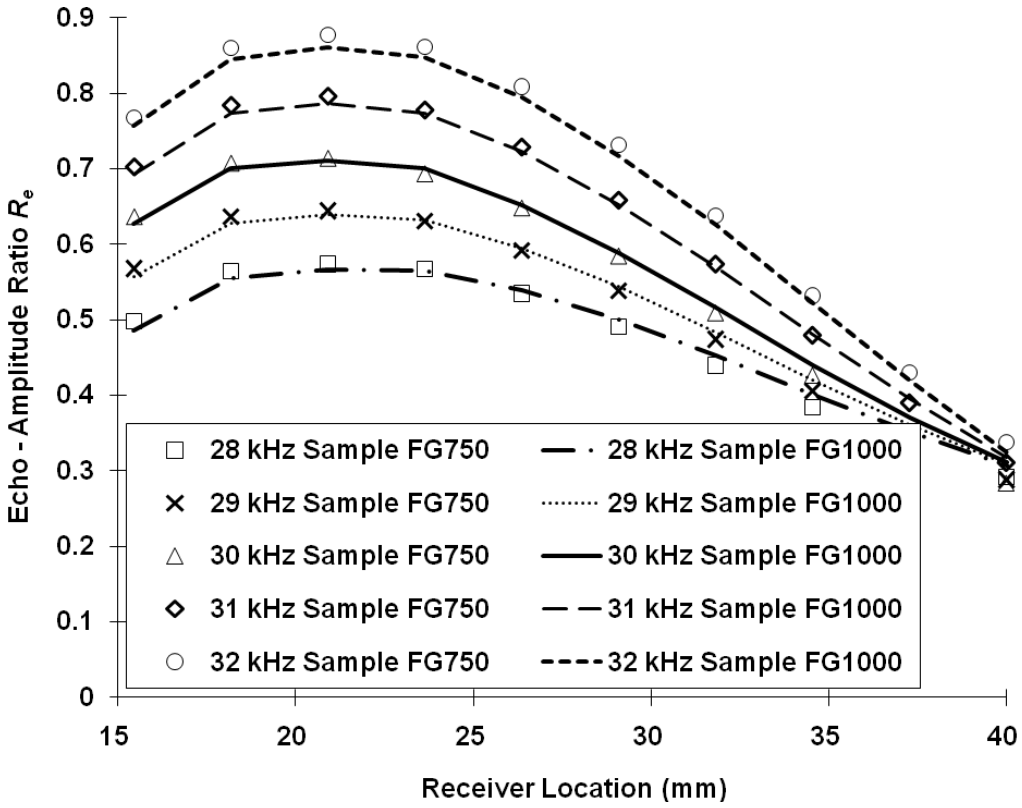

Figure 5-5 Echo - amplitude ratio R_e vs. lateral distance of receiving location

R_f and R_e are affected by the input frequency but to a lesser extent. However it should be pointed out that both R_f and R_e are constant for a specific measurement location and a specific wave frequency. The grout lengths of Sample FG750 and Sample FG1000 are different. As shown in Figure 5-4, R_f obtained from Sample FG750 is almost the same as that from Sample FG1000 measured at the same location. This is expected because R_f compares the input signal amplitudes before the signal travels through the grout and

should not be affected by the grout length. Based on results shown in Figure 5-5, it can also be concluded that R_e is not affected by the grout length. This is because R_e compares the echo amplitudes after the echo traveled through the same grout.

Considering Equation [2-1] applying to Point B (Figure 1-2), $A_a = A_{fB}$ and $A_b = A_{eB}$ and combining Equations [5-1] and [5-2], the amplitude ratio at B is

$$R_B = \frac{A_b}{A_a} = \frac{A_{eB}}{A_{fB}} = \frac{A_{eC} R_f}{A_{fC} R_e} \qquad [5\text{-}3]$$

With the consideration of the boundary condition at the ground end as discussed in Chapter 2, the attenuation and amplitude ratio along the bolt axis are defined in Equations [2-2]. Applying Equation [5-3] to Equation [2-2] gives:

$$-\alpha L = \ln(R_B) - \ln(K_b) = \ln\left(\frac{A_{eC} R_f}{A_{fC} R_e}\right) - \ln(K_b) \qquad [5\text{-}4]$$

Let's introduce the amplitude ratio, R_c, at Point C

$$R_C = \frac{A_{eC}}{A_{fC}} \qquad [5\text{-}5]$$

and a location correction factor, K_l

$$K_l = \frac{R_f}{R_e} \qquad [5\text{-}6]$$

Equation [5-3] becomes:

$$R_B = R_C K_l \qquad [5\text{-}7]$$

and Equation [5-4] becomes:

$$-\alpha L = \ln(R_C K_l) - \ln(K_b) = \ln(R_C K_l / K_b) \qquad [5\text{-}8]$$

Equation [5-7] relates the amplitude ratios at locations B and C with a location correction factor, K_l. Equation [5-8] can be used to calculate attenuation at Pint B using waveforms recorded at Point C (Figure 1-2) on the grout surface. For the simulated cases, the results of K_l for input frequencies of 28 kHz to 32 kHz in this study are shown in Figure 5-6.

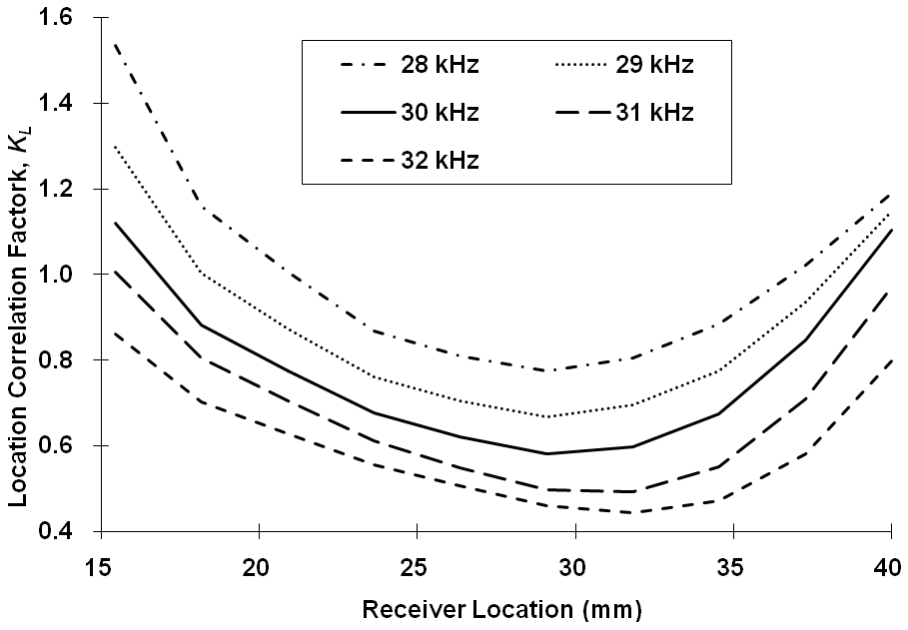

Figure 5-6 Location correction factor K_l vs. lateral distance of receiving location

In field and laboratory tests, it is often difficult to find an accurate location to install the receiving transducer. Therefore, it is necessary to identify a location range where the measured results are not very sensitive to the location. Based on the results shown in Figure 5-6, the suitable location for the receiver is evaluated to be between 27 mm and 32 mm measured from the bolt axis center (Point B in Figure 1-2).

We developed a method previously (Cui and Zou 2006) for determining the boundary correction factor K_b and the attenuation coefficient α for attenuation along the axis of a fully grouted rock bolt (Figure 1-1). In this study, the same method is used for Samples FG750 and FG1000. Both the location correction factor and boundary correction factor are calculated and the results are shown in Table 5-2. The K_l values listed in Table 5-2 are obtained at the lateral location of 29 mm measured from the center of the rebar. The same distance will be used for the installation of the receiving transducer in the experimental verification, which will be discussed in the next section.

Table 5-2 Attenuation coefficients and correction factors (Chapter 5)

Frequency (kHz)	28	29	30	31	32
Attenuation coefficient α (m^{-1})	0.42	0.42	0.43	0.44	0.43
Boundary Correction factor, K_b	0.82	0.82	0.84	0.91	1.01
Location Correction factor, K_l	0.63	0.55	0.48	0.47	0.48

5.4 EXPERIMENTAL VERIFICATION

To validate the numerical results, laboratory tests are performed on a rock bolt sample (Sample LFG500 in Table 5-1).

The instruments used in the test are shown in Figure 4-5 and was discussed in Chapter 4. The numerical modeling results in the previous section indicated that the most suitable receiver location was a distance of 27 mm to 32 mm measured from the bolt axis. The receiving transducer is therefore installed at approximately 29 mm to bolt axis in these tests. The input signals used in experiments are discussed in Chapter 4. The input signals had frequencies ranged from 28 kHz to 32 kHz, the same as used in the numerical study. The recorded wave data are analyzed using the same methods for numerical modeling.

Waveforms obtained using this proposed transmission-echo-off-path equipment set-up shown in Figure 1-2 are compared with waveforms obtained by Cui and Zou (2006) who used the previous transmission-through set-up shown in Figure 1-1. It can be concluded that both methods can obtain clear and analyzable waveforms. However, the proposed transmission-echo-off-path method is practical for performing field tests. Figure 5-7 shows a typical waveform recorded on the grout surface (Point C) from test conducted on Sample LFG500.

With the input frequency from 28 kHz to 32 kHz, the travel time is calculated to be approximately 350 to 300 μs after adjustment by the lateral travel time Δt as illustrated in Figure 5-3. The wave group velocity is estimated to be between 2800 m/s and 3100 m/s, with the higher velocity corresponding to higher frequency. The obtained group velocity is slightly higher than that determined by the numerical solution (2730 m/s to 2850 m/s), most likely due to measurement noises in the tests; nevertheless, they are comparable with previous results completed by Madenga et al (2006).

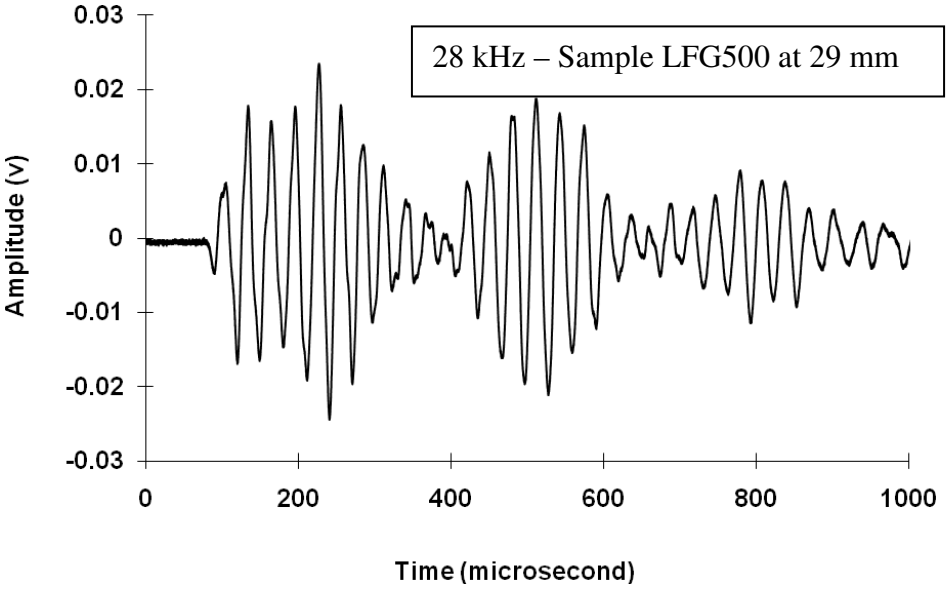

Figure 5-7 Typical measured waveforms – Sample LFG500

The measured waveform data are analyzed to determine the amplitude ratio (R_c) at the measurement location C. As discussed earlier, the sensor-recorded amplitude ratio (R_m) during a test is lower than the amplitude ratio (R_c) in Equation [5-8] due to a fixed energy loss at the contact interface between the transducers and bolts. As discussed in Chapter 2, the following fixed energy loss factor is used to represent this effect:

$$K_f = \frac{R_c}{R_m} \qquad [5\text{-}9]$$

Zou et al (2007) reported that because the energy loss due to attenuation in a relatively short free bolt (rebar) was ignorable the sensor recorded amplitude ratio (R_m) in a free bolt was caused by the fixed energy loss.

For specific test equipment, the fixed energy loss for a free bolt is the same as that for a grouted bolt. Therefore, R_c for grouted rock bolts can be estimated based on sensor recorded amplitude ratio (R_m) on a grouted bolt and K_f obtained from free bolt measurements using the equipment set-up as shown in Figure 1-1. Detailed discussion of this method was given by Zou et al (2007). In this study, this method is used to calculate R_c for Sample LFG500 at 29 mm location on the grout surface and the results is shown in Figure 5-8.

Based on the numerical results of this study, it has been concluded that attenuation coefficient (α), boundary correction factor (K_b) and location correction factor (K_l) are not dependent upon the grout length of a rock bolt. The results in Table 5-2 for Sample FG750 (750 mm) or Sample FG1000 (1000 mm) are therefore valid for rock bolts with any different grout length (L), if they have the same diameter and physical properties. Thus the amplitude ratio (R_c) for any rock bolt with a different grout length can be calculated using Equation [5-8].

It should be noted that the above conclusion (i.e., α, K_b, K_l being not dependent upon grout length) is based on the numerical results only. Experimental tests should be conducted to verify this conclusion. If the calculated (R_c) based on parameters obtained from numerical studies matches the experimental results on Sample LFG500, the above conclusion is proved.

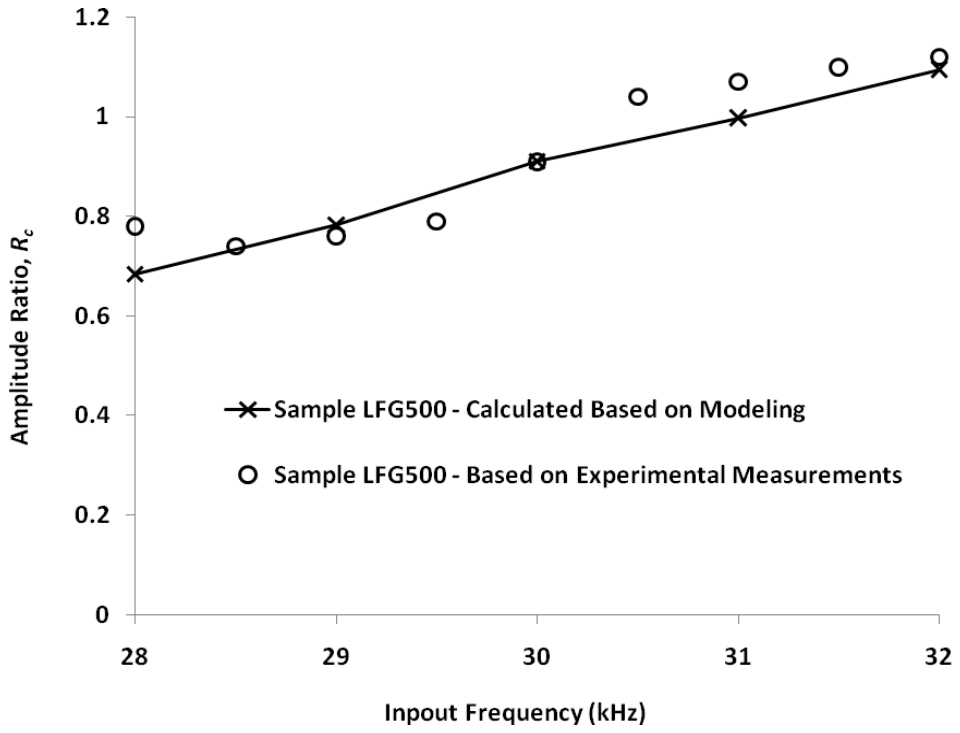

Figure 5-8 Comparison of amplitude ratios – Sample LFG500

The amplitude ratio at Point C (Figure 1-2), at a lateral distance of 29 mm from the centre-axis of the rebar (Point B in Figure 1-2) in a rock bolt with a grout length of 500 mm (Sample LFG500) is calculated using Equation [5-8] with the parameters in Table 5-2. The calculated and the experimental results for various input signal frequencies are presented in Figure 5-8. It can be seen that the numerical results match the experimental ones well. Therefore, it can be considered that the parameters would be the same for rock

bolts with different grout lengths, implying that α, K_b, K_l are not functions of grout lengths.

The results of this study indicate that it is practically possible to receive meaningful signals by installing the receiving transducer on the grout surface. With the data recorded on the grout surface, the grout length can be estimated using attenuation and wave velocity of ultrasonic guided waves with reasonable accuracy.

CHAPTER 6 EFFECTS OF MISSING GROUT

One of the challenges in field monitoring of grouted rock bolts is to detect the defects of the bolt or grout. Although the ultrasonic guided wave method has demonstrated potential for monitoring grout qualities, further study is required to use this method to detect grout defects.

In this chapter numerical modeling on grouted rock bolts is performed to assess the effects of a portion of missing grout at the ground end. Based on the numerical modeling used in Chapter 5, four grouted rock bolt models are created to compare the attenuation and group velocity in fully grouted rock bolts and rock bolts with a portion of missing grout at the ground end as shown in Figure 6-1. One laboratory sample is used to verify the results obtained from the numerical study.

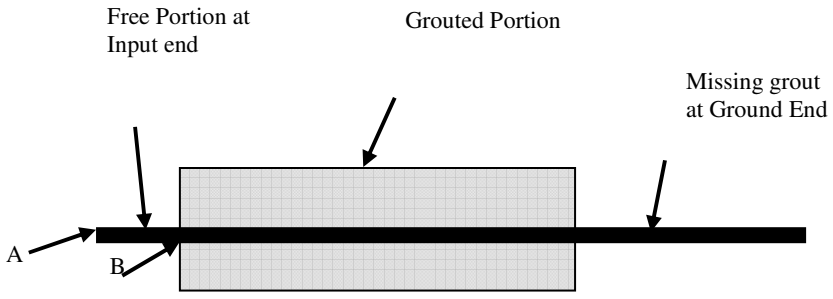

Figure 6-1 Rock bolt with a portion of missing grout

6.1 MODEL AND INPUT PARAMETERS

Geometries of rock bolt models used in this chapter are specified in Table 6-1. The sample IDs of MG stands for rock bolts with a portion of missing grout at the ground end. The ultrasonic guided wave behaviour is compared for the two groups of grouted rock

bolts (Figures 1-2 and 6-1): fully grouted rock bolts (Samples FG750 and FG1000), and rock bolts with a missing grout length (Samples MG750 and MG1000).

The input parameters and element sizes of these models are the same as those shown in Table 4-1 and Table 4-2. The LS-DYNA input file for modeling rock bolts with a missing grout length at the ground end (MG750) is provided in Appendix C.

Table 6-1 Chapter 6 model geometries

Sample ID	Free Length		Bolt diameter (mm)	Grouted Rebar length (mm)	Total Grout length (mm)	Total Rebar length (mm)	Diameter of concrete cylinder (mm)
	at input end (mm)	at ground end (mm)					
Sample FG750	50	0	20	750	750	800	160
Sample FG1000	50	0	20	1000	1000	1050	160
Sample MG750	50	1500	20	750	750	2300	160
Sample MG1000	50	1500	20	1000	1000	2550	160
Sample LMG500	50	1500	20	500	500	2050	160

To save computing time, the symmetrical condition of the sample is considered and only one quarter of the sample is created as shown in Figure 4-2. One of the finite element models (MG750) is shown in Figure 6-2.

As discussed in Chapter 5, when a receiver transducer is installed on the grout surface, clear and analyzable signals can be received only for input signals within a narrow range of input frequency that is between 28 kHz and 31 kHz. The input wave frequency in this chapter is limited to this range.

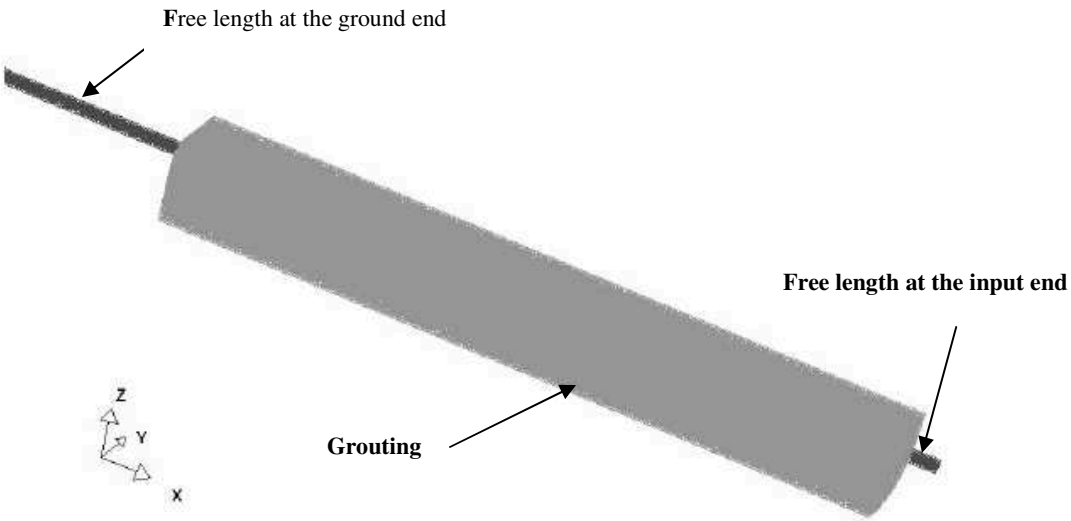

Figure 6-2 Finite element model – Sample MG750 (quarter size)

An ultrasonic wave at a specified frequency is transmitted to the rebar at the input end (Point A in Figure 6-1) and the waveforms at the central of the rock bolt (rebar) are studied. As discussed in Chapter 5, the echo obtained at Point B (Figure 6-1 and Figure 1-2) is not clear enough to perform detailed analysis due to the complicated boundary condition. The waveform data at Point A are used to perform the analyses. The typical input group and the echo waveforms obtained at Point A of Samples FG750 and MG750 are shown in Figures 6-3a) and 6-3b), respectively. The input frequency is 31 kHz.

It can be observed from Figure 6-3 that the maximum amplitude of the echo groups of Samples FG750, the fully grouted rock bolt, and MG750, the rock bolt with a missing grout length, arrived at almost the same time, indicating that the echo groups traveled the same period of time.

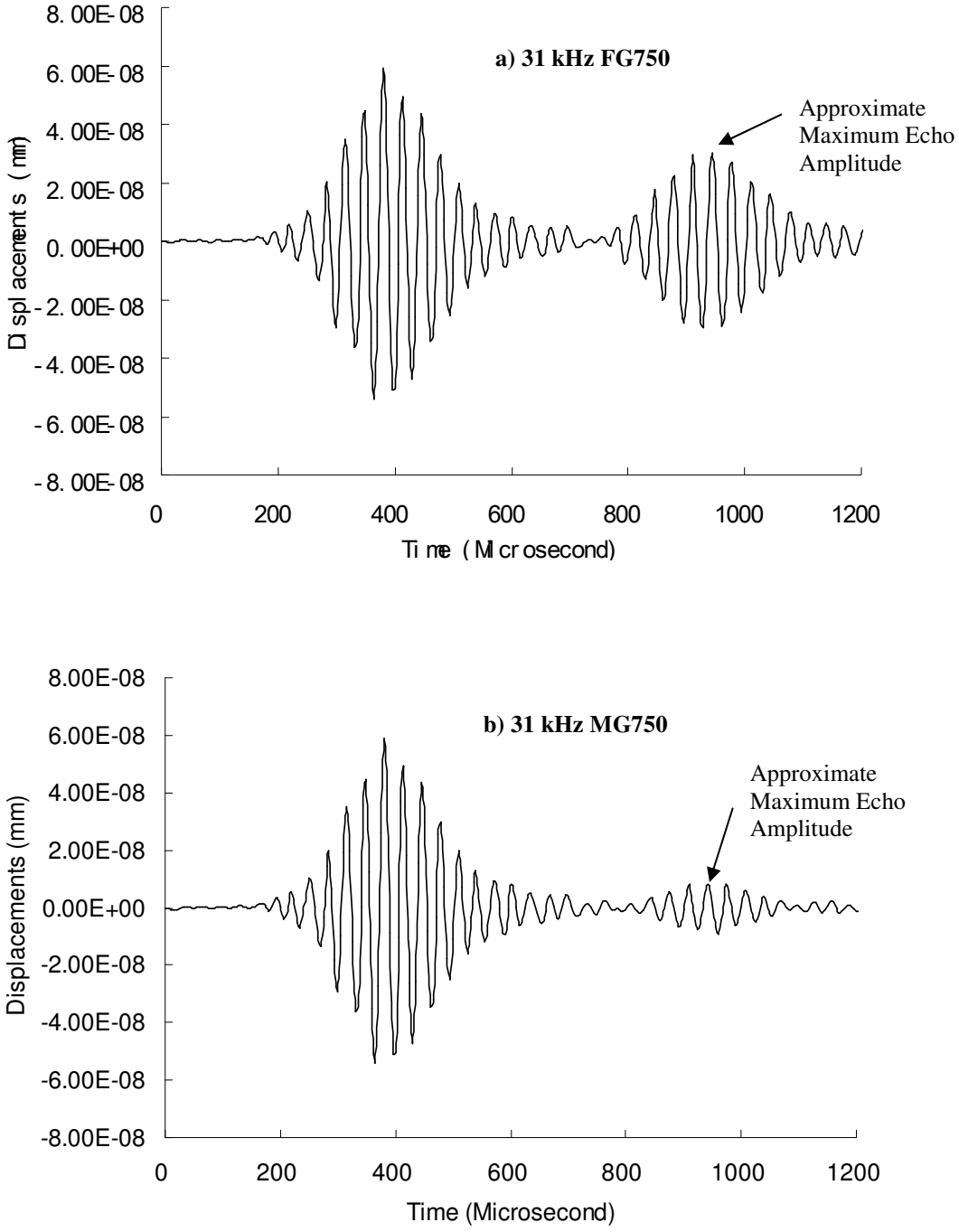

Figure 6-3 Typical waveforms for Samples FG750 and MG750

Although sample MG750 has longer rebar at the ground end, its grout length is the same as FG750. The echo of Sample MG750 is most likely reflected from the same locations (the end of the grout) as Sample FG750. It is also noticeable that the echo amplitude of Sample MG750 is smaller than that of Sample FG750, indicating an energy loss at the first reflection point (the end of the grout) of Sample MG750. The same is observed when the waveforms of Samples FG1000 and MG1000 are compared.

6.2 ANALYSIS OF WAVE TRAVEL TIME

Theoretically, the travel time can be determined by the time intervals between the locations of the maximum amplitude of the input group and the echo. With the acquired travel time and the bolt length, the group velocity can be calculated.

As discussed before, because the echo at Point B (Figures 1-2 and 6-1) is not clear, the wave traveling time at Point B is obtained based on the wave traveling time estimated at Point A subtracting the wave traveling time in the free potion at the input end, which can be estimated based on the bolt free length and wave group velocity in free bolts provided by Madenga et al (2004). The time intervals at Point B (Figure 1-2 and Figure 6-1) between the maximum amplitude of the input group and echo are shown in Figure 6-4 for each of the four models. From Figure 6-4, it can be concluded that the echo for rock bolts with a portion of missing grout is reflected from the end of the grout, regardless of the rebar length at the ground end.

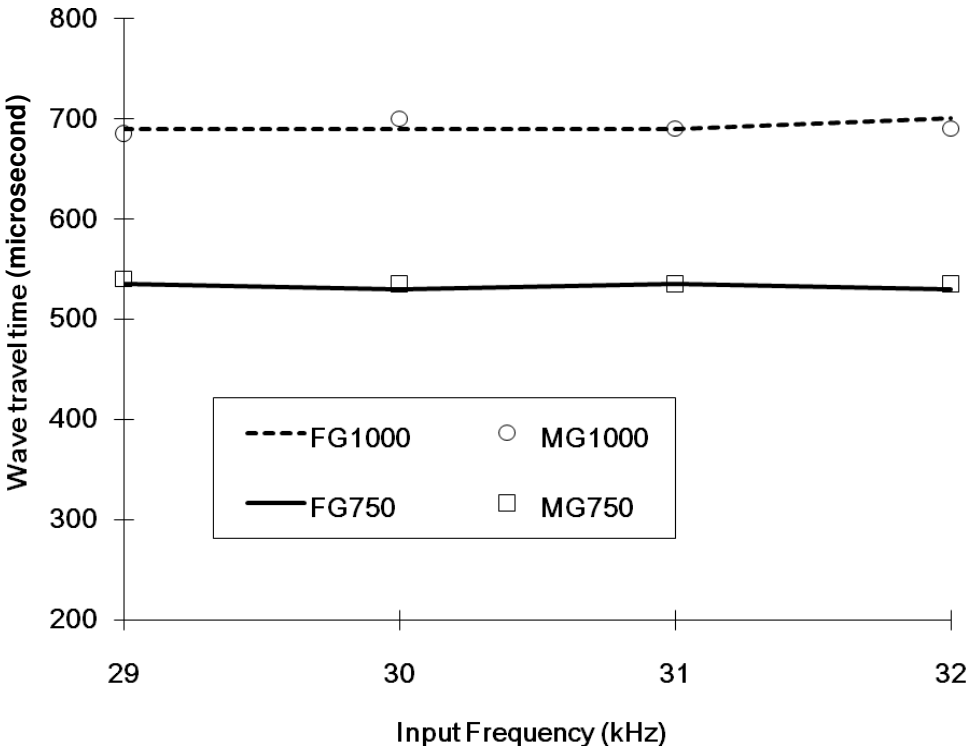

Figure 6-4 Wave travel time in rock bolts with a portion of missing grout

6.3 ANALYSIS OF WAVE ATTENUATION

As discussed above, the echo amplitudes from rock bolts with a missing grout length (Sample MG750 and MG1000) are smaller than those from fully grouted rock bolts (Samples FG750 and FG1000).

Figure 6-5 shows the amplitude of the input group along the axis of the grouted portion of Samples FG750 and MG750. As discussed by Zou et al (2007), the amplitude near both ends of the rock bolts is affected by the boundary condition and is much higher than that at the central portion of rock bolts.

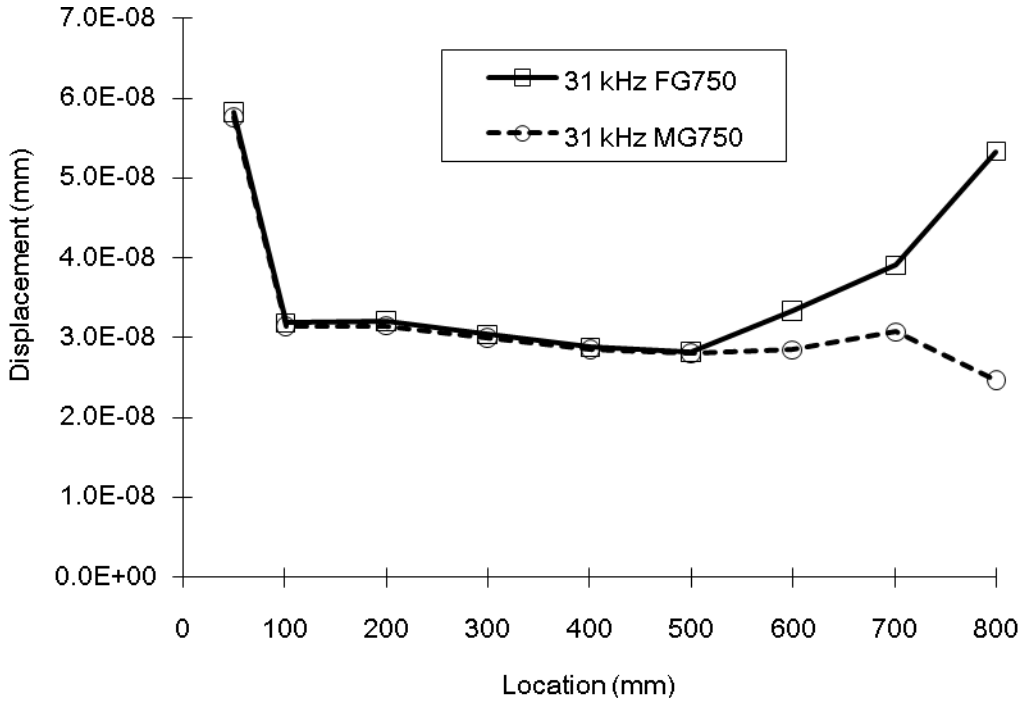

Figure 6-5 Wave amplitude along the axis of rock bolts

It can be observed from Figure 6-5 that the amplitude is the same near the input ends of both bolts (the fully grouted bolt and the bolt with a portion of missing grout at the ground end). However, the amplitude near the reflection surface (the end of the grout) is different. It is expected that the attenuation near the input end is the same for both types of rock bolts, because the boundary conditions are the same. However, the attenuation is different near the reflection surface at the ground end because their boundary conditions are different.

A method is suggested to calculate the attenuation at the reflection ends. Using Equation [2-2], the attenuation along the axis of the grouting portion of Samples FG750 and FG1000 can be expressed as follows:

$$-\alpha L_{FG750} = \ln(R_{F750}) - \ln(K_b) = \ln\left(R_{FG750} / K_b\right) \qquad [6\text{-}1]$$

$$-\alpha L_{FG1000} = \ln(R_{FG1000}) - \ln(K_b) = \ln\left(R_{FG1000} / K_b\right) \quad [6\text{-}2]$$

where, L_{FG750} and L_{FG1000} are grouted rebar lengths of Samples FG750 (750 mm) and FG1000 (1000 mm); and R_{FG750} and R_{FG1000} are the amplitude ratio of the echo and input group of the two samples, respectively.

For rock bolts with a missing grout length at the ground end (Samples MG750 and MG1000), the boundary effect is different from that of fully grouted rock bolts (Samples FG750 and FG1000). Cui (2006) concluded that the boundary correction factor is not a function of grout length. In this study, K_m is used to represent the boundary correction factor for rock bolts with a portion of missing grout at the ground end.

As discussed above, an energy loss occurs at the reflection surface and this loss reduces the echo energy of bolts with a missing grout length at the ground end. To consider this energy loss, a correction factor G is used to account for the wave energy propagating into the un-grouted portion and the value of G is assumed to be not a function of grout length (this assumption will be verified later). Thus for rock bolts with a portion of missing grout at the ground end, Equation [2-2] is modified as follows:

$$-\alpha L = \ln(R) - \ln(K_m) - \ln(G) \quad [6\text{-}3]$$

Equation [6-3] is based on an assumption that G is not a function of grout length, which has to be verified. If this assumption is valid, the attenuation along the axis of Samples MG750 and MG1000 can be expressed as follows:

$$-\alpha L_{MG750} = \ln(R_{MG750}) - \ln(K_m) - \ln(G) = \ln\left(R_{MG750} / K_m G\right) \quad [6\text{-}4]$$

$$-\alpha L_{MG1000} = \ln(R_{MG1000}) - \ln(K_m) - \ln(G) = \ln\left(R_{MG1000} / K_m G\right) \quad [6\text{-}5]$$

where, L_{MG750} and L_{MG1000} are the grouted rebar lengths of Samples MG750 (750 mm) and MG1000 (1000 mm). R_{MG750} and R_{MG1000} are the amplitude ratio of the echo and input group of the two samples.

Combining Equations [6-1] and [6-4] and considering the fact that $L_{MG750} = L_{FG750}$, the following equation can be derived as:

$$\ln\left(R_{FG750} / K_b\right) = \ln\left(R_{MG750} / K_m G\right) \quad \Rightarrow \quad \frac{R_{MG750}}{R_{FG750}} = \frac{K_m G}{K_b} \qquad [6\text{-}6]$$

Using the same concept, Equation [7-7] can be derived for Samples FG1000 and MG1000 (Equations [6-2] and [6-5]).

$$\frac{R_{MG1000}}{R_{FG1000}} = \frac{K_m G}{K_b} \qquad [6\text{-}7]$$

If the assumption that G is not a function of the grout length is true, then the following equation can be derived from Equations [6-6] and [6-7].

$$\frac{R_{MG750}}{R_{FG750}} = \frac{R_{MG1000}}{R_{FG1000}} = \frac{K_m G}{K_b} \qquad [6\text{-}8]$$

Figure 6-6 shows the ratios $\frac{R_{MG750}}{R_{FG750}}$ and $\frac{R_{MG1000}}{R_{FG1000}}$ obtained at the input end (Point A in Figure 1-2). It can be concluded that the two ratios are approximately equal, indicating that the assumption regarding G is valid.

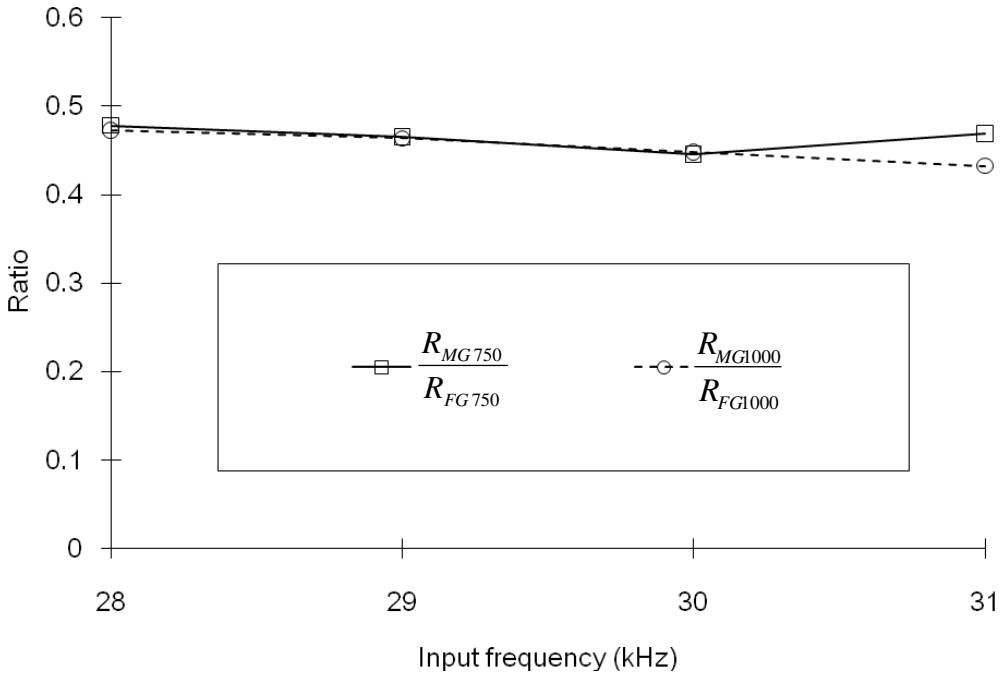

Figure 6-6 Comparison of amplitude ratios for fully grouted rock bolts and rock bolts with a portion of missing grout

It is difficult to separate the effects of the two parameters K_m and G. Because both of them are constants for a specific input frequency and not related to the grout length, these two parameters can be combined as a new factor, $K_{MG} = K_m G$, to represent both effects of boundary conditions and the energy loss at the first reflection point for rock bolts with a portion of missing grout. Equation [6-3] can be rewritten as Equation [6-9].

$$-\alpha L = \ln(R) - \ln(K_{MG}) \qquad [6\text{-}9]$$

Cui and Zou (2006) provided a method for determining the attenuation coefficient α and the boundary correction factor K_b. In this study, the same method is used to obtain α and K_b of FG750 and FG1000 (fully grouted rock bolts). Cui and Zou (2006) commented that α is a constant value for rock bolts with the same rebar and grout diameters. Therefore, theoretically α of MG750 and MG1000 is the same as that of

FG750 and FG1000. However, K_{MG} of MG750 and MG1000 is not the same as K_b of FG750 and FG1000 due to different boundary conditions, but can be achieved using the same method. Detailed of the method to obtain α and K_b can be found in Cui and Zou (2006). The obtained attenuation coefficients and boundary correction factors are shown in Table 6-2.

Equation [5-9] in Chapter 5 provided a method to correlate the amplitude ratio obtained at the grout surface (Point C in Figure 1-2) to that at Point B (Figure 1-2). This correlation is completed using the measurement location factor, K_l. The measurement location correction factors K_l at 29 mm from the rebar (Point C in Figure 1-2) are included in Table 6-2 for the use of the experimental verification in the next section.

Table 6-2 Attenuation coefficients and correction factors (Chapter 6)

Wave Frequency (kHz)	28	29	30	31
Attenuation coefficient α	0.42	0.42	0.43	0.44
Correction factor for the measurement location, K_l	0.63	0.55	0.48	0.47
Boundary correction factor, K_b - full grouted rock bolts	0.82	0.82	0.84	0.91
Boundary Correction factor, K_{MG} - rock bolts with missing grout	0.58	0.57	0.53	0.52

6.4 EXPERIMENTAL VERIFICATION

To verify the numerical results, laboratory tests are performed on a laboratory sample, LMG500. The geometry of this sample is given in Table 6-1.

The instruments used in the test are the same as those discussed in Chapter 4. The input signals used are at frequencies from 28 kHz to 31 kHz, which are the same as those used in the numerical modeling. The receiving signals are picked up by a receiving transducer

installed on the grout surface (Point C in Figure 1-2) at 29 mm measured from the rebar axis (Point B in Figure 1-2). The recorded data are analyzed using the same methods as in numerical modeling.

Figure 6-7 shows a typical waveform recorded at Point C of Sample LMG500. It can be observed that the data received on the grout surface of rock bolts with a portion of missing grout is clear and analyzable.

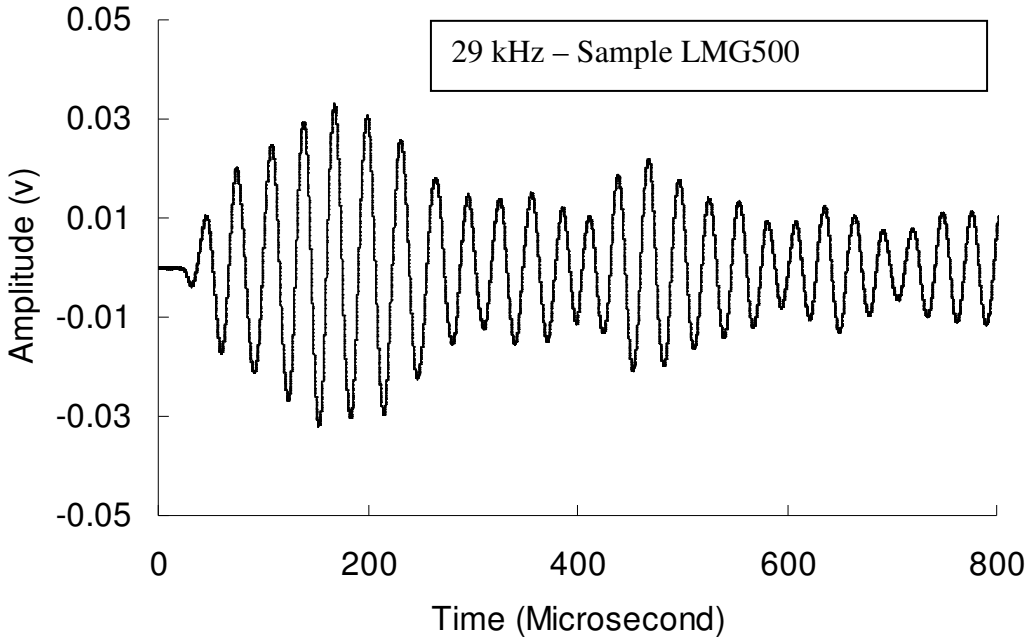

Figure 6-7 Typical waveform – Sample LMG500

Chapter 5 provided a method to correlate the wave travel time measured on the grouting surface (Point C in Figure 1-2) to the central of the rebar (Point B in Figure 1-2). Based on the wave travel time in the fully grouted portion of the rock bolts, the group velocity along the central of the rebar is estimated to be in a range between 2650 m/s and 3000 m/s. The results are similar to the experimental results (approximately 2700 m/s) obtained by Madenga et al (2004) with slight difference. This difference may be the result of errors due to noises.

The test results of amplitude ratio of Sample LMG500 at Point C (Figure 1-2) are shown in Figure 6-8. The amplitude ratio at Point C (Figure 1-2), at a lateral distance of 29 mm from the central of the rebar (Point B in Figure 1-2), is also calculated using Equation [6-9] and parameters obtained from numerical modeling shown in Table 6-2. The calculated results shown in Figure 6-7 match the experimental ones well. It can be concluded from the above results that the numerical modeling results have sufficient accuracy and that rock bolts with defects of a missing grout length at the ground end can be identified by the ultrasonic guided wave method with reasonable accuracy.

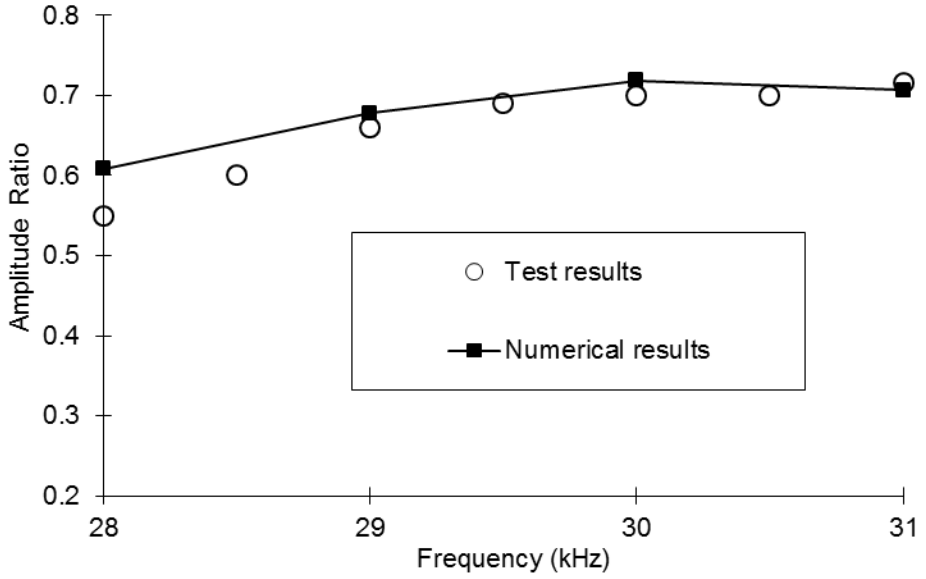

Figure 6-8 Amplitude ratio – Sample LMG500

CHAPTER 7 EFFECTS OF INSUFFICIENT REBAR LENGTH

In Chapter 6, rock bolts with a typical defect of a missing grout portion at the ground end are analyzed and studied. Another typical defect of grouted rock bolts is the insufficient rebar length at the ground end (the actual bolt length is shorter than expected) as shown in Figure 7-1 and will be studied in this chapter.

Four numerical models are created to assess the effects of an insufficient rebar length at the ground end. One laboratory sample is tested to verify the results obtained from the numerical study.

7.1 MODEL AND INPUT PARAMETERS

Geometries of rock bolt models used in this chapter are specified in Table 7-1. Input parameters and element sizes of these models are the same as those shown in Table 4-1 and Table 4-2.

Table 7-1 Chapter 7 model geometries

Sample ID	Free Length		Bolt diameter (mm)	Grouted Rebar length (mm)	Total Grout length (mm)	Total Rebar length (mm)	Diameter of concrete cylinder (mm)
	at input end (mm)	at ground end (mm)					
Sample FG500	50	0	20	500	500	550	160
Sample FG750	50	0	20	750	750	800	160
Sample IR500	50	0	20	500	1000	550	160
Sample IR750	50	0	20	750	1250	800	160
Sample LIR500	50	0	20	500	1000	550	160

The sample IDs of IR stands for rock bolts with an insufficient rebar length at the ground end. The ultrasonic guided wave behaviour are compared for the two groups of grouted

rock bolts: fully grouted rock bolts (Samples FG500 and FG750), and rock bolts with an insufficient rebar length (Samples IR500 and IR750).

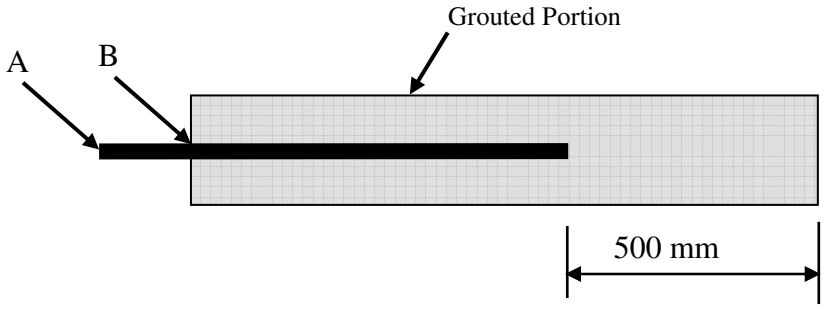

Figure 7-1 Rock bolt with an insufficient rebar length

The LS-DYNA input file for modeling a typical rock bolt with an insufficient rebar length at the ground end (IR750) is provided in Appendix D. To save computing time, the symmetry condition of the sample is considered and only one quarter of the sample is created.

An ultrasonic wave at a specified frequency is transmitted to the rebar at the input end (Point A in Figure 7-1) and the waveforms obtained along the central of the rock bolt (rebar) are studied. Input signals used in this chapter are limited to frequency between 28 kHz and 31 kHz. As discussed before, the echo obtained at Point B is not clear enough to perform detailed analysis due to the complicated boundary condition and the waveform data at Point A are analyzed instead.

The typical input group and the echo waveforms obtained at Point A (Figure 7-1) of Samples FG500 and IR500 are shown in Figures 7-2a) and 7-2b), respectively. The input frequency is 31 kHz.

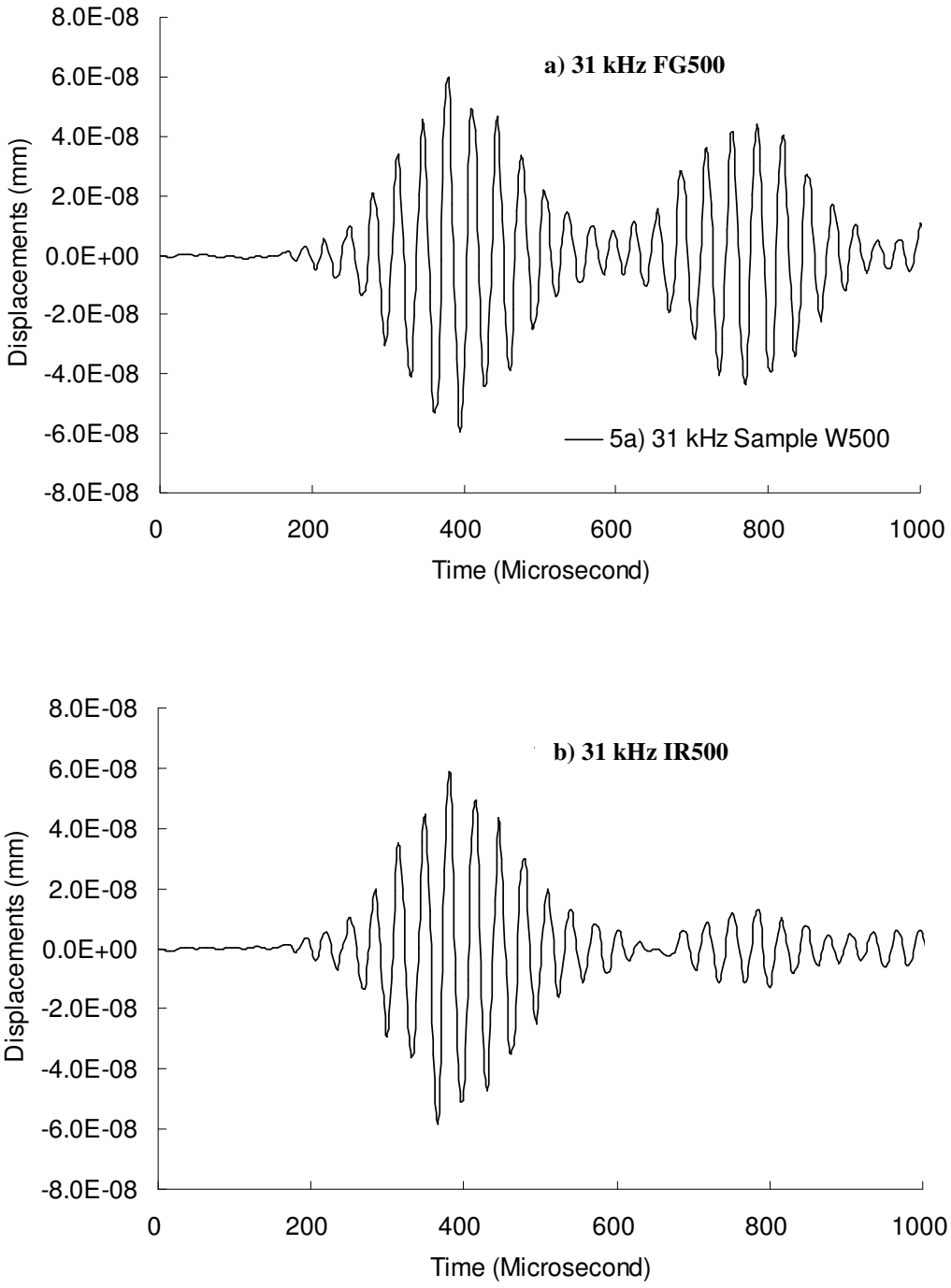

Figure 7-2 Typical waveforms of Samples FG500 and IR500

It can be observed from Figure 7-2 that the maximum amplitude of echo groups of Samples FG500, the fully grouted rock bolt, and IR500, the rock bolt with an insufficient

rebar length, arrived at almost the same time, indicating that their echo groups traveled the same length of time. Although Sample IR500 has longer grout, its rebar length is the same as FG500. The echo of Sample IR500 is apparently reflected from the end of the rebar.

It is noticeable that the echo amplitude of Sample IR500 is smaller than that of Sample FG500, indicating more energy loss at the first reflection point (the end of the rebar) of Sample IR500. The same is observed when the waveforms for Samples FG750 and IR750 are compared.

7.2 Analysis of Wave Travel Time

Because the echo at Point B (Figure 1-2) is not clear, the wave travel time at Point B is obtained based on the wave travel time estimated at Pint A subtracting the wave travel time in the free potion at the input end, which can be estimated based on the bolt free length and wave group velocity in free bolts. The time intervals at Point B between the maximum amplitude of the input group and echo are shown in Figure 7-3 for each of the four models. From Figure 7-3, it can be concluded that the echo for rock bolts with an insufficient rebar length is reflected from the end of the rebar, regardless of grout length.

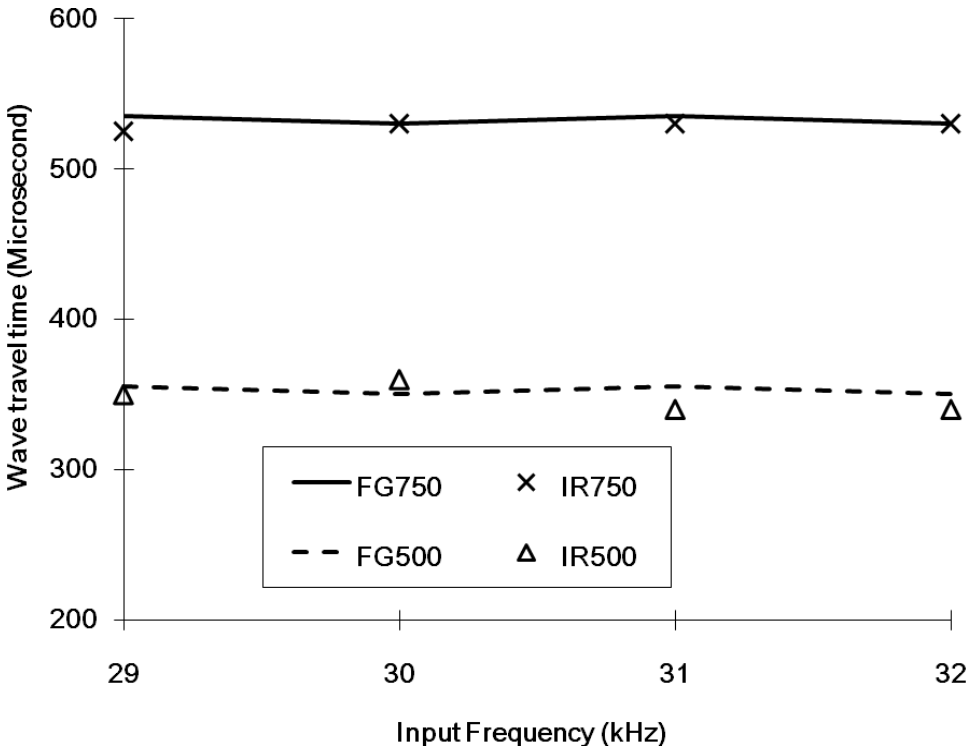

Figure 7-3 Wave travel time in rock bolts with an insufficient rebar length

7.3 ANALYSIS OF WAVE ATTENUATION

The echo amplitudes of rock bolts with an insufficient rebar length (Samples IR500 and IR750) are smaller than those of fully grouted rock bolts (Samples FG500 and FG750). As discussed in Chapter 6, the attenuation near the input end is the same for both the fully grouted rock bolts and the rock bolts with an insufficient rebar because the boundary conditions are the same. However their attenuation behaviour is different at locations near the reflection surface at the ground end because the boundary conditions are not the same.

Using Equation [2-2], the attenuation along the axis of Samples FG500 and FG750 can be expressed as follows:

$$-\alpha L_{FG500} = \ln(R_{FG500}) - \ln(K_b) = \ln\left(R_{FG500} / K_b\right) \quad [7\text{-}1]$$

$$-\alpha L_{FG750} = \ln(R_{FG750}) - \ln(K_b) = \ln\left(R_{FG750} / K_b\right) \quad [7\text{-}2]$$

where, L_{FG500} and L_{FG750} are grouted rebar lengths of Samples FG500 (500 mm) and FG750 (750 mm); and R_{FG500} and R_{FG750} are amplitude ratios of the echo and input group of the two samples, respectively.

For rock bolts with an insufficient rebar length at the ground end (Samples IR500 and IR750), the boundary effect is different from that of fully grout rock bolts. In this study, K_I is used to represent the boundary correction factor for rock bolts with an insufficient rebar length at the ground end.

An energy loss occurred at the reflection surface and this loss has reduced the echo energy of bolts with an insufficient rebar length at the ground end. A correction factor H is used to account for the wave energy propagating into the grout after the end of the rebar and the value of H is assumed to be not a function of grout length (this assumption will be verified later). Thus for rock bolts with an insufficient rebar length at the ground end, Equation [2-2] is modified as follows.

$$-\alpha L = \ln(R) - \ln(K_I) - \ln(H) \quad [7\text{-}3]$$

If the assumption that H is not a function of grout length is valid, the attenuation along the axis of Samples IR500 and IR750 can be expressed as follows:

$$-\alpha L_{IR500} = \ln(R_{IR500}) - \ln(K_I) - \ln(H) = \ln\left(R_{IR500} / K_I H\right) \quad [7\text{-}4]$$

$$-\alpha L_{IR750} = \ln(R_{IR750}) - \ln(K_I) - \ln(H) = \ln\left(R_{IR750} / K_I H\right) \quad [7\text{-}5]$$

where, L_{IR500} and L_{IR750} are the grouted rebar lengths of Samples IR500 (500 mm) and IR750 (750 mm). R_{IR500} and R_{IR750} are the amplitude ratios of the echo and input group of the two samples, respectively.

Combining Equations [7-1] and [7-4] and considering the fact $L_{IR500} = L_{FG500}$, the following equation can be derived as:

$$\ln\left(R_{FG500} / K_b\right) = \ln\left(R_{IR500} / K_I H\right) \quad \Rightarrow \quad \frac{R_{IR500}}{R_{FG500}} = \frac{K_I H}{K_b} \qquad [7\text{-}6]$$

Using the same concept, Equation [8-7] can be derived for Samples FG750 and MG750.

$$\frac{R_{IR750}}{R_{FG750}} = \frac{K_I H}{K_b} \qquad [7\text{-}7]$$

If the above assumption regarding H (H is not a function of the grout length) is correct, the following equation can be derived from Equation [7-6] and [7-7].

$$\frac{R_{IR500}}{R_{FG500}} = \frac{R_{IR750}}{R_{FG750}} = \frac{K_I H}{K_b} \qquad [7\text{-}8]$$

Figure 7-4 shows $\frac{R_{IR500}}{R_{FG500}}$ and $\frac{R_{IR750}}{R_{FG750}}$ obtained at the input end (Point A in Figure 7-1). It can be seen that the two ratios are approximately equal, indicating that the assumption regarding H is valid.

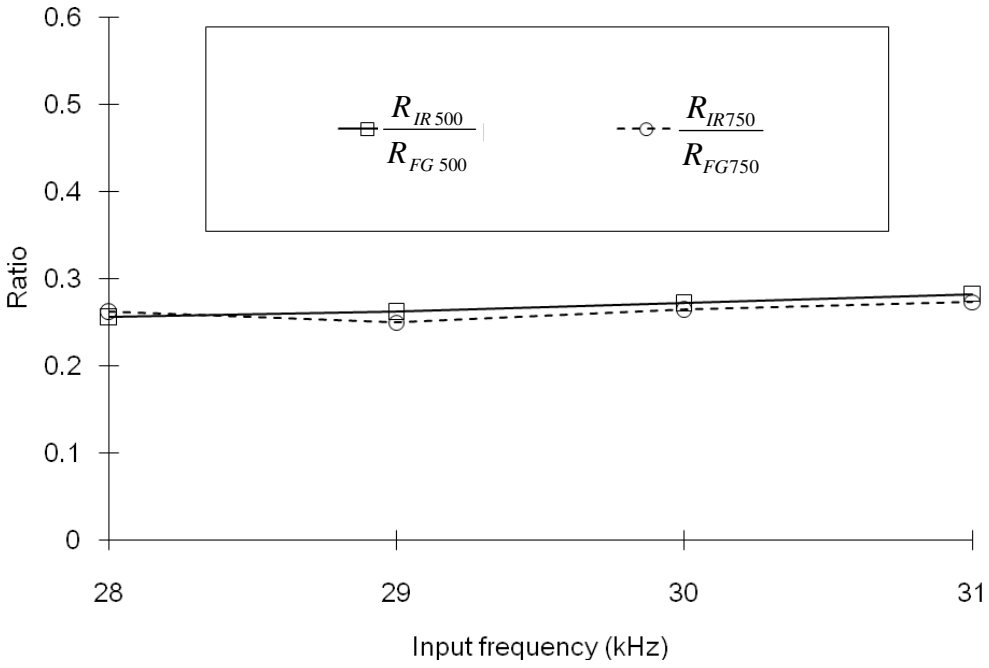

Figure 7-4 Comparison of amplitude ratios for full grouted rock bolts and rock bolts with an insufficient rebar length

The two parameters K_I and H can be combined as a new factor $K_{IR} = K_I H$ to represent both effects of boundary conditions and the energy loss at the first reflection point on rock bolts with an insufficient rebar length. The Equation [7-3] can be rewritten as Equation [7-9].

$$-\alpha L = \ln(R) - \ln(K_{IR}) \qquad [7\text{-}9]$$

Using the method discussed in Chapters 5 and 6, the attenuation coefficient α and the boundary correction factor K_b for fully grouted rock bolt samples (FG500 and FG750), and the α and K_{IR} can be achieved for rock bolts samples with an insufficient rebar length (IR500 and IR750). The obtained attenuation coefficients and boundary corrections factors are illustrated in Table 7-2.

Equation [5-9] in Chapter 5 provided a method to correlate the amplitude ratio obtained at grout surface (Point C in Figure 1-2). The measurement location correction factor K_l at 29 mm from the rebar (Point C in Figure 1-2) is also included in Table 7-2.

Table 7-2 Attenuation coefficients and correction factors (Chapter 7)

Wave Frequency (kHz)	28	29	30	31
Attenuation coefficient α	0.42	0.42	0.43	0.44
Correction factor for the measurement location K_l	0.63	0.55	0.48	0.47
Boundary Correction factor, K_b - full grouted rock bolts	0.82	0.82	0.84	0.91
Boundary Correction factor, K_{IR} - rock bolts with an insufficient rebar length	0.31	0.32	0.32	0.31

7.4 EXPERIMENTAL VERIFICATION

To verify the numerical results, laboratory tests are performed on Sample LIR500. The geometry of this sample is given in Table 7-1.

The instruments used in the test are the same as discussed in the Chapter 4. The input signals used are at frequencies from 28 kHz to 31 kHz, which are the same as in numerical modeling. The reflected signals are picked up by a receiving transducer installed on the grout surface at 29 mm measured from the rebar axis (Point C in Figure 1-2). The recorded data are analyzed using the same methods as in numerical modeling.

Figure 7-5 shows a typical waveform obtained at Point C of Sample LIR500. Figure 7-5 indicates that the data received on the grout surface of rock bolts with an insufficient rebar length at the ground end is clear and analyzable.

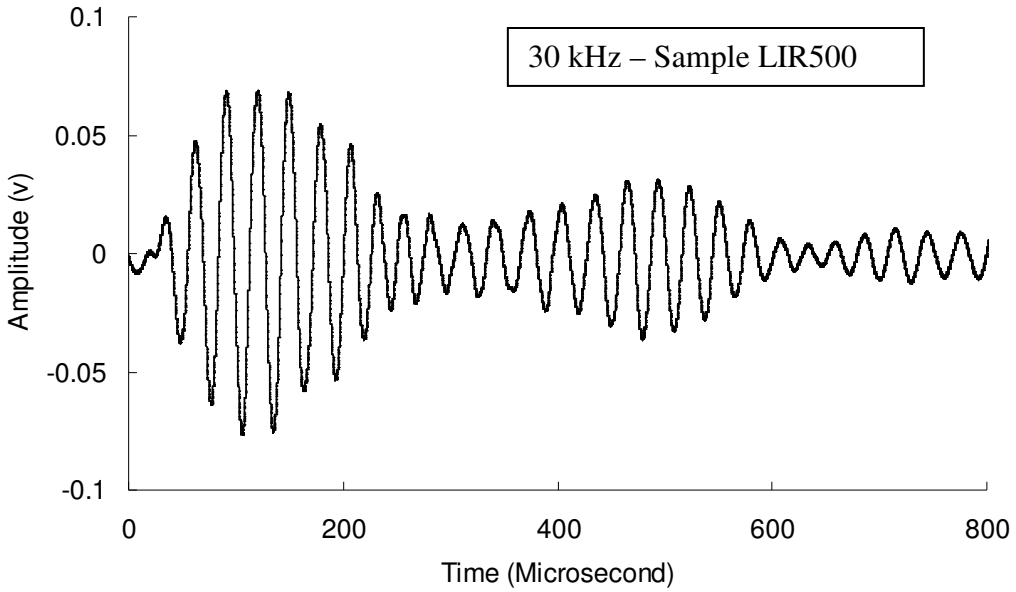

Figure 7-5 Typical waveform – Sample LIR500

Based on the wave travel time in the fully grouted portion of the rock bolts, the group velocity along the central axis of the rebar is estimated to be in a range between 2650 m/s and 2900 m/s. The results are similar to the experimental results (approximately 2700 m/s) obtained by Madenga et al (2004) with slight difference, which may be the result of errors due to noises.

The test results of amplitude ratio at Point C (Figure 1-2) are shown in Figures 7-6. To verify the accuracy of the numerical results, the amplitude ratio of Sample IR500 is also calculated using Equation [7-9] and with parameters obtained from numerical modeling shown in Table 7-2. The calculated results shown in Figure 7-6 match the experimental ones well. This leads to the conclusion that the numerical modeling results have sufficient accuracy.

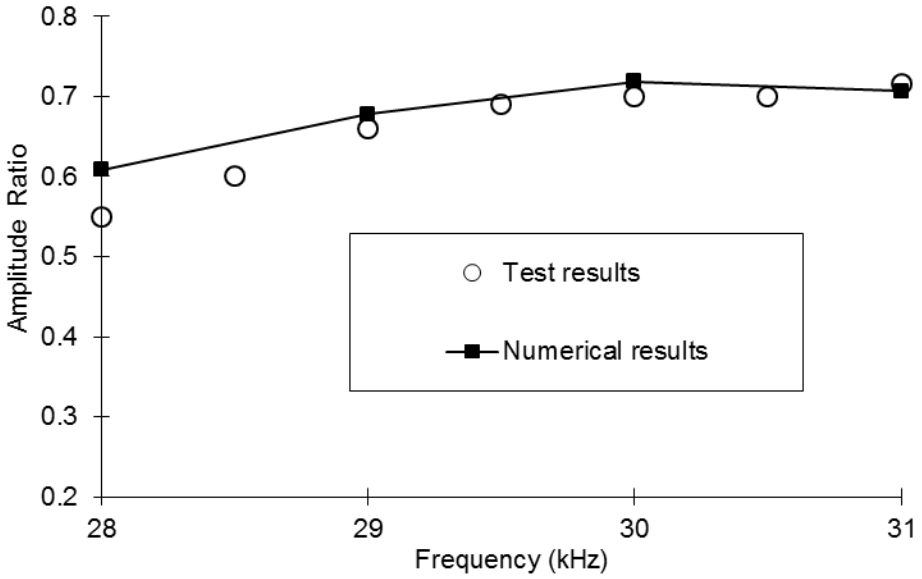

Figure 7-6 Amplitude ratio – Sample LIR500

Comparing factors provided in Table 6-2 and Table 7-2, it is found that α, K_b and K_l for fully grouted rock bolts are the same as those for defected rock bolts with different grout lengths. It can also be observed that K_{MG} and K_{IR} are different. Therefore, it is theoretically possible to identify the difference between rock bolts with an insufficient rebar and rock bolts with a portion of missing grout at the ground end based on the signals measured on the grouting surface near the input end. The fully grout length can also be approximately estimated based on group velocity. If the designed grout length is known, rock bolt defects can be initially identified by group velocity and confirmed by attenuation evaluation.

CHAPTER 8 EFFECTS OF A VOID IN GROUT

In Chapters 6 and 7, two typical defects in grouted rock bolts (an insufficient rebar length or a portion of missing grout at the ground end) are studied. The existence of voids in grout is another typical defect in grouted rock bolts and is studied in this chapter.

Based on the research completed in Chapters 6 and 7, the received echo is reflected at the first reflection point and the attenuation near the reflection point is not the same for different boundary conditions (types of defects). Therefore, it is expected that, for a rock bolt with a void in grout, ultrasonic guided wave echo is reflected at the surface of the void, and the attenuation may be affected by the size of the void due to different boundary conditions.

Grouted rock bolt models are created to study rock bolts with a void in grout. To simplify this problem, the void surface is considered to be perpendicular to the rebar as shown in Figure 8-1. Laboratory tests are used to verify the results obtained from the numerical study.

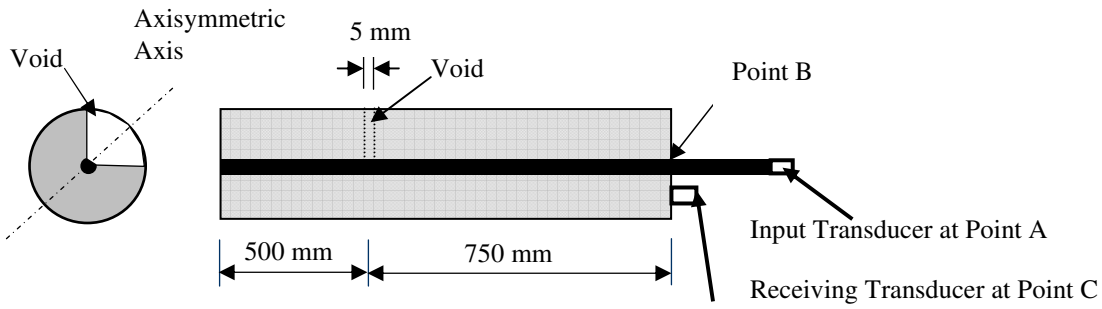

Figure 8-1 Grouted rock bolts with a void

8.1 MODEL AND INPUT PARAMETERS

The models studied in this chapter are rock bolts with a grout length of 1250 mm and a void at the location shown in Figure 8-1. It is found that if the void is too close to the input end, the reflected echo overlaps with the input group and it is difficult to analyze. With a void location at 750 mm measured from the grouting surface at the input end, the input group and echo can be clearly separated. Ultrasonic guided wave behaviours are compared for rock bolts with a void size of 25%, 50%, 75% and 100% of the grouted cross section area.

The geometries of these four models are presented in Table 8-1. Other input parameters of the model are listed in Table 4-1. The sample IDs of V stands for rock bolts with a void. The element sizes used in these models are listed in Table 4-2. The LS-DYNA input file for modeling a typical rock bolts with a void in grout (Sample V75) is provided in Appendix E.

Table 8-1 Chapter 8 Model geometries

Sample Number	Total length (mm)	Grout length (mm)	Free length (mm)	Bolt diameter (mm)	Void Area (%)	Diameter of concrete cylinder (mm)
Sample V25	1300	1250	50	20	25	160
Sample V50	1300	1250	50	20	50	160
Sample V75	1300	1250	50	20	75	160
Sample V100	1300	1250	50	20	100	160
Sample LV50	1100	800	300	20	50	160

To save computing time, the symmetry condition of the sample is considered based on a symmetry axis shown in Figure 8-1 and only a half of the sample is modeled. A typical finite element model (Sample V75) is shown in Figure 8-2. The boundary conditions of the models are presented in Figure 4-4.

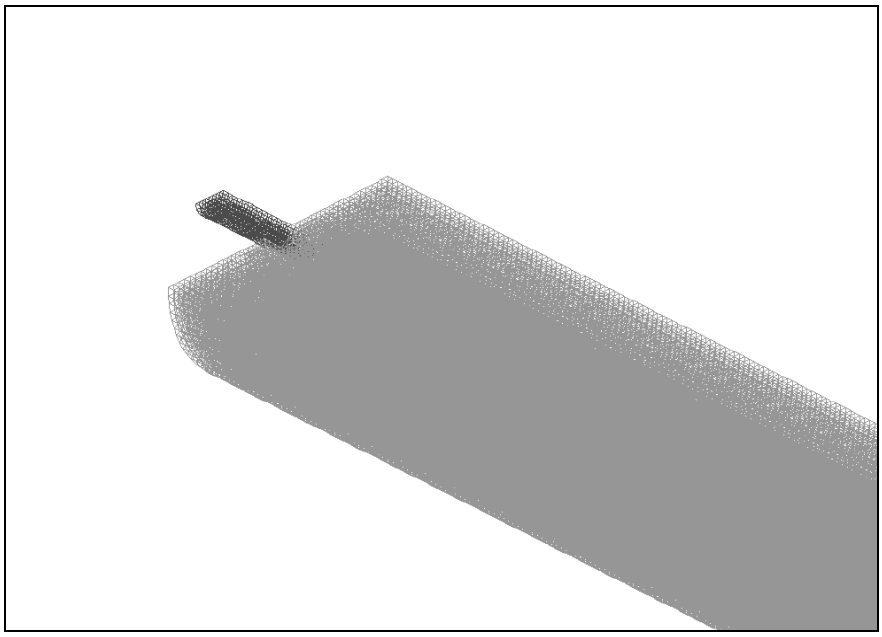

Figure 8-2 Finite element model – Sample V75 (half size)

As discussed before, when a receiver is installed on the grout surface, clear and analyzable signals are received only for input signals within a narrow range of wave frequencies. It is found that the frequency between 29 kHz and 31 kHz is most suitable for the proposed study and the input wave frequency is limited to this range.

8.2 STUDY OF VOID EFFECTS ON ULTRASONIC GUIDED WAVE ATTENUATION

Typical waveforms for Samples V25, V50, V75 and V100 are illustrated in Figures 8-3a) to 8-3d). The input frequency for these waveforms is 30 kHz. These waveforms are obtained at the input end (Point A in Figure 8-1).

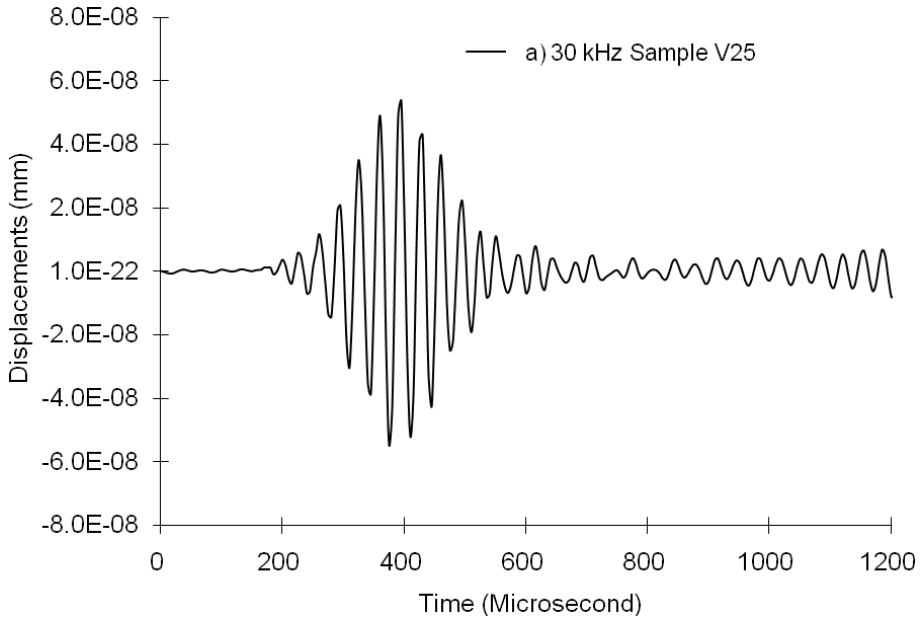
a) 30 kHz Sample V25
8.0E-08
6.0E-08
4.0E-08
2.0E-08
1.0E-22
-2.0E-08
-4.0E-08
-6.0E-08
-8.0E-08
Displacements (mm)
0
200
400
600
800
1000
1200
Time (Microsecond)

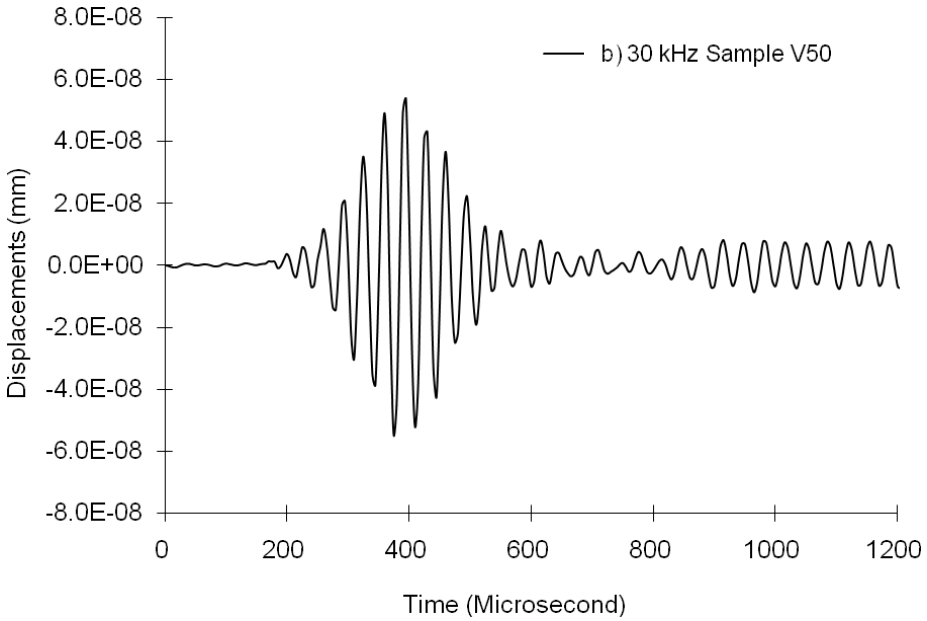
b) 30 kHz Sample V50
8.0E-08
6.0E-08
4.0E-08
2.0E-08
0.0E+00
-2.0E-08
-4.0E-08
-6.0E-08
-8.0E-08
Displacements (mm)
0
200
400
600
800
1000
1200
Time (Microsecond)

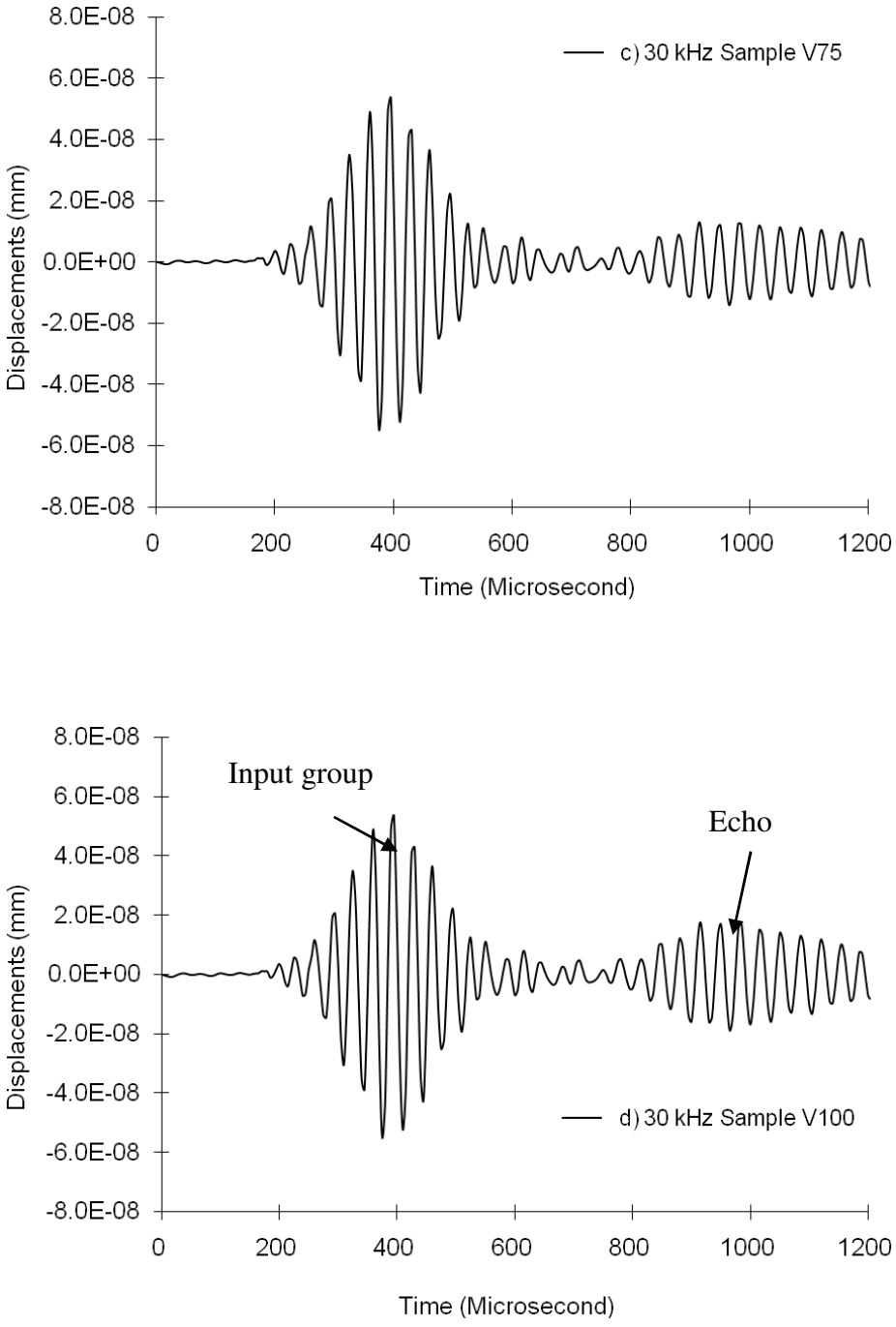

Figure 8-3 Typical waveforms for Samples V25, V50, V75 and V100

As discussed before, the echo obtained at the input end (Point A in Figure 8-1) is expected to be reflected from the first reflection point. The echo of the Figures 8-3b), 8-3c) and 8-3d) are arrived at almost the same time, indicating that their echo are reflected from the same location (the void). It also can be observed that higher echo amplitudes are obtained for rock bolts with a greater void.

Theoretically, the travel time can be determined by the time intervals between the maximum amplitude of the input group and the echo. However, due to the echo of the waveforms are relatively weak, the maximum amplitude of echo is very difficult to identify, especially for rock bolts having a relatively small void in grout. With the numerical models and laboratory samples used in this study, no reliable conclusions regarding the effects of the void on the wave group velocity and travel time are achieved. Study in this chapter focuses on the effects of a grout void on the attenuation of ultrasonic guided waves in a rock bolts with a void in grout.

The echo of Sample V25 (Figure 8-3a)) is very weak. It can be concluded that it is difficult to practically identify a relatively small void using ultrasonic guided waves. Similar observations are obtained from other waveforms which are obtained using input signals with different frequencies.

Figure 8-4 shows the amplitude ratios of Samples V50, V75 and V100, respectively, recorded at the input end (Point A of Figure 8-1). The echo of Sample V25 is too weak to perform analyses.

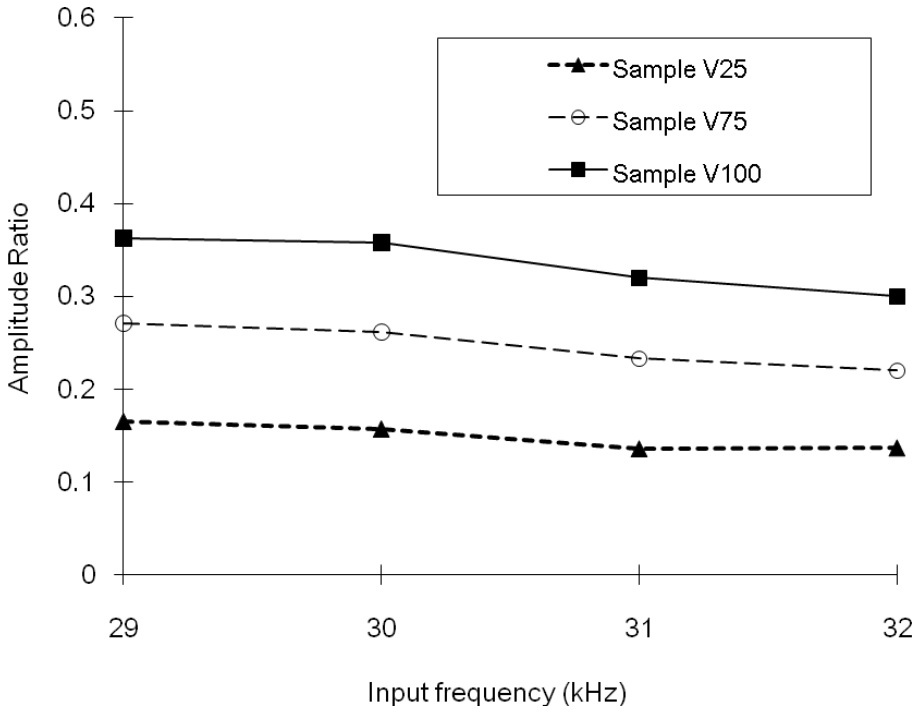

Figure 8-4 Amplitude ratio for rock bolts with a grout void

In this study, attenuation coefficient α of grouted rock bolts, except at the location closing the void, is considered the same as of fully grouted rock bolts. The boundary correction factor K_b of fully grouted rock bolts cannot be directly used for rock bolts with a void in grout due to their different boundary conditions. In this study, K_v is used to represent the void-boundary correction factor of rock bolts with a void and Equation [2-2] is thus modified as Equation [8-1] for rock bolts with a void.

$$-\alpha L = \ln(R) - \ln(K_v) = \ln(R / K_v) \qquad [8\text{-}1]$$

With the amplitude ratio, *R*, obtained at the input end (Point A in Figure 8-1), K_v can be back-calculated using Equation [8-1]. The attenuation coefficients and boundary corrections factors for Samples V50, V75 and V100 are given in Table 8-2.

Table 8-2 Attenuation coefficients and correction factors (Chapter 8)

Frequency (kHz)	Attenuation Coefficient α (m^{-1})	Boundary correction factor K_v		
		Sample V50	Sample V75	Sample V100
29	0.42	0.310	0.509	0.682
30	0.42	0.295	0.492	0.672
31	0.43	0.259	0.444	0.610
32	0.44	0.265	0.426	0.580

Based on the results shown on Table 8-2, it can be concluded that the void-boundary correction factor, K_v, is greater for rock bolts with a larger void in the grout. Figure 8-5 shows a nearly proportional relationship between the boundary correction factor and the size of the void (in percentage of the grout area).

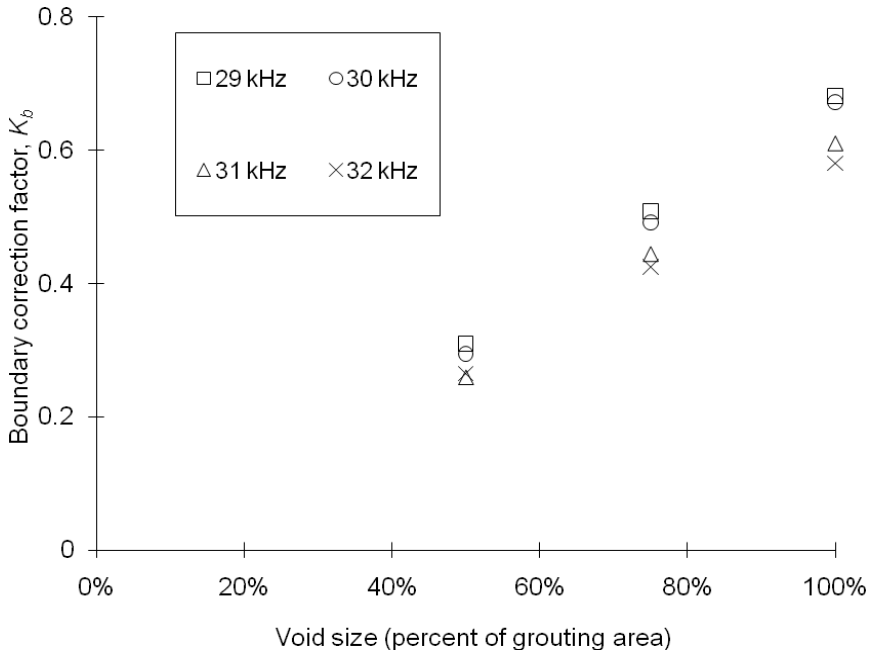

Figure 8-5 Boundary Correction Factors – Samples V50, V75 and V100

8.3 MEASUREMENT LOCATIONS RELATIVE TO THE VOID

As discussed in Chapter 5, the receiving transducer may be installed on the grout surface at the input end at the location as shown in Figure 1-2, and Equation [5-9] can be used to consider the effect of measurement location for grouted bolts without voids in grout. This conclusion is obtained for rock bolts with a symmetric condition. However, because the void is at one side of the rock bolt, waveforms obtained at different locations related to the void may be not the same.

It is understood that the echo is reflected from the void surface. Thus if the receiving transducer is directly over the void, the echo is expected to be stronger (higher amplitude) than at other locations. During this study it is verified that, at locations with the same distance measured from the central of the rebar, the amplitude of the echo varies at different locations and stronger echoes are received on the grout surface over the void than on the other side. The strongest echo is received directly over the central of the void and the weakest at the central of the other side (grout). This location is illustrated on the diametrical line in Figure 8-6.

Figures 8-6a) shows typical waveforms (Sample V75) obtained on the grouting surface directly over the central of the void and Figures 8-6b) shows the waveforms on the other side. The input signal of these waveforms is 30 kHz and measurement locations are 29 mm measured from the central of the rebar. Figure 8-6 clearly shows that the echo of waveform obtained over the void is greater than that over the non-void side.

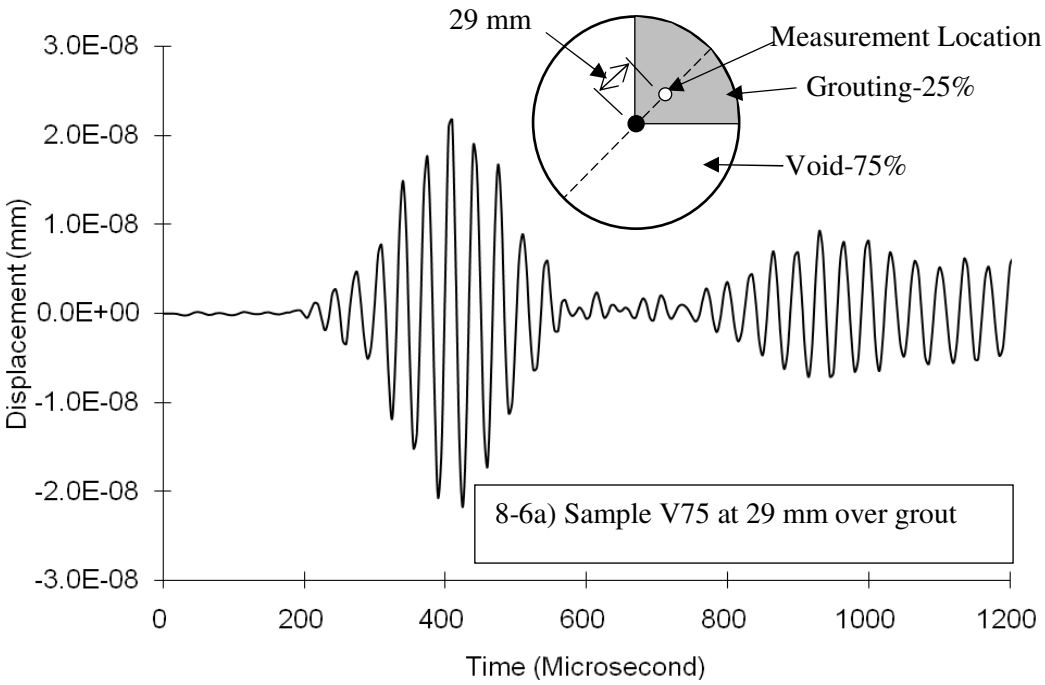

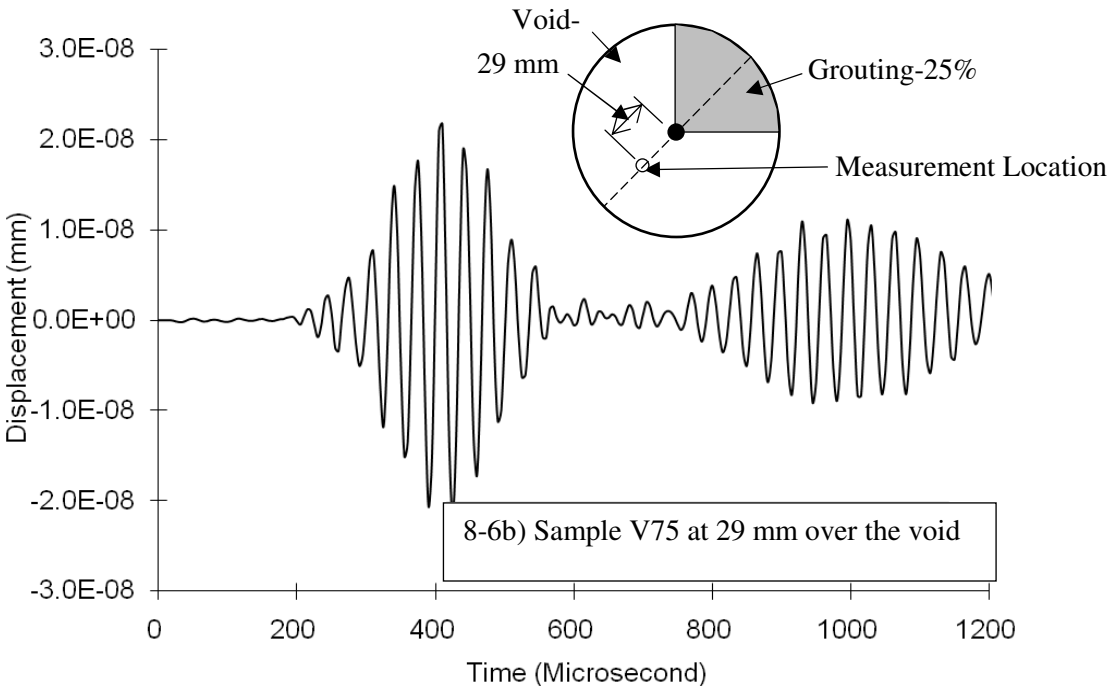

Figure 8-6 Typical waveforms for rock bolts with a grout void

Chapter 5 provided a method to correlate the wave travel time measured on the grouting surface (Point C in Figure 1-2) to location Point B (Figures 1-2 and 8-1). This method is used for rock bolts with a void in grout. It is found that the wave travel time measured over the void may be slightly different from that over the grout as shown in Figure 8-6 and Figure 8-9. However, the received wave is relatively weak and the results are significantly scattered. No accurate conclusion could be made based on numerical and laboratory tests performed in this chapter. The wave travel time may not be accurate for estimating the grout length of a rock bolt with a void in grout.

Equation [5-8] provided a method to correlate the amplitude ratio obtained at Point A and Point C in Figure 1-2. Measurement location correction factor, K_l, is studied for locations with 29 mm measured from the central of the rebar. With the same measurement distance to the central of the rebar (cycle locations), the obtained K_l is generally relatively low over the void side and high over the grouting side. The lowest values are obtained at the location along the axis over the central of the void and the highest along the same axis but over the central of the other side at locations shown in Figure 8-6.

Figures 8-7a), 8-7b) and 8-7c) show K_l obtained along the symmetry axis for Samples V50, V75 and V100. As can be seen, the K_l on the grouting surface at different locations is not the same. Lower K_l is shown over the central of the void.

From experiment tests, K_l for Sample V50 with the measurement location over the central of the void and the non-void side on the grout surface with a 29 mm distance measured from the central of the rebar is provided in Table 8-3, which is the same as illustrated in Figure 8-7a).

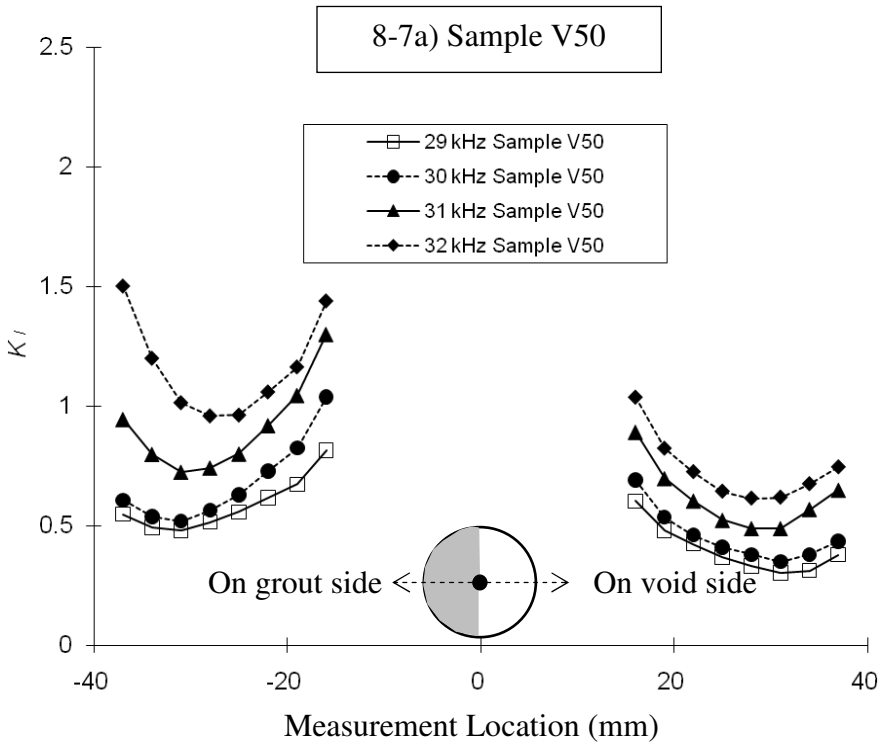
8-7a) Sample V50
29 kHz Sample V50
30 kHz Sample V50
31 kHz Sample V50
32 kHz Sample V50
2.5
2
1.5
1
0.5
0
K I
On grout side
On void side
-40
-20
0
20
40
Measurement Location (mm)

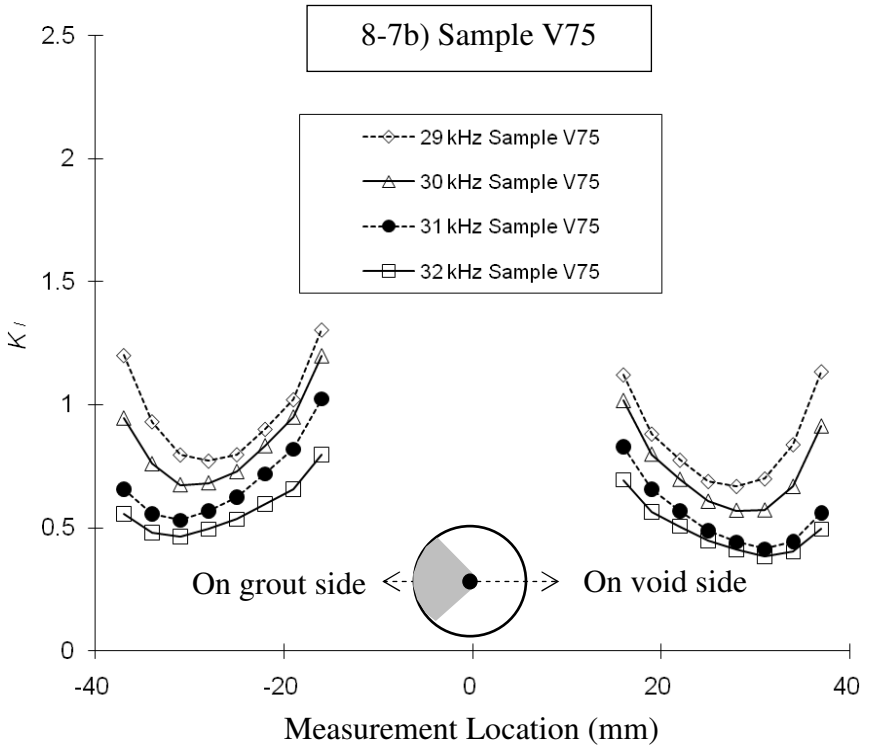
8-7b) Sample V75
29 kHz Sample V75
30 kHz Sample V75
31 kHz Sample V75
32 kHz Sample V75
2.5
2
1.5
1
0.5
0
K I
On grout side
On void side
-40
-20
0
20
40
Measurement Location (mm)

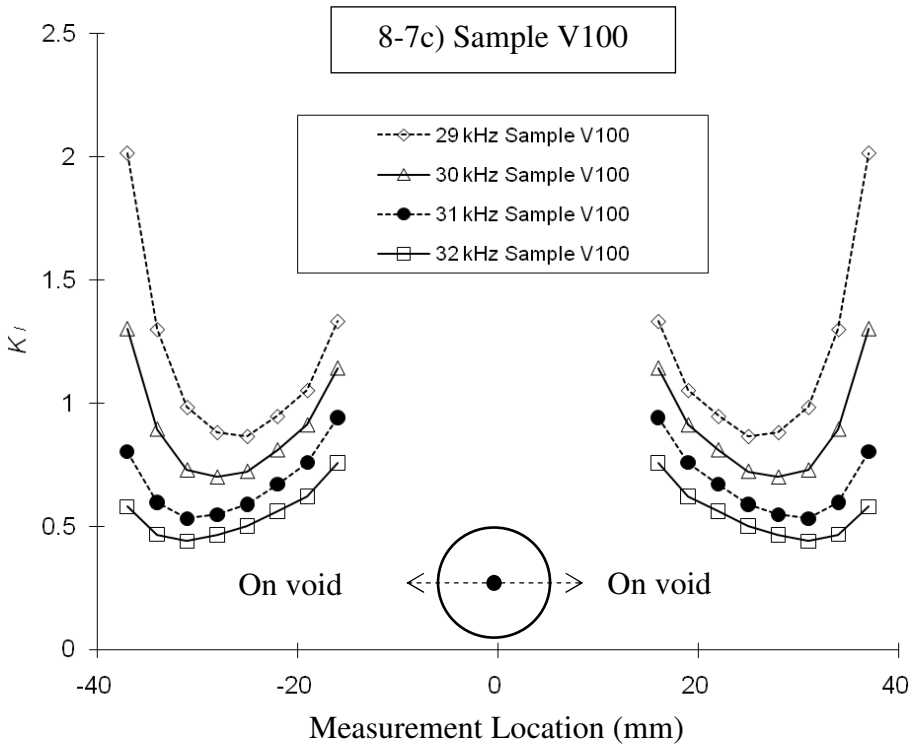

Figure 8-7 Measurement location correlation factors

Table 8-3 Measurement location correction factors (Sample V50)

Frequency (kHz)	29	30	31	32
K_l over the central of the grout side	0.52	0.56	0.74	0.96
K_l over the central of the void	0.33	0.38	0.49	0.61

8.4 EXPERIMENT VERIFICATION

To verify the numerical results above, laboratory tests are performed on a rock bolt, Sample LV50. The geometry of Sample LV50 is illustrated in Figure 8-8 and Table 8-1.

Chapter 5 concluded that K_l is not related to the length measured from the grouting surface at the input end to the first reflection point. For the studied case, the first

reflection point is the void. To verify the above conclusion, the length to the first reflection point for Sample LV50 (500 mm) is assigned to differ from Sample V50 (750 mm). If the conclusion obtained in Chapter 5 is valid for the studied case, the measured amplitude ratio for Sample LV50 (500 mm to void) should be the same as the calculated results based on Tables 8-2 and 8-3, which are obtained from Sample V50 (750 mm to void).

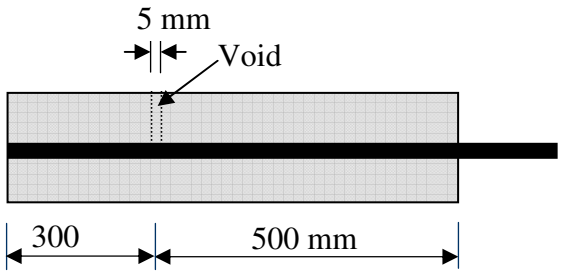

Figure 8-8 Sample LV50

The instrument used in this study is the same as used in Chapter 5. The experiments are conducted by exciting input signals at different frequencies into the input end of the bolt sample (Point A in Figure 8-1). The signal at the grouting surface (Point C in Figure 8-1) is picked up by a transducer and the whole waveform is recorded digitally. During tests, the receiving transducer is installed at 29 mm measured from the central of the rebar. The obtained data are analyzed using the same methods for numerical models.

Figures 8-9a) and 8-9b) show waveforms obtained on the grouting surface at locations shown in Figures 8-6a) and 8-6b), respectively. The input frequency is 31 kHz. The obtained amplitude ratio *R* is shown in Figure 8-10. The amplitude ratio of Sample LV50 is also calculated based on parameters from numerical modeling shown in Tables 8-2 and 8-3 and the result are also shown in Figure 8-10.

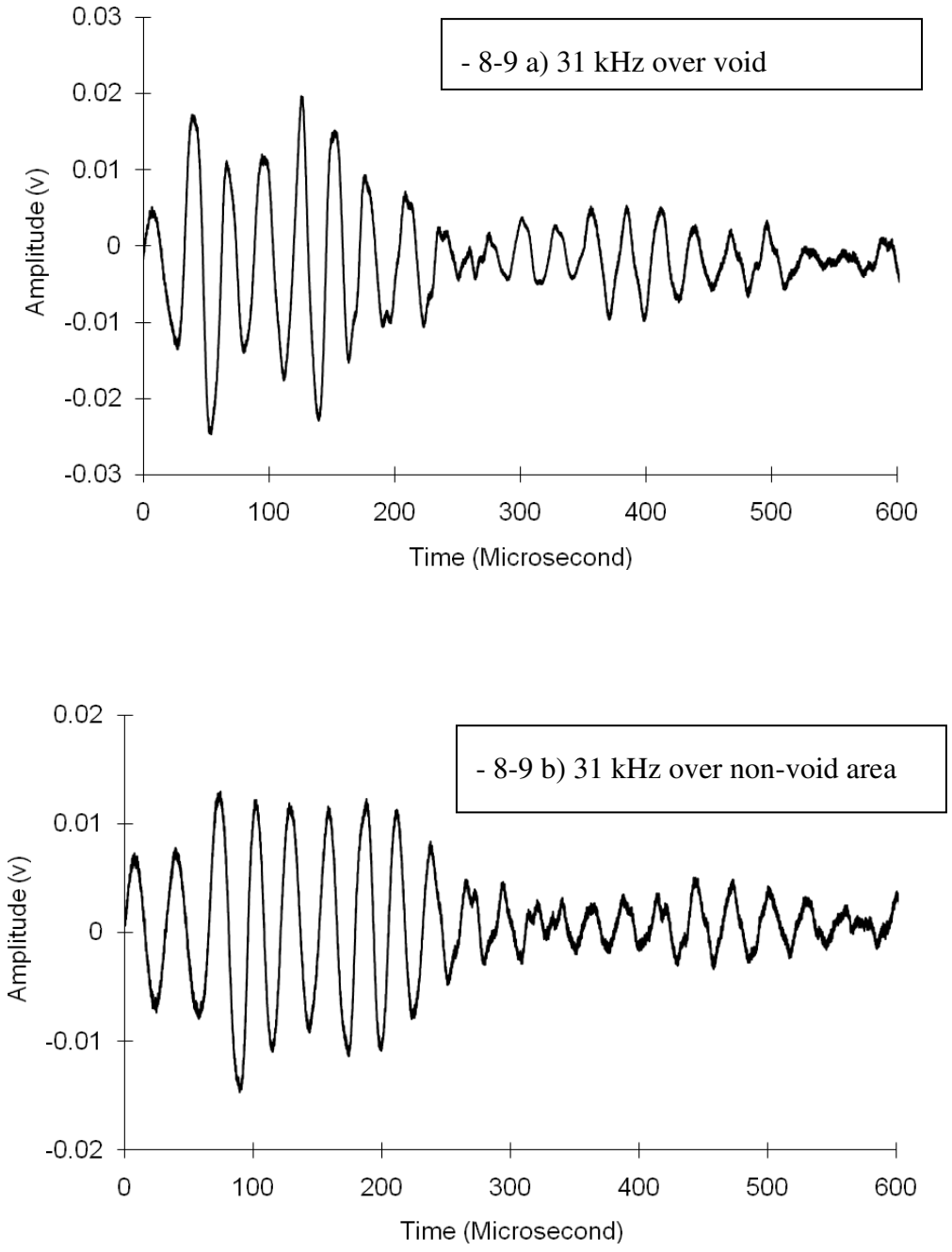

Figure 8-9 Waveforms – Sample LV50

Based on results shown in Figure 8-10, it can be concluded that the numerical results match the experimental ones very well. In addition, it also can be concluded that the

measurement location correction factor K_l is likely not a function of the length to the first reflection point for the studied case.

It can be concluded that it is possible to identify the void by installing the receiving transducer on the grouting surface. The amplitude ratio obtained on the grouting surface is affected by the measurement location. The amplitude ratio obtained over the void is higher than that obtained over the non-void side on the grouting surface.

The conclusions obtained from numerical models are verified by an experimental test. The results show that the numerical modeling has sufficient accuracy.

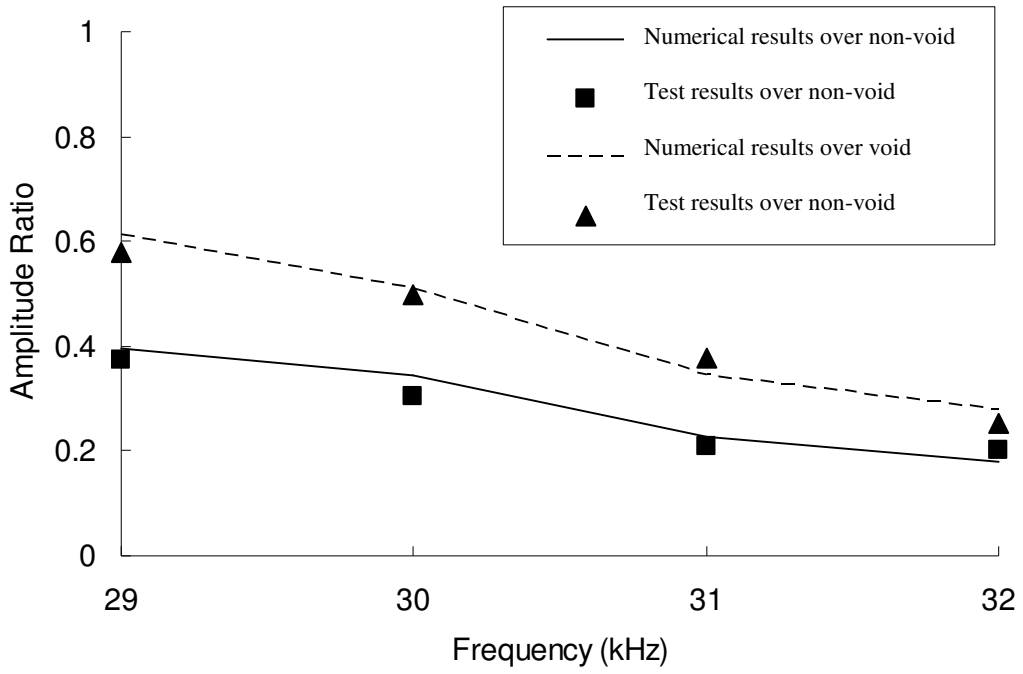

Figure 8-10 Amplitude ratio – Sample LV50

CHAPTER 9 CONCLUSIONS AND RECOMMENDATIONS

Conclusions

The research provides evidence that it is possible to receive meaningful signals by installing the receiving transducer on the grout surface and by using the location correction factor developed in this research. The research also demonstrated that the proposed method could identify three typical installation defects, namely, insufficient rebar length, missing grout at the ground end, and a void in grout.

The proposed field test method of installing the receiving transducer on the grout surface at the input end of the rock bolt is studied. The effects of the measurement location are analyzed by numerical models and experiments are conducted to verify the results. A location correction factor is introduced to correlate the amplitude ratio along the bolt and that on the grout surface. This factor is found to vary with the measurement location and wave frequency but it is constant at a specific location and for a specific wave frequency.

The results indicate that it is possible to receive meaningful signals by installing the receiving transducer on the grout surface and that by using the location correction factor. It is also possible with the data recorded on the grout surface to determine the attenuation and wave velocity of guided waves in grouted rock bolts with reasonable accuracy. The study also shows the proper measurement location of 27 to 32 mm from the bolt center.

Numerical studies are performed for fully grouted rock bolts and rock bolts with insufficient rebar and with missing grout at the ground end. The result of numerical modeling indicates that echo of rock bolts with insufficient rebar length is reflected from the end of the rebar; and the echo of rock bolts with missing grout at the ground end is reflected from the end of the grouting. The travel time can be used to evaluate the approximate fully grouted rebar length with reasonable accuracy for rock bolts with these two types of defects.

The wave attenuation along the fully grouted segment of full grouted rock bolts and rock bolts with insufficient rebar and with missing grout at the ground end is considered the same. However, the boundary effects at the first reflection point at the ground end are different for different types of conditions. Correction factors are used to represent the wave energy loss for the two types of defects – insufficient rebar length and missing grout at the ground end, in this study. A practical method is developed to determine these correction factors. The values of these correction factors are different and may provide a means of identifying the type of bolt defects.

Numerical studies are performed for rock bolts with a void in grout. The results of modeling indicate that the boundary effects at the fist reflection point (the void) are not the same for different sizes of voids. The amplitude ratio measured by transducer installed on the grout surface is affected by the receiver transducer installation location and the location of the void. The amplitude ratio obtained over the void is higher than obtained over the non-void side on the grouting surface.

The results obtained from numerical models are verified by experiments and the results match the numerical results very well. This further supports accuracy of numerical modeling results.

Recommendations

This study focus on the feasibility of the proposed test method and the wave behaviour in rock bolts with some typical defects. The geometry and parameters used in the numerical modeling and the materials used to make experimental samples are limited (for example, only a grout diameter of 160 mm is used). The conclusions obtained from this study need to be verified in field tests and further researches are still required as follows:

- Field tests to verify the validity of this method is still required. Full scale experiments or field experiments are recommended for the future research.

- The effects of the grout length on the attenuation and group velocity are studied in the reported research. Further research regarding effects of grouted quality (for different grout materials) on wave behaviour is required before this method can be used practically.

- In both of the numerical study and laboratory test, clear and analyzable signals could only be received for tests with input signals having a narrow range of frequencies. In this study, it was found that the suitable frequency was affected by the sample diameter (160 mm), and transducer used in laboratory tests was selected based on trial tests on rock bolt samples. However, the rock bolts in field may have a different diameter and the rock mass surrounding the rock bolt may also play an important role to affect the suitable frequency and the transducer selection. Further study is required.

- It is known from this research that the grouting status at the ground end affects the echo. When performing in-situ tests, the grout will be between the rebar and the surrounding rocks, which properties (Young's Modulus, Poisson's Ratio and ect.) may vary in a wide range. This variation of the rock mass may affect the echo received. Further research is required. In addition, study on the possibility of using this method to identify the rock mass properties may also be considered.

- Based on the study in this thesis, it seems possible to detect the grout length and rock bolts with typical defects in the field tests. Further study may be required to find other applications of this method.

BIBLIOGRAPHY

Achenbach, J. D. Wave propagation in elastic solids, Applied Mathematics and Mechanics, North-Holland Publishing Company, Amsterdam, The Netherland, 1973

American standard test method (ASTM) E 610-82, Standard Definitions of Terms Relating to Acoustic Emission, ASTM International, West Conshohocken, PA, 1982

Beard, M. D., Lowe, M. J. S., and Cawley, P. Development of a guided wave inspection technique for rock bolts; Insight, vol. 44, No. 1, pp 19-23, 2002

Beard, M.D and Lowe, M.J.S. Non-destructive testing of rock bolts using guided ultrasonic waves, Intl Journal of Rock Mechanics & Mining Science, vol. 40, pp 527-536, 2003

Beard, M.D., Lowe, M.J.S., and Cawley, P. Ultrasonic guided waves for inspection of grouted tendons and bolts, Journal of Materials in Civil Engineering, vol. 15, No. 3, pp 212-218, 2003

Berkhout, A. J. Applied seismic wave theory. Appendix E. Elsevier, Amsterdam, The Netherland, pp. 377, 1987

Blitz, J. and Simpson, G., Ultrasonic methods of non-destructive testing, Springer-Verlag, New York, LLC., 1991

Boadu, F. K. Fractal characterization of fractures: effect of fractures on seismic wave velocity and attenuation, Unpublished Ph.D Thesis, Georgia Institute of Technology, Atlanta, USA, 1994

Bolstad, D. and Hill, J., U.S. Bureau of mines rock bolting research, Proceedings of the international symposium on rock bolting, Abisko, Sweden, pp. 313-320, 1983

Bowles, J.E., Foundation analysis and design, McGraw-Hill, New York, LLC., ISBN 0-07-912247-7, 1997

Choquet, P., Rock Bolting Practical Guide, Canada Center for Mineral and Energy, 1991

Cui, Y., Study of Group Velocity and Attenuation of Ultrasonic Guided Waves in Grouted Rock Bolts, Master Thesis of Dalhousie University, 2005

Cui, Y. and Zou, D. H., Numerical simulation of attenuation and group velocity of guided ultrasonic wave in grouted rock bolts, J. of Applied Geophysics. Vol. 59(1), pp. 79-87, 2006

Cui, Y. and Zou, D. H. Assessing the effects of insufficient rebar and missing grout in grouted rock bolts using guided ultrasonic waves (accepted), Journal of Applied Geophysics, Vol. 79 (2012), pp.64-70, 2012

Dywidag-Systems International (DSI), Product index, 2010

Federal Highway Administration (FHWA), Design and Construction of Driven Pile Foundations, FHWA HI 97-013, 1997

Federal Highway Administration (FHWA), Context sensitive rock slope design solutions, FHWA-CFL/TD-11-002, 2011

Ge, M. and Kaiser, P. K., Practical application of an innovative microseismic source location, Geotechnical and Geological Engineering, vol. 10, pp: 163-184, 1992

Ge, M., Mrugala, M. and Iannacchione, A.T., Microseismic monitoring at a limestone mine, Geotechnical and Geological Engineering, vol. 27, pp: 325-339

Gibowicz, S. J. and Kidjko, A. An introduction to mining seismology, Academic Press, San Diego, CA, USA, 1994

Gilkey, H. J., Chamberlin, S.J. and Beal, R.W., Bond between concrete and steel, Eng. Rep. No. 26, Lowa Eng. Exp. Sta., Lowa State College, Ames, 1956.

Han, S., Lee, I., Lee, Y. and Lee, J. Evaluation of rock bolt integrity using guided ultrasonic waves, Geotechnical Testing Journal, vol. 32, No. 1, pp: 31-38, 2009

Hawkes, J.M. and Evans, R.H., Bond stresses in reinforced concrete columns and beams, Struct. Eng., 29(12), pp: 323-327, 1951

Hoek, E., Kaiser, P. K. and Bawden, Support of underground excavations in hard rock, Taylor & Francis, London, England, 2000

Ivanovic, A, Neilson, R. D. and Rodger, A. A., Lumped parameter modeling of ground anchorage systems, Geotechnical Engineering, 1499(2), 103-113, 2001

Kelly, A.M., and Jager, A.J., Critically evaluate techniques for the in-situ testing of steel tendon grouting effectiveness as a basis for reducing fall of ground injuries and fatalities, Final Project Report Under the Auspices of CSIR to the Safety in Mines Research Advisory Committee, South Africa, Project No. GAP 205, 1996

Kilic, A., Yasar, E. and Celik, A.G., Effect of grout properties on the pull-out load capacity of fully grouted rock bolt, Tunneling and Underground Space Technology, vol. 17, pp 355-362, 2002

Kim, K. Y. and Sachse, W., Point-source/Point-receiver method, Modern acoustical techniques for the measurement of mechanical properties, Academic Press, Waltham, Massachusetts, 2001

Klimentos, T. and McCann, C., Relationships between compressional wave attenuation, porosity, clay content and permeability of sandstones, Geophysics, vol. 55, 998-1014, 1990

Lee, J.S., Kim, H.J., Lee, I.M., Hand, S.I. and Lee, Y.J., Rock bolt integrity evaluation in tunneling using ultrasonic NDT techniques, Proceedings of 33rd ITA-AITES Word Tunnel Congress – Underground Space – The 4th Dimension of Metropolises, Vol. 1, pp: 321-326, 2007

Levy, M., Modern acoustical techniques for the measurement of mechanical, properties, Academic Press, Waltham, Massachusetts, 2001.

Livermore Software Technology Corporation. LS-DYNA, Version: PC-DYNA_960, Livermore, CA, US, 2001

Luo, J.L. A new rock bolt design criterion and knowledge-based expert system for stratified roof, Virginia Polytechnic Institute and State University, Unpublished Ph.D. thesis, Blacksburg, Virginia, USA, 1999

Madenga, V. Application of guided waves to grout quality testing of rock bolts, M.A.Sc Thesis, Dalhousie University, Halifax, NS, Canada, 2004

Madenga, V., Zou D. H. and Zhang C.S., Effects of curing time and frequency on ultrasonic wave velocity in grouted rock bolts, Journal of Applied Geophysics, Vol. 59(1), pp: 79-87, 2006

McVay, M.C., Alvarez V., Zhang L., Perez A., Gibsen A., Estimating driven pile capacities during construction, Civil and Coastal Engineering, University of Florida, US, 2002

Milne, G., Condition monitoring and integrity assessment of rock anchorages, published PhD thesis, University of Aberdeen, U.K., 1999

O'connell, R. D., and Budiansky, B. Seismic velocities in dry and saturated cracked solids, J. Geophys. Res., vol., 79, pp5412-5426, 1974

Peng, S. Coal mine ground control, John Wiley & Sons Inc., pp. 131-173, New Yord, LLC., 1984

Phillips, S.H.E., Factors affecting design of anchorages in rock, Cementation research report R48/70, Cementation Research Ltd., London, UK, 1970

Pile Dynamics Inc. (PDI). GRLWEAP Background Report, 4535 Renaissance Parkway, Cleveland. OH, 44128, USA. www.pile.com, 2005

Pile Dynamics Inc. (PDI). CAPWAP Background Report, 4535 Renaissance Parkway, Cleveland. OH, 44128, USA. www.pile.com, 2006

Rabcewicz, L. V., Principles of dimensioning the supporting system for the NATM, Water power (March)-88, 1973

Rose, J.L., Ultrasonic Waves in Solid Media, Cambridge University Press, Cambridge, UK, 1999

Starkey, A., Internal Report, Univ. of Aberdeen, U.K., 2000

Sundholm, S., The quality control of rock bolts, Proceeding of the Society for Rock Mechanics, vol. l 6, No. 2, pp1255-1264, 1988

Tadolini, S. and Koch, R., Cable supports for improved longwall gateroad stability, Proceeding of 12th Conference on Ground Control in Mining, Morgantown, WV, pp. 9-15, 1993

Tang, X.M. and Cheng, A., Handbook of geophysical exploration seismic exploration, Vol. 24, Quantitative borehole acoustic methods, Elsevier, ISBN 0-08-044051-7, 2004

Tavakoli, M. B. and Evans, J. A., The effect of bone structure on ultrasonic attenuation and velocity, Ultrasonics, vol. 30, 389-395, 1992

TiePie engineering, Multi Channel Software User Manual, Sneek, The Netherlands, 2012

Thurner, H.F., Instrument for non-destructive testing of grouted rock bolts, 2nd International Symposium on Filed Measurements in Geomechanics, Balkema, Rotterdam, pp 135-143, 1988

Vrkljan, I., Nondestructive procedure for testing grouting quality of rockbolt anchors, Proceedings of the Congress of the International Society for Rock Mechanics, vol. 9, No. 2, pp 1475-1478, 1999.

Wang, C. He, W. Ning, J. and Zhang, C., Propagation properties of guided wave in the anchorage structure of rock bolts, Journal of Applied Geophysics, Vol. 69, pp: 131-139, 2009

Weigal, W., Channel iron for roof control, Engineering and Mining Journal, vol. 144, pp. 70-72, 1943

Widjaja, B., Wave Equation Analysis and Pile Driving Analyzer for Driven Piles: 18th Floor Office Building Jakarta Case, International Civil Conference “Towards Sustainable Civil Engineering Practice”, Surabaya, 2006

Xanthakos, P. P., Ground anchors and anchored structured, John Wiley & Sons Inc., ISBN 0-471-52520-0, New York, LLC., 1991

Yilmaz, O., Seismic data processing, SEG Investigations in Geophysics No. 2, Society of Exploration Geophysicists, 1987

Zhang, C. H., Zou, D.H. and Madenga, V. Numerical simulation of wave propagation in grouted rock bolts and the effects of mesh density and wave frequency, Int'l J. of Rock Mechanics and Mining Science & Geomechanics Abs, Vol. 43 (4), pp. 634-639, 2006

Zhang, C. H., Li, Y., Zhao, Y. S. and Zou, D.H. Study on optimum excitation wave in grout quality nondestructive testing of rock bolt, Chinese Journal of Rock Mechanics and Engineering, Vol. 25, No. 6, pp: 1240-1245, 2009

Zou, D.H., Analysis of in situ rock bolt loading status. International Journal of Rock Mechanics & Mining Sciences, SINOROCK 2004 Paper 3A 08, vol. 41, 2004

Zou, D. H., Cui, Y., Madenga, V., and Zhang, C. Effects of frequency and grouted length on the behaviour of Guided Ultrasonic Wave Propagating in Rock Bolts, Int'l J. of Rock Mechanics and Mining Science, Vol. 44(6), pp. 813-819, 2007

Zou, D.H. , Cheng, J.L., Yue, R.J., Yang, F.Z., Cui, Y. and Zhu, Y.Y. Investigation of grouted rock bolts using guided ultrasonic waves, 2010 International Conference on Mine Hazards Prevention and Control, pp. 130-135, 2010,

Zou, D. H. and Cui, Y. A new approach for field instrumentation in grouted rock bolt monitoring using guided ultrasonic waves, Journal of Applied Geophysics, Vol. 75 (2011), pp.506-512

Zou, D. H. and Cui, Y. Assessing Effects of grouting voids in grouted rock bolts using guided ultrasonic waves (in press – submitted to Journal of Applied Geophysics), 2012

APPENDIX A MATLAB INPUT FILE OF FILTER

This input file is used to filter the recorded raw waveforms to narrow the frequency band around each testing frequency suggested by Madenga et al (2006).

```
% fielter for lowpass

clear; close all;
clc
[dat,datpath]=uigetfile('*,txt','select a file:');
s=[datpath,'\'dat];
S=load(s);
[N]=size(S);
st=max(N)*(2e-7);
fs=1/(2e-7);
x=zeros(N);
[b,a]=butter(9,25*1000/(fs/2))
x=filtfilt(b,a,S)
f=[dat(1:8) '_' 'low.txt'];
dlmwrite(f,x)

% fielter for highpass

clear; close all;
clc
[dat,datpath]=uigetfile('*,txt','select a file:');
s=[datpath,'\'dat];
S=load(s);
[N]=size(S);
st=max(N)*(2e-7);
fs=1/(2e-7);
```

```
x=zeros(N);
[b,a]=butter(9,15*1000/(fs/2),'high', 's')
x=filtfilt(b,a,S)
f=[dat(1:8) '_' 'high.txt'];
dlmwrite(f,x)
```

APPENDIX B LS-DYNA INPUT FILE OF SAMPLE FG750

This is a typical input file for the study of the new approach of the field test method.

```
*KEYWORD
*TITLE
model of dynamic respond of rock bolt
*include
load_curve_25.k
*CONTROL_CONTACT
5.000E-02,0.000E+00,0,0,1,0,0,0
0,0,0,0,0.000E+00,0,0,0
*CONTROL_OUTPUT
1,0,0,0,0.000E+00,1,99000,0
0
*CONTROL_SOLUTION
0
*CONTROL_TERMINATION
8.00,0,0.000E+00,0.000E+00,25.0
*CONTROL_TIMESTEP
0.000E+00,0.000E+00,0,0.000E+00,0.000E+00,0,0,0
*DATABASE_NODOUT
0.500E-02
*DATABASE_BINARY_D3PLOT
0.5,0
*DATABASE_BINARY_D3THDT
0.50E-03,0
*DATABASE_EXTENT_BINARY
0,0,0,1,0,1,0,0
0,0,0,0,0,0
$*damping_global
$  0,1.5
*damping_part_mass
  1,10,0.05,0
*damping_part_mass
  2,10,0.5,0
*DEFINE_CURVE
 10,,1,,
 0.0,5
 11,5
*control_damping
100,1.0e-3,0.995,0,0.9
$
$ DEFINITION OF MATERIAL     1
```

```
$
*MAT_PLASTIC_KINEMATIC
1,7.840E-03,2.100E+05,0.300,2.100E+04,2.00,0.000E+00
0.000E+00,0.000E+00,0.000E+00
*HOURGLASS
1,0,0.000E+00,0,0.000E+00,0.000E+00
*SECTION_SOLID
1,1,0
*PART
rock bolt
1,1,1,0,1,0
$
$ MATERIAL CARDS
$
$
$ DEFINITION OF MATERIAL     2
$
*MAT_ELASTIC
2,2.405E-03,3.700E+04,0.250,,,
*HOURGLASS
2,0,0.000E+00,0,0.000E+00,0.000E+00
*SECTION_SOLID
2,1,0
*PART
surrounding rock
2,2,2,0,2,0
$
$ NODES
$
*NODE
$
*NODE
1,0.000000000E+00,0.000000000E+00,-10.0000000,2,6
2,0.000000000E+00,0.000000000E+00,-7.50000000,2,6
3,0.000000000E+00,0.000000000E+00,-5.00000000,2,6
4,0.000000000E+00,3.82683420,-9.23879528,0,0
……
((nodes between are not listed)
……
126556,800.000000,79.8454056,-4.97099543,0,0
126557,800.000000,80.0000000,0.000000000E+00,3,4
$
$ ELEMENT CARDS FOR SOLID ELEMENTS
$
*ELEMENT_SOLID
1,1,1,10,13,4,2,11,14,5
```

2,1,10,19,22,13,11,20,23,14
3,1,19,28,31,22,20,29,32,23
4,1,28,37,40,31,29,38,41,32
5,1,37,46,49,40,38,47,50,41
6,1,46,55,58,49,47,56,59,50
……
(elements between are not listed)
……
115939,2,126466,126488,126490,126468,126467,126489,126491,126469
115940,2,126488,126510,126512,126490,126489,126511,126513,126491
115941,2,126510,126532,126534,126512,126511,126533,126535,126513
115942,2,126532,126554,126556,126534,126533,126555,126557,126535
$
$ NODAL TIME HISTORY BLOCKS
$
*DATABASE_HISTORY_NODE
$...>....1....>....2....>....3
251,253,255,321,323,85144
85146,85148,85150,85152,85154
85156,85158,85160,85162,85164
2671
2869
3067
3271
3469
3667
3871
4069
$
$ PRESSURE LOADS
$
*LOAD_SEGMENT
1,1.00,0.000E+00,1,4,5,2
*LOAD_SEGMENT
1,1.00,0.000E+00,2,5,6,3
*LOAD_SEGMENT
1,1.00,0.000E+00,4,7,8,5
*LOAD_SEGMENT
1,1.00,0.000E+00,5,8,9,6
*LOAD_SEGMENT
1,1.00,0.000E+00,3,6,156,154
*LOAD_SEGMENT
1,1.00,0.000E+00,154,156,157,155
*LOAD_SEGMENT
1,1.00,0.000E+00,6,9,158,156
*LOAD_SEGMENT

```
1,1.00,0.000E+00,156,158,159,157
*LOAD_SEGMENT
1,1.00,0.000E+00,9,8,256,158
*LOAD_SEGMENT
1,1.00,0.000E+00,158,256,257,159
*LOAD_SEGMENT
1,1.00,0.000E+00,8,7,258,256
*LOAD_SEGMENT
1,1.00,0.000E+00,256,258,259,257
*END
```

APPENDIX C LS-DYNA INPUT FILE OF SAMPLE MG750

This is a typical input file for the study of rock bolts with a portion of missing grout.

```
*KEYWORD
*TITLE
model of dynamic respond of rock bolt
*include
load_curve_25.k
*CONTROL_CONTACT
5.000E-02,0.000E+00,0,0,1,0,0,0
0,0,0,0,0.000E+00,0,0,0
*CONTROL_OUTPUT
1,0,0,0,0.000E+00,1,99000,0
0
*CONTROL_SOLUTION
0
*CONTROL_TERMINATION
0.100,0,0.000E+00,0.000E+00,25.0
*CONTROL_TIMESTEP
0.000E+00,0.000E+00,0,0.000E+00,0.000E+00,0,0,0
*DATABASE_NODOUT
0.500E-02
*DATABASE_BINARY_D3PLOT
0.5,0
*DATABASE_BINARY_D3THDT
0.50E-03,0
*DATABASE_EXTENT_BINARY
0,0,0,1,0,1,0,0
0,0,0,0,0,0
$*damping_global
$  0,1.5
*damping_part_mass
  1,10,0.05,0
*damping_part_mass
  2,10,0.5,0
*DEFINE_CURVE
 10,,1,,
 0.0,5
 11,5
*control_damping
100,1.0e-3,0.995,0,0.9
$
$ DEFINITION OF MATERIAL     1
$
```

```
*MAT_PLASTIC_KINEMATIC
1,7.840E-03,2.100E+05,0.300,2.100E+04,2.00,0.000E+00
0.000E+00,0.000E+00,0.000E+00
*HOURGLASS
1,0,0.000E+00,0,0.000E+00,0.000E+00
*SECTION_SOLID
1,1,0
*PART
rock bolt
1,1,1,0,1,0
$
$ MATERIAL CARDS
$
$
$ DEFINITION OF MATERIAL     2
$
*MAT_ELASTIC
2,2.405E-03,3.700E+04,0.250,,,
*HOURGLASS
2,0,0.000E+00,0,0.000E+00,0.000E+00
*SECTION_SOLID
2,1,0
*PART
surrounding rock
2,2,2,0,2,0
$
$ NODES
$
*NODE
1,0.000000000E+00,0.000000000E+00,-10.0000000,2,6
2,0.000000000E+00,0.000000000E+00,-7.50000000,2,6
3,0.000000000E+00,0.000000000E+00,-5.00000000,2,6
4,0.000000000E+00,3.82683420,-9.23879528,0,0
5,0.000000000E+00,3.13595653,-7.05310202,0,0
……
((nodes between are not listed)
……
136071,2299.875,9.23879528,-3.82683444,0,0
136072,2299.875,10,0,3,4
136073,2303,7.05310202,-3.13595676,0,0
136074,2303,7.5,0,3,4
136075,2303,9.23879528,-3.82683444,0,0
136076,2303,10,0,3,4
$
$ ELEMENT CARDS FOR SOLID ELEMENTS
$
```

```
*ELEMENT_SOLID
1,1,1,10,13,4,2,11,14,5
2,1,10,19,22,13,11,20,23,14
3,1,19,28,31,22,20,29,32,23
4,1,28,37,40,31,29,38,41,32
5,1,37,46,49,40,38,47,50,41
6,1,46,55,58,49,47,56,59,50
7,1,55,64,67,58,56,65,68,59
8,1,64,73,76,67,65,74,77,68
……
(elements between are not listed)
……
121950,1,13266,135909,135911,13268,13267,135910,135912,13269
121951,1,11769,135762,135761,11768,13268,135911,136009,14266
121952,1,13268,135911,136009,14266,13269,135912,136010,14267
121953,1,11768,135761,135760,11767,14266,136009,136011,14268
121954,1,14266,136009,136011,14268,14267,136010,136012,14269
$
$ NODAL TIME HISTORY BLOCKS
$
*DATABASE_HISTORY_NODE
$...>....1....>....2....>....3
136004
13265,13267,13269,14267,14269
99840,99842,99844,99846,99848
99850,99852,99854,99856,99858
99860
13163
12965
12767
12563
12365
12167
11963
7511,7513,7515,9517,9519,94340
94342,94344,94346,94348,94350
94352,94354,94356,94358,94360
7409,7411,7413,9449,9451
7313,7315,7317,9385,9387
6911,6913,6915,9117,9119
6509,6511,6513,8849,8851
6113,6115,6117,8585,8587
5711,5713,5715,8317,8319
5309,5311,5313,8049,8051
4913,4915,4917,7785,7787
4511,4513,4515,7517,7519
```

```
$
$ PRESSURE LOADS
$
*LOAD_SEGMENT
1,1.00,0.000E+00,135898,135901,135902,135899
*LOAD_SEGMENT
1,1.00,0.000E+00,135899,135902,135903,135900
*LOAD_SEGMENT
1,1.00,0.000E+00,135900,135903,136005,136003
*LOAD_SEGMENT
1,1.00,0.000E+00,136003,136005,136006,136004
*LOAD_SEGMENT
1,1.00,0.000E+00,135901,135904,135905,135902
*LOAD_SEGMENT
1,1.00,0.000E+00,135902,135905,135906,135903
*LOAD_SEGMENT
1,1.00,0.000E+00,135903,135906,136007,136005
*LOAD_SEGMENT
1,1.00,0.000E+00,136005,136007,136008,136006
*LOAD_SEGMENT
1,1.00,0.000E+00,135906,135905,136073,136007
*LOAD_SEGMENT
1,1.00,0.000E+00,136007,136073,136074,136008
*LOAD_SEGMENT
1,1.00,0.000E+00,135905,135904,136075,136073
*LOAD_SEGMENT
1,1.00,0.000E+00,136073,136075,136076,136074
*END
```

APPENDIX D LS-DYNA INPUT FILE OF SAMPLE IR750

This is a typical source for the study of rock bolts with an insufficient rebar.

```
*KEYWORD
*TITLE
model of dynamic respond of rock bolt
*include
load_curve_25.k
*CONTROL_CONTACT
5.000E-02,0.000E+00,0,0,1,0,0,0
0,0,0,0,0.000E+00,0,0,0
*CONTROL_OUTPUT
1,0,0,0,0.000E+00,1,99000,0
0
*CONTROL_SOLUTION
0
*CONTROL_TERMINATION
6.00,0,0.000E+00,0.000E+00,25.0
*CONTROL_TIMESTEP
0.000E+00,0.000E+00,0,0.000E+00,0.000E+00,0,0,0
*DATABASE_NODOUT
0.500E-02
*DATABASE_BINARY_D3PLOT
0.5,0
*DATABASE_BINARY_D3THDT
0.50E-03,0
*DATABASE_EXTENT_BINARY
0,0,0,1,0,1,0,0
0,0,0,0,0,0
$*damping_global
$  0,1.5
*damping_part_mass
  1,10,0.05,0
*damping_part_mass
  2,10,0.5,0
*DEFINE_CURVE
 10,,1,,
 0.0,5
 11,5
*control_damping
100,1.0e-3,0.995,0,0.9
$
$ DEFINITION OF MATERIAL     1
$
```

```
*MAT_PLASTIC_KINEMATIC
1,7.840E-03,2.100E+05,0.300,2.100E+04,2.00,0.000E+00
0.000E+00,0.000E+00,0.000E+00
*HOURGLASS
1,0,0.000E+00,0,0.000E+00,0.000E+00
*SECTION_SOLID
1,1,0
*PART
rock bolt
1,1,1,0,1,0
$
$ MATERIAL CARDS
$
$
$ DEFINITION OF MATERIAL     2
$
*MAT_ELASTIC
2,2.405E-03,3.700E+04,0.250,,,
*HOURGLASS
2,0,0.000E+00,0,0.000E+00,0.000E+00
*SECTION_SOLID
2,1,0
*PART
surrounding rock
2,2,2,0,2,0
$
$ NODES
$
*NODE
$
*NODE
1,0.000000000E+00,0.000000000E+00,-10.0000000,2,6
2,0.000000000E+00,0.000000000E+00,-7.50000000,2,6
3,0.000000000E+00,0.000000000E+00,-5.00000000,2,6
4,0.000000000E+00,3.82683420,-9.23879528,0,0
5,0.000000000E+00,3.13595653,-7.05310202,0,0
6,0.000000000E+00,2.50000000,-5.00000000,0,0
7,0.000000000E+00,7.07106781,-7.07106781,0,0
8,0.000000000E+00,6.03553391,-6.03553391,0,0
9,0.000000000E+00,5.00000000,-5.00000000,0,0
10,3.12500000,0.000000000E+00,-10.0000000,2,6
……
((nodes between are not listed)
……
210043,1300.00000,58.1818199,0.000000000E+00,3,4
210044,1300.00000,61.7148170,-3.84663033,0,0
```

210045,1300.00000,61.8181839,0.000000000E+00,3,4
210046,1300.00000,65.3383865,-4.07134485,0,0
210047,1300.00000,65.4545441,0.000000000E+00,3,4
210048,1300.00000,68.9632416,-4.29613876,0,0
210049,1300.00000,69.0909119,0.000000000E+00,3,4
210050,1300.00000,72.5893555,-4.52101231,0,0
210051,1300.00000,72.7272720,0.000000000E+00,3,4
210052,1300.00000,76.2167435,-4.74596453,0,0
210053,1300.00000,76.3636398,0.000000000E+00,3,4
210054,1300.00000,79.8454056,-4.97099543,0,0
210055,1300.00000,80.0000000,0.000000000E+00,3,4
$
$ ELEMENT CARDS FOR SOLID ELEMENTS
$
*ELEMENT_SOLID
1,1,1,10,13,4,2,11,14,5
2,1,10,19,22,13,11,20,23,14
3,1,19,28,31,22,20,29,32,23
4,1,28,37,40,31,29,38,41,32
5,1,37,46,49,40,38,47,50,41
6,1,46,55,58,49,47,56,59,50
7,1,55,64,67,58,56,65,68,59
8,1,64,73,76,67,65,74,77,68
9,1,73,82,85,76,74,83,86,77
10,1,82,91,94,85,83,92,95,86
……
(elements between are not listed)
……
192792,2,209854,209876,209878,209856,209855,209877,209879,209857
192793,2,209876,209898,209900,209878,209877,209899,209901,209879
192794,2,209898,209920,209922,209900,209899,209921,209923,209901
192795,2,209920,209942,209944,209922,209921,209943,209945,209923
192796,2,209942,209964,209966,209944,209943,209965,209967,209945
192797,2,209964,209986,209988,209966,209965,209987,209989,209967
192798,2,209986,210008,210010,209988,209987,210009,210011,209989
192799,2,210008,210030,210032,210010,210009,210031,210033,210011
192800,2,210030,210052,210054,210032,210031,210053,210055,210033
$
$ NODAL TIME HISTORY BLOCKS
$
*DATABASE_HISTORY_NODE
$...>....1....>....2....>....3
155,251,4261,4363,4465,4561
4663,4765,4861,4963,5059
5161,5263,5359,5461
$

```
$ PRESSURE LOADS
$
*LOAD_SEGMENT
1,1.00,0.000E+00,1,4,5,2
*LOAD_SEGMENT
1,1.00,0.000E+00,2,5,6,3
*LOAD_SEGMENT
1,1.00,0.000E+00,4,7,8,5
*LOAD_SEGMENT
1,1.00,0.000E+00,5,8,9,6
*LOAD_SEGMENT
1,1.00,0.000E+00,3,6,156,154
*LOAD_SEGMENT
1,1.00,0.000E+00,154,156,157,155
*LOAD_SEGMENT
1,1.00,0.000E+00,6,9,158,156
*LOAD_SEGMENT
1,1.00,0.000E+00,156,158,159,157
*LOAD_SEGMENT
1,1.00,0.000E+00,9,8,256,158
*LOAD_SEGMENT
1,1.00,0.000E+00,158,256,257,159
*LOAD_SEGMENT
1,1.00,0.000E+00,8,7,258,256
*LOAD_SEGMENT
1,1.00,0.000E+00,256,258,259,257
*END
```

APPENDIX E LS-DYNA INPUT FILE OF SAMPLE V75

This is a typical input file for the study of rock bolts with a void in grout

```
*KEYWORD
*TITLE
model of dynamic respond of rock bolt
*include
load_curve_25.k
*CONTROL_CONTACT
5.000E-02,0.000E+00,0,0,1,0,0,0
0,0,0,0,0.000E+00,0,0,0
*CONTROL_OUTPUT
1,0,0,0,0.000E+00,1,99000,0
0
*CONTROL_SOLUTION
0
*CONTROL_TERMINATION
5.000,0,0.000E+00,0.000E+00,25.0
*CONTROL_TIMESTEP
0.000E+00,0.000E+00,0,0.000E+00,0.000E+00,0,0,0
*DATABASE_NODOUT
0.500E-02
*DATABASE_BINARY_D3PLOT
0.5,0
*DATABASE_BINARY_D3THDT
0.50E-03,0
*DATABASE_EXTENT_BINARY
0,0,0,1,0,1,0,0
0,0,0,0,0,0
$*damping_global
$  0,1.5
*damping_part_mass
  1,10,0.05,0
*damping_part_mass
  2,10,0.5,0
*DEFINE_CURVE
 10,,1,,
 0.0,5
 11,5
*control_damping
100,1.0e-3,0.995,0,0.9
$
$ DEFINITION OF MATERIAL     1
$
*MAT_PLASTIC_KINEMATIC
```

1,7.840E-03,2.100E+05,0.300,2.100E+04,2.00,0.000E+00
0.000E+00,0.000E+00,0.000E+00
*HOURGLASS
1,0,0.000E+00,0,0.000E+00,0.000E+00
*SECTION_SOLID
1,1,0
*PART
rock bolt
1,1,1,0,1,0
$
$ MATERIAL CARDS
$
$
$ DEFINITION OF MATERIAL 2
$
*MAT_ELASTIC
2,2.405E-03,3.800E+04,0.250,,,
*HOURGLASS
2,0,0.000E+00,0,0.000E+00,0.000E+00
*SECTION_SOLID
2,1,0
*PART
surrounding rock
2,2,2,0,2,0
$
$ NODES
$
*NODE
1,0.00000000E+00,-7.07106781E+00,-7.07106781E+00,0,0
2,0.00000000E+00,-9.23879528E+00,-3.82683444E+00,0,0
3,0.00000000E+00,-1.00000000E+01,0.00000000E+00,3,4
4,0.00000000E+00,-6.03553391E+00,-6.03553391E+00,0,0
5,0.00000000E+00,-7.05310202E+00,-3.13595676E+00,0,0
6,0.00000000E+00,-7.50000000E+00,0.00000000E+00,3,4
7,0.00000000E+00,-5.00000000E+00,-5.00000000E+00,0,0
8,0.00000000E+00,-5.00000000E+00,-2.50000000E+00,0,0
9,0.00000000E+00,-5.00000000E+00,0.00000000E+00,3,4
10,3.57142878E+00,-7.07106781E+00,-7.07106781E+00,0,0
……
((nodes between are not listed)
……
238690,1.35000000E+03,6.00000000E+01,0.00000000E+00,3,4
238691,1.35000000E+03,6.38888092E+01,-3.98144984E+00,0,0
238692,1.35000000E+03,6.40000000E+01,0.00000000E+00,3,4
238693,1.35000000E+03,6.78756485E+01,-4.22869253E+00,0,0
238694,1.35000000E+03,6.80000000E+01,0.00000000E+00,3,4

```
238695,1.35000000E+03,7.18640366E+01,-4.47603130E+00,0,0
238696,1.35000000E+03,7.20000000E+01,0.00000000E+00,3,4
238697,1.35000000E+03,7.58539505E+01,-4.72346592E+00,0,0
238698,1.35000000E+03,7.60000000E+01,0.00000000E+00,3,4
238699,1.35000000E+03,7.98454056E+01,-4.97099543E+00,0,0
238700,1.35000000E+03,8.00000000E+01,0.00000000E+00,3,4
$
$ ELEMENT CARDS FOR SOLID ELEMENTS
$
*ELEMENT_SOLID
1,1,1,10,13,4,2,11,14,5
2,1,10,19,22,13,11,20,23,14
3,1,19,28,31,22,20,29,32,23
4,1,28,37,40,31,29,38,41,32
5,1,37,46,49,40,38,47,50,41
6,1,46,55,58,49,47,56,59,50
7,1,55,64,67,58,56,65,68,59
8,1,64,73,76,67,65,74,77,68
9,1,73,82,85,76,74,83,86,77
10,1,82,91,94,85,83,92,95,86
……
(elements between are not listed)
……
223770,2,238557,238577,238579,238559,238558,238578,238580,238560
223771,2,238577,238597,238599,238579,238578,238598,238600,238580
223772,2,238597,238617,238619,238599,238598,238618,238620,238600
223773,2,238617,238637,238639,238619,238618,238638,238640,238620
223774,2,238637,238657,238659,238639,238638,238658,238660,238640
223775,2,238657,238677,238679,238659,238658,238678,238680,238660
223776,2,238677,238697,238699,238679,238678,238698,238700,238680
$
$ NODAL TIME HISTORY BLOCKS
$
*DATABASE_HISTORY_NODE
$...>....1....>....2....>....3
229,285,5282,5170,5054,4942
4826,5398,5510,5626,5910
$
$ PRESSURE LOADS
$
*LOAD_SEGMENT
1,1.00,0.000E+00,1,4,5,2
*LOAD_SEGMENT
1,1.00,0.000E+00,2,5,6,3
*LOAD_SEGMENT
1,1.00,0.000E+00,4,7,8,5
```

```
*LOAD_SEGMENT
1,1.00,0.000E+00,5,8,9,6
*LOAD_SEGMENT
1,1.00,0.000E+00,1,136,137,4
*LOAD_SEGMENT
1,1.00,0.000E+00,4,137,138,7
*LOAD_SEGMENT
1,1.00,0.000E+00,136,139,140,137
*LOAD_SEGMENT
1,1.00,0.000E+00,137,140,141,138
*LOAD_SEGMENT
1,1.00,0.000E+00,7,138,226,8
*LOAD_SEGMENT
1,1.00,0.000E+00,8,226,227,9
*LOAD_SEGMENT
1,1.00,0.000E+00,138,141,228,226
*LOAD_SEGMENT
1,1.00,0.000E+00,226,228,229,227
*LOAD_SEGMENT
1,1.00,0.000E+00,139,286,287,140
*LOAD_SEGMENT
1,1.00,0.000E+00,140,287,288,141
*LOAD_SEGMENT
1,1.00,0.000E+00,286,289,290,287
*LOAD_SEGMENT
1,1.00,0.000E+00,287,290,291,288
*LOAD_SEGMENT
1,1.00,0.000E+00,141,288,376,228
*LOAD_SEGMENT
1,1.00,0.000E+00,228,376,377,229
*LOAD_SEGMENT
1,1.00,0.000E+00,288,291,378,376
*LOAD_SEGMENT
1,1.00,0.000E+00,376,378,379,377
*LOAD_SEGMENT
1,1.00,0.000E+00,291,290,436,378
*LOAD_SEGMENT
1,1.00,0.000E+00,378,436,437,379
*LOAD_SEGMENT
1,1.00,0.000E+00,290,289,438,436
*LOAD_SEGMENT
1,1.00,0.000E+00,436,438,439,437
*END
```